THE CONTRIBUTION OF GLOMERULAR ACTIVITY MAPS TO OLFACTORY PERCEPTUAL JUDGEMENTS IN MICE

Thesis submitted for the degree of

Doctor of Philosophy of University College London

Edward F Bracey

Department of Neuroscience, Physiology and Pharmacology

UNIVERSITY COLLEGE LONDON

2013

Declaration

I, Edward Finlay Bracey, confirm that the work presented in this thesis is my own. This work has recently been published (Edward F. Bracey, Bruno Pichler, Andreas T. Schaefer, Damian J. Wallace and Troy W. Margrie, *Perceptual judgements and chronic imaging of altered odour maps indicate comprehensive stimulus template matching in olfaction,* Nat Commun. 2013 Jul 3;4:2100. doi: 10.1038/ncomms3100).

Edward Finlay Bracey

Abstract

Odours are first represented in the brain as spatiotemporal maps of activity in the olfactory bulb (OB). Imaging and electrophysiological studies have shown that these maps are both temporally and spatially complex and unique to each odour. Behavioural tasks that probe perceptual differences between odours suggest that odours that evoke similar spatial activity maps in the OB are perceived as similar. However, combination of lesion and behavioural experiments of either the olfactory epithelium or bulb has suggested that rodents can detect and discriminate between odours using minimal stimulus-related input. This has led to a consensus in the field that sensory inputs to the olfactory system contain significant redundant signal and that spatial activity maps are unnecessary for odour coding. The work presented here used a go/no-go behavioural paradigm to investigate the ability of mice not just to detect or discriminate odours after nasal epithelial lesion but also to recognise odours – which enables odour *quality* perception to be probed. Intrinsic optical imaging was used in the same animals, to observe changes in odour-evoked signals in the OB before and after lesion. The results revealed that even moderate changes to intrinsic activity maps caused deficits in both odour discrimination and recognition, suggesting that perception of odour quality was significantly altered.

Reduction in odour inputs could be equivalent to reducing the intensity of inputs, so alterations to odour quality perception after changes in odour

concentration were also examined. Recognition scores were reduced when mice were presented with a familiar odour at an unfamiliar concentration, suggesting odour perception was also significantly altered by reduction of stimulus intensity. In order to determine whether reductions in recognition score caused by lesioning and change in odour concentration had different perceptual origins, mice were trained to generalise across odour concentrations and tested for recognition after lesion. This revealed that impaired recognition after lesion resulted, not from experiencing an altered odour concentration, but from perception of apparent novel odour qualities. Consistent with this, intrinsic imaging data revealed that relative intensity of glomerular activity following lesions was altered compared with maps recorded in shams or by varying odour concentration.

Long-standing theories of sensory coding suggest that sensory systems actively match odours in the environment with stored stimulus templates. Odours familiar before lesioning were re-learnt more rapidly after lesioning than novel odours were learnt either before or after lesioning. This suggests that stored templates of familiar odours were compared to moderately altered incoming inputs and, with reinforcement, were rapidly incorporated into those templates.

In all, this work suggests that odour quality perception requires comprehensive matching of input patterns to stored representations, suggesting that spatial activity maps are a crucial component of odour coding.

.

Acknowledgements

This PhD has been an exercise in consciousness-raising that has affected all parts of my life, scientific and otherwise. Two people have been instrumental in this process, without whom I would no doubt have fallen at the first hurdle. First my PI, Professor Troy Margrie. I thank him for his patience, support and tolerance of my numerous shortcomings. For his implicit and explicit scientific guidance. He has always been available to give scientific support and advice and I know this is by no means a given in many student-PI relationships. I feel lucky to have been privy to the world-class, often daring science he produces. The second person is Dr Bruno Pichler. His rigorous help in matters practical and analytical has been invaluable.

To Paul Chadderton, Andreas Schaefer, Diogo Pimentel, Hannah Bergman and Damien Haydon-Wallace for guiding me at the start, helping me to kick-start the project. To Frances Edwards for ultimately starting me on this path. To Martyn Stopps, Greg James, Keith Fairhall, Duncan Farquharson and Alan Ling and their teams for electronic and technical assistance. Thanks also to other members of the lab past and present and others in the neuroscience community for their advice, support and good times. Agota, Alex A, Alex B, Anja, Charlie, Christian, Danielle, Ede, Jesper, Kate, Mateo, Molly, Tom.

Outside the science world, I would like to thank my family: Ma, Pops, Nadry, Del and V for their concern, unwavering support and regular courage-upbucking.

To Pops for your binary help at the eleventh hour and to you and V for Felix. To Granny and Mart for canny glimpses of warmth and welcome in the darker days. To Grandpa, Tim and Brett, Ele, Uncle J and Auntie S.

To my friends who make the rest of my life so colourful; Sheans, Mims, Dafni, Mike, JP, beaker et al., Mundy, Kels, Ali, Chithru, Kimmers, Marky, Chris and Gordon. To Tyrone. To Ninja. A special mention must go to Dr Christian A-private-practice Klettner and Michael T-nothing-to-wear Delahaye; you have been more than bastions to me, you have been an absolute set of bastions.

I would like to thank the BBSRC for funding my work, and giving me the chance to work in the Government Office for Science for three months.

I owe you all a great deal.

Contents

Chapter One: Introduction

1.1. The olfactory sense as a model system for investigating sensory processing

Specialised neural networks in our brains create approximations of the environment using information from sensory organs. These approximations are thought to dictate the version of reality we perceive and ultimately influence the choices we make. How neural networks use sensory information to generate a coherent representation or template of a stimulus is only partially understood. Basic principles of neural activity and connectivity within and between various sensory networks are well documented but debate still surrounds precisely which neurons communicate with each other, how firing patterns of neuronal populations change under different stimulus conditions, and the computations that whole sensory networks perform.

In most mammals, the olfactory sense plays a major role in behaviours crucial for survival, such as mating, finding food, avoiding predators, homing, recognising kin and mother-infant attachment. In some ways the olfactory system is simpler than other sensory systems, making it a useful tool for investigating certain aspects of sensory perception. Furthermore, olfactory deficits have been found to precede many neurodegenerative diseases (R. S. Wilson et al., 2009; W. Li et al., 2010; R. L. Doty, 2012), so a thorough understanding of the limits of olfactory processing may inform clinical research.

The *olfactory bulb* (OB) is the brain structure in mammals that receives stimulus information – in the form of neural activity - from the main odour-detecting sensory organ, the *olfactory epithelium* (OE) **(Figure 1.1A)**. The OB is a sensory network that first processes and then relays odour-evoked neural activity to downstream cortical and subcortical brain structures such as the *piriform cortex*, *amygdala* and *entorhinal cortex*, where activity is processed further and integrated with other stimulus-related information (S. Nagayama et al., 2010).

The OB in rodents is easily accessed, recorded from and manipulated without damaging other brain structures. It consists of functional units that are easy to define anatomically (M. Meister and T. Bonhoeffer, 2001) and, unlike similar structures in other sensory systems, the outputs of the OB project directly into cortical areas rather than first being processed by the thalamus (D. C. Willhite et al., 2006). These features make the OB an ideal model system for identifying computations that must occur in order to transform peripheral signals from sensory organs into neuronal activity patterns that can be interpreted by the cortex and ultimately used to generate sensory perceptions.

1.2. Olfactory sensation

1.2.1. Detection, signal transduction and first representation of odours in the OB

The first feat a sensory system must perform in order to generate a sensory percept is *stimulus detection*. This function is mediated in most sensory systems by a few types of specialised receptor cell that respond to specific stimulus-features. In the human retina, for example, all colours in the spectrum of visible light are represented by combining the activity evoked in three types of *cone photoreceptor* cell, each activated by a specific range of light wavelengths. Odour stimulus detection, however, presents the brain with a unique problem: hundreds of thousands of distinct chemical odour molecules occur in the natural world: a handful of receptor types cannot easily detect them all. The olfactory system overcomes this problem by expressing hundreds of different types of odour receptors, referred to as *olfactory receptors* (ORs). ORs are expressed in the dendrites of olfactory receptor neurons (ORNs) in the olfactory epithelium (OE) **(Figure 1.1A, B**). The mouse genome contains approximately 1300 functional OR genes (X. Zhang and S. Firestein, 2002) while humans, being more adapted to visual phenomena, express 400 (B. Malnic, 2007). Each OR has a high affinity for small range of odours with similar molecular features but may also be activated by odours with more distinct features presented in higher concentrations (P. Duchamp-Viret et al., 2000). The relative non-specificity and large number of OR subtypes thus allows the olfactory system to detect many thousands of odours (V. N. Murthy, 2011).

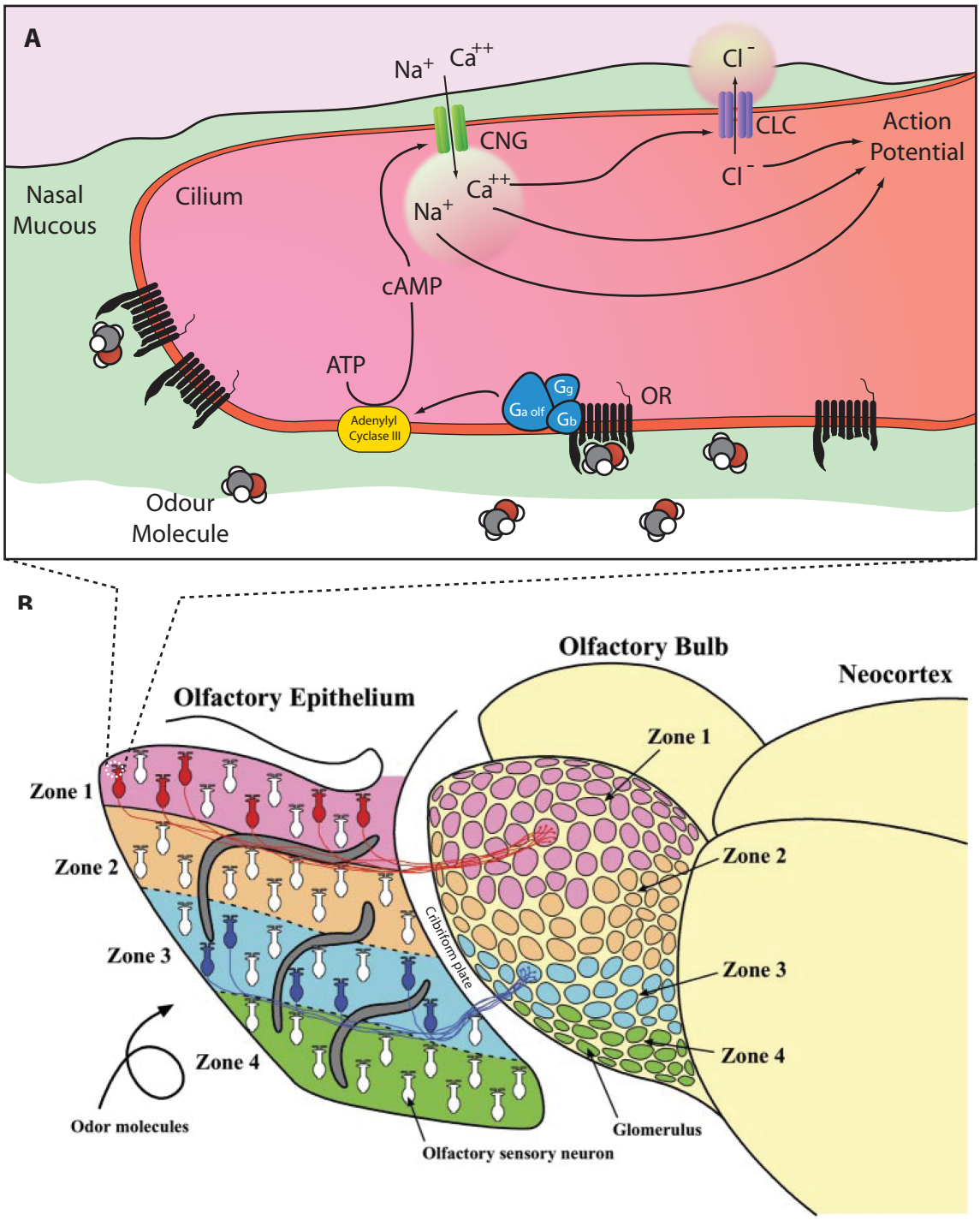

Figure 1.1. Transduction and representation of odour signals in the OE and OB
A. Olfactory receptor neuron (ORN) signal transduction pathway. Binding of an odour molecule to the olfactory receptor (OR) causes it to change conformation, allowing it to bind and activate the (blue) Golf G-protein. The G-protein activates adenylyl cyclase (yellow), causing an intracellular rise in the second messenger cyclic adenosine monophosphate (cAMP). This opens cyclic-nucleotide gated (CNG, green) cation channels in the membrane. CNG opening permits an influx of calcium and sodium ions into the ORN, depolarising the membrane and also activating chloride channels (CLC, purple). Because intracellular chloride levels are high w.r.t. extracellular levels, CLC opening depolarises the membrane further, resulting in an action potential.
B. Diagram of the olfactory bulb and epithelium. ORNs (red or blue) expressing the same OR are dispersed throughout the olfactory epithelium but converge on one glomerulus in the OB (adapted from K. Mori 2006)

Odours that diffuse or are inhaled into the nose dissolve into the mucous lining of the olfactory epithelium where they are bound by ORs. ORs are G-protein couple receptors (GPCRs) (D. T. Jones and R. R. Reed, 1989; H. A. Bakalyar and R. R. Reed, 1990) that are thought to open cyclic-nucleotide gated (CNG) ion channels in the ORN membrane (T. Nakamura and G. H. Gold, 1987; S. J. Kleene, 2008) when activated. The resultant calcium and sodium ion influx activates chloride channels, leading to chloride efflux (U. B. Kaupp, 2010), which further depolarises ORNs, triggering action potentials **(Figure 1.1A)**. ORN axons pass through the basement membrane of the olfactory epithelium where they fasciculate into mesaxons. From there, they are chaperoned by specialised glia (olfactory ensheathing cells) through the cribriform plate of the ethmoid bone and into the OB (G. M. Shepherd et al., 2004). In the OB, ORN axons pass through the *olfactory nerve layer* and terminate in the *glomerular layer*, in defined spherical bundles of neuropil referred to as *glomeruli* **(Figure 1.1B)**. Glomeruli in the mouse are 50 - 100 m in diameter and consist of dense networks of capillaries and the axons and dendrites of various bulbar neurons, including the apical dendrites of the main output neurons of the OB, the *mitral and tufted* (M/T) cells.

Each ORN expresses only one of the hundreds of OR gene subtypes (L. Buck and R. Axel, 1991). Apart from four broad, overlapping zones, the OR subtypes are stochastically distributed across the OE (K. Miyamichi et al., 2005; K. Mori et al., 2006; V. N. Murthy, 2011). However, all ORNs in the OB expressing a particular OR project to one of two glomeruli in the glomerular layer (K. J. Ressler et al., 1994; R. Vassar et al., 1994; P. Mombaerts et al., 1996) **(Figure**

1.1B). Each OR is most responsive to a small range of odour molecules, so each glomerulus - and the M/T cells and bulbar neurons that synapse in it - can be considered a *functional unit* that encodes a particular *molecular receptive range* (MRR) (K. Imamura et al., 1992; K. Mori et al., 1992; K. Katoh et al., 1993; K. Mori and Y. Yoshihara, 1995; V. N. Murthy, 2011). Each odour activates glomeruli with different MRRs to varying extents, so a given odour at a given concentration activates a specific combination of glomeruli, with each glomerulus being activated to a different degree (M. Meister and T. Bonhoeffer, 2001; M. Wachowiak and L. B. Cohen, 2003). In this way, each odour is first represented in the brain as a unique spatial map of glomerular activity (K. M. Guthrie and C. M. Gall, 1995b; B. A. Johnson et al., 1998; B. A. Johnson et al., 1999; B. A. Johnson and M. Leon, 2000; L. Belluscio and L. C. Katz, 2001; M. Meister and T. Bonhoeffer, 2001; B. D. Rubin and L. C. Katz, 2001). Glomeruli in the bulb are loosely arranged so that many with similar MRRs are clustered (B. A. Johnson et al., 1998; B. A. Johnson et al., 1999; B. A. Johnson and M. Leon, 2000; L. Belluscio and L. C. Katz, 2001; B. D. Rubin and L. C. Katz, 2001). This means that odours with similar molecular features activate similar patterns of glomerular activity, a phenomenon known as *chemotopy* (see **intrinsic imaging section** below). Chemotopic odour-evoked spatial activity maps have been proposed by some to be crucial for accurate odour perception (B. A. Johnson and M. Leon, 2007). ORNs expressing the same OR project to one of two glomeruli in the OB, so each bulb contains two neural maps of odour space; one dorsolateral and one ventromedial (B. A. Johnson et al., 1998; B. A. Johnson et al., 1999; B. A. Johnson and M. Leon, 2000; M. Wachowiak and L. B. Cohen, 2001).

As well as a spatial pattern of activity, inputs entering the OB have a significant temporal component, which is also thought to be crucial for accurate odour perception (A. T. Schaefer and T. W. Margrie, 2007; S. Junek et al., 2010). Odours enter the nose of a rodent in rhythmic cycles dependent on the rate of respiration or active sniffing (D. W. Wesson et al., 2008b). This means that ORNs are activated in phase with the sniff cycle. Furthermore, spatial activity patterns evolve both over the course of a sniff (H. Spors et al., 2006), and over multiple sniffs (H. Spors and A. Grinvald, 2002).

Thus, inputs to the OB are spatially and temporally complex. The importance of odour-evoked spatial activity maps to accurate odour perception has been contested (B. Slotnick and N. Bodyak, 2002; B. A. Johnson and M. Leon, 2007). Determining the relevance of this coding motif to olfactory perception is the main goal of this thesis.

1.2.2. OB anatomy and connectivity

Raw signals from ORNs are transformed substantially by the OB before being relayed by output neurons to higher brain centres (E. Yaksi et al., 2007). The precise nature and function of this processing are still debated (M. Yokoi et al., 1995; M. Luo and L. C. Katz, 2001; N. E. Schoppa and N. N. Urban, 2003; K. Mori et al., 2006; T. A. Cleland et al., 2012) but the major cell types and connections thought to effect the actions of the OB are well documented.

The OB comprises six distinct layers which are, from superficial to deep; the olfactory nerve (ON) layer, glomerular layer, external plexiform layer (EPL), mitral cell layer, internal plexiform layer (IPL) and the granule cell (GC) layer **(Figure 1.2A)**. In the glomerular layer, 12,000 **ORN** axons converge onto a single glomerulus (G. M. Shepherd et al., 2004). Each axon is thought to form approximately 10 synapses (J. R. Klenoff and C. A. Greer, 1998), so a single glomerulus contains at least 100,000 ORN synapses. In the glomerulus, ORNs synapse with the dendrites of *external tufted* (ET) cells, M/T cells and intrinsic OB interneurons called *periglomerular* (PG) cells **(Figure 1.2B)**. ORNs are thought to synapse with M/T cells but the major mode of ORN excitation of M/T cells has more recently been proposed to come indirectly via ET cell glutamatergic synapses (A. Hayar et al., 2004; A. Hayar et al., 2005; M. Wachowiak and M. T. Shipley, 2006).

A glomerulus contains the apical dendritic tufts of approximately 100 **M/T cells** whose somas are positioned within two to five glomerular spacings beneath the glomerulus they innervate (N. Buonviso and M. A. Chaput, 1990; N. Buonviso et

al., 1991). The apical tuft is thought to compartmentalise subthreshold inputs from the glomerular layer, allowing it to integrate signals before they proceed into the apical dendrite (M. Djurisic et al., 2008). Apart from their connections with ORNs and ET cells, M/T cells make reciprocal dendrodendritic synapses with PG cells. Dendrodendritic synapses are uncommon in other brain areas but well conserved in the olfactory systems of most species, suggesting they are an important feature of odour coding (N. N. Urban and A. C. Arevian, 2009). Reciprocal dendrodendritic connections comprise of the N-Methyl-D-Aspartate (NMDA) receptor-dependent synapses that M/T cells make onto PG cells, and the γ-aminobutyric acid (GABA) receptor-dependent synapses PG cells make onto M/T cells in return (V. Aroniadou-Anderjaska et al., 1999; J. M. Christie et al., 2001). M/T cells also have secondary dendrites that ramify in the EPL where they form dendrodendritic synapses with *granule cells* (see below). M/T cell axons gather at the posterolateral surface of the OB to form its main output, the lateral olfactory tract (LOT). The LOT projects to brain areas involved in olfactory processing including the *anterior olfactory nucleus (AON), taenia tecta, olfactory tubercle, entorhinal cortex, medial amygdala* and, most extensively, to the *primary olfactory (piriform) cortex* (L. B. Haberly and J. L. Price, 1977).

PG cell dendrites ramify in part of the glomerulus that their cell bodies lie next to (A. J. Pinching and T. P. Powell, 1971a), (**Figure 1.2A)**. Apart from connections with M/T cells, PG cells form presynaptic GABA-ergic synapses with ORNs and make dendrodendritic synapses with ET cells (A. Hayar et al., 2005). PG cell axons form GABA-mediated inhibitory synapses onto cell bodies and dendrites of PG cells and M/T cell apical dendritic tufts of glomeruli two to

four glomerular spacings away (T. Kosaka and K. Kosaka, 2011). The dendritic tufts of **ET cells** ramify extensively in the glomerulus (J. Ma and G. Lowe, 2007). Most have a single axon that branches in the glomerular layer and forms abundant glutamatergic synapses with M/T cell apical tufts, PG cell dendrites and SA cells. **Short axon cells** are found in most layers of the OB and are thought to play a key role in bulbar processing (J. L. Aungst et al., 2003). In the glomerular layer, their dendrites ramify in three to four glomeruli where they are thought to receive and integrate signals from ET cells (A. J. Pinching and T. P. Powell, 1971b). Despite their name, SA cells have extensive axons that project to glomeruli hundreds of μm away from their somas. In those glomeruli, they are thought to form inhibitory GABAergic synapses onto ET cells (J. D. Whitesell et al., 2013) and excitatory glutamatergic synapses onto PG cells (J. L. Aungst et al., 2003; J. D. Whitesell et al., 2013). SA cells are also found in deeper layers (B. J. Davis et al., 1978). These have yet to be properly categorised, although some SA cells in the EPL and GCL have been reported to form GABA-ergic synapses onto granule cells (R. T. Pressler and B. W. Strowbridge, 2006; M. D. Eyre et al., 2008).

Granule cells (GCs) are thought to provide the major source of inhibition in the OB. Over 80% of connections in the EPL are reciprocal dendrodendritic synapses between M/T cell secondary dendrites and granule cell dendritic spines (J. S. Isaacson and B. W. Strowbridge, 1998). M/T cell excitation of GCs is -amino-3-hydroxy-5-methyl-4-isoxazolepropionic acid (AMPA) and NMDA receptor-dependent, while GCs release GABA onto M/T cells, which act on $GABA_A$ receptors, causing recurrent inhibition. GCs receive inputs from M/T

cells that belong to many different glomeruli (W. Rall et al., 1966; J. L. Price and T. P. Powell, 1970; D. C. Willhite et al., 2006) and dendrodendritic synapses between M/T cells not only cause recurrent inhibition of M/T cells but can inhibit the other M/T cells the GC is connected to if activation of GCs is strong enough (N. N. Urban and B. Sakmann, 2002). GCs lack an axon, so synapses made onto M/T cells are their only output. The dendrites of GCs span only one or two glomerular spacings, whereas M/T cell secondary dendrites can span 10 - 12 glomerular spacings (E. Orona et al., 1984). Precise connectivity rules between M/T cells have yet to be determined, although viral tracing (D. C. Willhite et al., 2006) and single unit recordings (A. L. Fantana et al., 2008) suggest that M/T cell connectivity may be selective rather than distance-dependent.

Many other interneurons have been described in the OB (e.g. Van Gehuchten cells, satellite cells, piriform cells and multipolar cells) and their precise physiological features are still being investigated (T. Kosaka and K. Kosaka, 2011). The OB also receives extensive *centrifugal inputs* from both olfactory cortical regions (A. M. Boyd et al., 2012; F. Markopoulos et al., 2012) and neuromodulatory areas of the brain (J. H. McLean and M. T. Shipley, 1987b; C. Gomez et al., 2005; G. C. Petzold et al., 2009; A. M. Boyd et al., 2012).

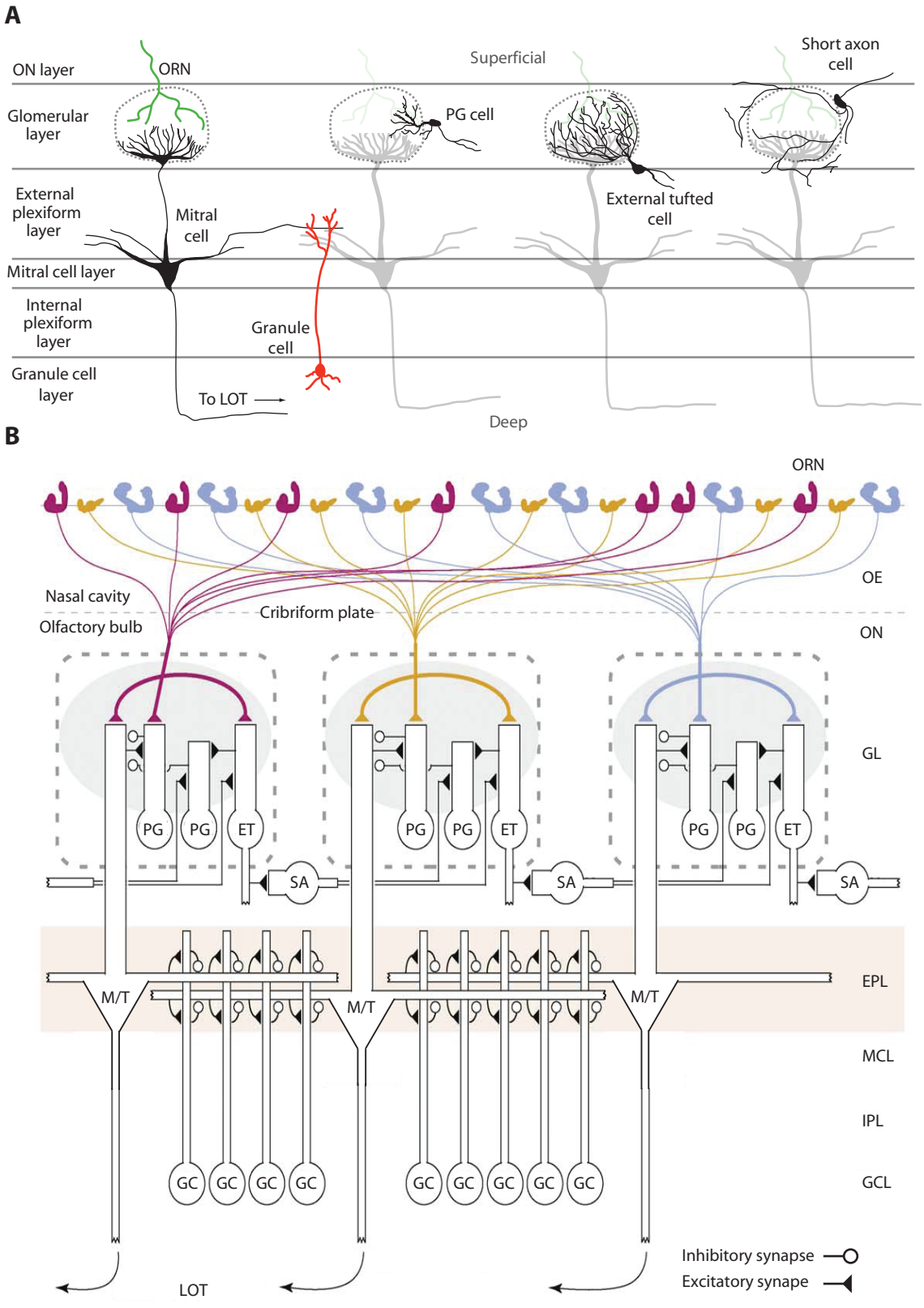

Figure 1.2. Major cell types and connections of the olfactory bulb

A. Morphology, position in layered structure and dendritic arborisation of major bulbar neurons. Olfactory nerve (ON) layer, olfactory receptor neuron (ORN), lateral olfactory tract (LOT).

B. Major connections in the olfactory bulb. Olfactory receptor neuron (ORN), mitral/tufted cell (M/T), granule cell (GC), periglomerular cell (PG), external tufted cell (ET). (adapted from T. A. Cleland 2009).

1.2.3. OB function

M/T cells are the major input to higher olfactory centres, so understanding the computations the OB performs that shape their firing is crucial to understanding olfactory perception. The precise role of the OB is still debated. It has been proposed to perform normalisation of odour inputs (M. Yokoi et al., 1995; M. Wachowiak et al., 2002), pattern decorrelation (E. Yaksi et al., 2007) and synchronisation of outputs (S. Lagier et al., 2004; B. Bathellier et al., 2006; S. Marella and B. Ermentrout, 2010).

Normalisation of odour inputs is thought to allow the OB to remain responsive to a wide range of odour concentrations (M. Wachowiak et al., 2002). Desensitisation of ORNs at high-odour concentrations may contribute to normalisation (J. Reisert and H. R. Matthews, 2001; S. J. Kleene, 2008; J. Lecoq et al., 2009), but M/T cell activity does not vary as widely as ORN responses across large changes in odour intensity, (M. Chalansonnet and M. A. Chaput, 1998) suggesting that bulbar circuitry compresses or normalises inputs from ORNs (M. Wachowiak et al., 2002). The precise bulbar mechanism for normalisation is unknown, but connections in both the glomerular layer and EPL have been proposed to mediate it (J. P. McGann et al., 2005; T. A. Cleland et al., 2007; M. L. Fletcher et al., 2009). In the glomerular layer, PG cells may perform *intra*glomerular normalisation either by inhibition of ORN input, mediated by presynaptic $GABA_B$ receptors (V. Aroniadou-Anderjaska et al., 2000; J. P. McGann et al., 2005) or by feed-forward inhibition of M/T cell throughput (T. A. Cleland, 2009). *Interglomerular* inhibition, mediated by ET

cells activating SA cells, which in turn stimulate PG cells from neighbouring glomeruli, has also been postulated to reduce M/T cell activity uniformly throughout the bulb (T. A. Cleland et al., 2007). In the EPL, lateral interactions mediated by M/T cells inhibiting other M/T cells via GCs, have been proposed to effect normalisation (T. A. Cleland et al., 2007). Normalisation of M/T cell activity patterns over changes in odour intensity may contribute to the phenomenon of *concentration invariance*, where odour identity is maintained despite changes in stimulus concentration (R. Gross-Isseroff and D. Lancet, 1988; R. Homma et al., 2009; T. A. Cleland et al., 2012).

Pattern decorrelation is a network motif proposed to reduce similarities between representations of sensory stimuli that overlap (S. W. Kuffler, 1953). ORN activity patterns in the olfactory system evoked by chemically similar odours can overlap significantly (K. Mori et al., 2006), while M/T cell outputs for those same odours differ substantially (R. W. Friedrich et al., 2009). Pattern decorrelation in the OB is proposed to exaggerate differences between glomeruli activated to similar extents, enabling accurate identification of odours by downstream olfactory areas (M. Yokoi et al., 1995; K. Mori et al., 2006).

The OB has been proposed to perform pattern decorrelation by *lateral inhibition*, whereby one glomerulus inhibits the activity of similarly active but weaker glomeruli (M. Yokoi et al., 1995; A. C. Arevian et al., 2008). In the glomerular layer, lateral inhibition has been proposed to be mediated by a number of circuit motifs including; PG cells inhibiting either M/T cells (T. A. Cleland and P. Sethupathy, 2006) or ORN inputs of other glomeruli (D. Vucinic

et al., 2006), glutamatergic SA cells stimulating PG cells of other glomeruli (J. L. Aungst et al., 2003) and GABAergic SA cells inhibiting E/T cells of other glomeruli (J. D. Whitesell et al., 2013). Reciprocal synapses between GCs and M/T cells (N. N. Urban and B. Sakmann, 2002) in the EPL have also been suggested to mediate lateral inhibition (M. Yokoi et al., 1995; M. Luo and L. C. Katz, 2001; N. E. Schoppa and N. N. Urban, 2003). In this scenario, activation of granule cells by M/T cells can lead to inhibition of M/T cells from more weakly activated glomeruli (J. S. Isaacson and B. W. Strowbridge, 1998; N. E. Schoppa et al., 1998).

However, whether lateral inhibition in either the glomerular layer or EPL contributes to pattern decorrelation in the OB is debated (E. R. Soucy et al., 2009; T. A. Cleland and C. Linster, 2012). In other sensory areas, pattern decorrelation can be performed by local lateral inhibition because neuronal populations that respond to similar stimuli are clustered. Thus, populations that are most strongly activated can inhibit weaker neighbouring populations (contrast enhancement) (S. W. Kuffler, 1953). In the olfactory system, there is some chemotopic clustering of glomeruli with similar MRRs (B. A. Johnson et al., 1998; B. A. Johnson et al., 1999; L. Belluscio and L. C. Katz, 2001; M. Meister and T. Bonhoeffer, 2001) but glomeruli with quite different MRRs can be found juxtaposed (L. Belluscio and L. C. Katz, 2001; E. R. Soucy et al., 2009) suggesting chemotopy in the OB is not precise (E. R. Soucy et al., 2009). Thus, it is debated whether pattern decorrelation in the OB relies on non-specific centre surround inhibition (A. C. Arevian et al., 2008; M. T. Wiechert et al., 2010), more specific connectivity between glomeruli that does not rely on

proximity (D. C. Willhite et al., 2006; A. L. Fantana et al., 2008), or indeed on feed-forward *intra*glomerular inhibition that does not rely on lateral connections at all (T. A. Cleland and P. Sethupathy, 2006; T. A. Cleland and C. Linster, 2012).

Furthermore, why there should be two layers of lateral inhibition is unclear. Consequently, interactions in the EPL have been proposed instead to perform synchronisation of M/T cell activity (W. Rall and G. M. Shepherd, 1968; K. Mori et al., 1992; H. Kashiwadani et al., 1999; J. L. Aungst et al., 2003; N. E. Schoppa, 2006; J. D. Whitesell et al., 2013), which is proposed to improve probability of transmission of M/T cell signals to higher areas (N. E. Schoppa, 2006).

The function of interactions in the OB is still unclear because precise connectivity motifs in the glomerular and external plexiform layers have yet to be determined. Furthermore, numerous temporal features of OB signalling add further complexity (A. T. Schaefer and T. W. Margrie, 2007; B. Bathellier et al., 2008; K. M. Cury and N. Uchida, 2010; A. K. Dhawale et al., 2010; S. Junek et al., 2010; H. Spors et al., 2012). Precise mapping of bulbar connectivity patterns using techniques that combine functional recordings with *post-hoc* analysis of connectivity such as those described in the retina (K. L. Briggman et al., 2011) and visual cortex (E. A. Rancz et al., 2011) may help clarify some of the processes the bulb performs.

Centrifugal Modulation

Bulbar output is also thought to be modulated significantly by centrifugal innervation from olfactory cortical structures, such as the anterior olfactory nucleus (F. Markopoulos et al., 2012) and piriform cortex (M. T. Shipley and G. D. Adamek, 1984; A. M. Boyd et al., 2012), and by neuromodulatory areas, such as the raphe nucleus (G. C. Petzold et al., 2009), horizontal limb of the diagonal band (HDB) (K. A. Carson, 1984; P. E. Castillo et al., 1999) and locus coeruleus (LC) (M. Jiang et al., 1996). Neuromodulatory areas are involved in determining brain states such as arousal, attention and motivation. Various projections from these areas, mediated by serotonin, noradrenaline or acetylcholine have been proposed to change bulbar activity in a number of ways. These include reducing (J. H. McLean and M. T. Shipley, 1987b, 1987a; C. Gomez et al., 2005; G. P. Dugue and Z. F. Mainen, 2009; G. C. Petzold et al., 2009; S. Liu et al., 2012) or increasing bulbar sensitivity to odours (M. Jiang et al., 1996; O. Escanilla et al., 2008) and enhancing lateral inhibition, making similar odours easier to discriminate (P. E. Castillo et al., 1999; S. Devore et al., 2012; O. Escanilla et al., 2012).

The presence of extensive inputs from olfactory cortical and neuromodulatory areas indicates that the throughput of the OB is not simply passive but subject to significant top-down modulation by behavioural state. Linked with the marked changes in M/T cell output that intrinsic OB circuitry effects, this suggests that bulbar activity is crucial for accurate odour coding. However, some of the functions proposed above suggest that chemotopic organisation of odour representation – and therefore odour-evoked spatial activity in general -

may not be relevant or necessary for odour perception (X. C. Lu and B. M. Slotnick, 1994; T. A. Cleland and P. Sethupathy, 2006; D. C. Willhite et al., 2006; A. C. Arevian et al., 2008; A. L. Fantana et al., 2008; E. R. Soucy et al., 2009; M. T. Wiechert et al., 2010; T. A. Cleland and C. Linster, 2012).

1.3. Intrinsic optical signal imaging

1.3.1. Overview

Many theories about the function of sensory networks and how stimuli are represented within them have arisen from studies using techniques that allow activity in large neuronal populations to be monitored (B. A. Johnson et al., 1998; B. A. Johnson et al., 1999; B. A. Johnson and M. Leon, 2000; L. Belluscio and L. C. Katz, 2001; M. Meister and T. Bonhoeffer, 2001; J. A. Gottfried et al., 2006; C. Zelano et al., 2011). These techniques include multi-electrode recording (J. O'Keefe and J. Dostrovsky, 1971; J. O'Keefe, 1979; J. Zhou et al., 2012), imaging of fluorescent dyes or genetically encoded probes (G. Miesenbock et al., 1998; T. Mao et al., 2008) that report intracellular changes in calcium levels (R. W. Friedrich and S. I. Korsching, 1997; C. Stosiek et al., 2003; H. Spors et al., 2006: Friedrich, 2009 #186; K. M. Cury and N. Uchida, 2010; S. Junek et al., 2010) with either wide-field (M. Wachowiak and L. B. Cohen, 2003; E. R. Soucy et al., 2009) or two-photon microscopy (K. Svoboda et al., 1997; E. Yaksi and R. W. Friedrich, 2006; W. Mittmann et al., 2011), functional magnetic resonance imaging (fMRI) (J. A. Gottfried and C. Zelano, 2011; J. Li et al., 2011; C. Zelano et al., 2011) and intrinsic optical imaging (A. Grinvald et al., 1986; D. S. Kim and T. Bonhoeffer, 1994; A. Antonini et al., 1999; B. Lendvai, 2000; J. T. Trachtenberg, 2002; D. B. Polley, 2004; A. Mizrahi, 2005; T. Keck, 2008; I. M. Devonshire, 2010).

Much of what is known about spatial representations in the OB arises from studies using intrinsic optical imaging (B. D. Rubin and L. C. Katz, 1999; L.

Belluscio and L. C. Katz, 2001; B. D. Rubin and L. C. Katz, 2001; E. R. Soucy et al., 2009), which makes use of the intrinsic optical properties of neural tissue (D. K. Hill and R. D. Keynes, 1949). Changes in blood flow, haemoglobin oxygenation states (B. Chance et al., 1962; F. F. Jobsis, 1977; R. D. Frostig et al., 1990; A. Devor et al., 2003), neurite volume and in ionic salts extruded into the extracellular fluid (L. B. Cohen et al., 1972) have been proposed to affect light-scattering and absorption in neural tissue. Intrinsic signal imaging allows changes in optical properties to be monitored by recording light reflected from the surface of the imaging substrate (L. B. Cohen et al., 1972). Early recordings of neural activity in vivo using intrinsic signals were made in the visual and barrel cortices, where signals were shown to correlate well with neural activity, which was monitored in parallel by recording changes in voltage sensitive dyes (A. Grinvald et al., 1986). The temporal resolution of intrinsic signals can be as low as 500ms and spatial resolution is approximately 50 m (M. Meister and T. Bonhoeffer, 2001). Furthermore, intrinsic imaging is relatively non-invasive because it requires neither fluorescent dye loading (A. Grinvald et al., 1986) nor craniotomy, so it causes minimal stress to animals (A. Celerier et al., 2004; R. S. Stawski et al., 2009). This makes it ideal for use in conjunction with behavioural studies.

1.3.2. Intrinsic optical signal imaging and odour coding in the OB

Combination with histological (M. Meister and T. Bonhoeffer, 2001), voltage sensitive dye (L. Belluscio and L. C. Katz, 2001) or calcium sensitive dye imaging techniques (M. Wachowiak and L. B. Cohen, 2003) in the OB has shown that intrinsic signals reflect odour-evoked glomerular activity, (F. Xu et

al., 2000, **Figure 1.3A**). Imaging of the dorsal surface of the OB is estimated to allow the activity of approximately 20% of bulbar glomeruli to be observed (F. Pain et al., 2011) and spatial resolution is high enough to allow individual glomeruli in the OB to be discerned (B. D. Rubin and L. C. Katz, 1999; M. Wachowiak and L. B. Cohen, 2001).

The precise neural origin of the intrinsic signal in the OB is unknown (F. Pain et al., 2011). Odour-evoked responses may have different origins at different wavelengths (M. Meister and T. Bonhoeffer, 2001). Wavelengths of between 550 and 610nm are thought to represent changes in total haemoglobin and deoxyhemoglobin respectively, while above 707nm, changes in light scattering properties of the glomerular layer likely to be caused by axonal (L. B. Cohen et al., 1972) or glial (B. A. MacVicar and D. Hochman, 1991) swelling and ion exchange are thought to be more dominant (M. Meister and T. Bonhoeffer, 2001). Despite different origins, functional maps recorded at different wavelengths are reasonably similar (M. Meister and T. Bonhoeffer, 2001). Intrinsic signals in the OB have been shown to correlate with release of glutamate by ORNs and to be dependent on uptake by astrocytes (H. Gurden et al., 2006). Thus, it is thought that odour-evoked intrinsic-optical signals in the glomerular layer predominantly reflect presynaptic activity at the first synapse rather than bulbar interneurons or projection neurons. However, changes in bulbar blood flow have been proposed to rely on post-synaptic activation of glutamate receptors, suggesting that some component of odour-evoked intrinsic signals may originate from sources that are not purely presynaptic (E. Chaigneau et al., 2007).

As noted earlier, odour stimuli are first represented in the OB as spatiotemporal maps of activity (A. T. Schaefer and T. W. Margrie, 2007). Early studies using uptake of 14C-labeled glucose analogue 2-deoxyglucose (2DG) by active neurons (L. Sokoloff et al., 1977; W. B. Stewart et al., 1979; B. A. Johnson et al., 1998; B. A. Johnson et al., 1999; B. A. Johnson and M. Leon, 2000; B. A. Johnson et al., 2005a; B. A. Johnson et al., 2005b) or immediate early gene expression (K. M. Guthrie et al., 1993; K. M. Guthrie and C. M. Gall, 1995a, 1995b) allowed odour-evoked spatial activity in the OB to be monitored. However, these techniques monitor only neural activity elicited by a single exposure of an odour per animal as they rely on post-mortem analysis (W. B. Stewart et al., 1979). Intrinsic imaging and other optical techniques, such as calcium imaging (M. Wachowiak and L. B. Cohen, 2003) and fMRI (C. Martin et al., 2007) have allowed spatial activity evoked by different odours to be monitored in the same animals in vivo (L. Belluscio and L. C. Katz, 2001). In conjunction with presentation of large sets of odours, these techniques have been used to carefully characterise spatial representations of odours in the OB (B. A. Johnson et al., 1998; B. A. Johnson et al., 1999; B. D. Rubin and L. C. Katz, 1999; N. Uchida et al., 2000; L. Belluscio and L. C. Katz, 2001; B. A. Johnson et al., 2005a; B. A. Johnson et al., 2005b; E. R. Soucy et al., 2009; T. Imai et al., 2010). These studies show that most odours evoke activity in glomeruli that are clustered, rather than randomly distributed throughout the glomerular layer (B. A. Johnson et al., 1998; B. A. Johnson et al., 1999; B. A. Johnson and M. Leon, 2000; L. Belluscio and L. C. Katz, 2001), and that glomeruli are organised into loose chemotopic functional domains comprising

glomerular units that respond to odours with the same functional group or position of the functional group in molecules (L. Belluscio and L. C. Katz, 2001; K. Mori et al., 2006). For example, glomeruli in the anteromedial dorsal OB surface respond most strongly to aliphatic acids and aldehydes, while glomeruli in the rostroventral portion the dorsolateral surface respond largely to aliphatic ketones (K. Mori et al., 2006) (summarised in **Figure 1.3B**). Glomerular position within these domains is determined by features such as length and branching of carbon chains in an odour molecule and centroids of activity patterns have been shown to shift systematically across the domain as chain length changes (B. A. Johnson et al., 1999; N. Uchida et al., 2000; L. Belluscio and L. C. Katz, 2001; M. Meister and T. Bonhoeffer, 2001).

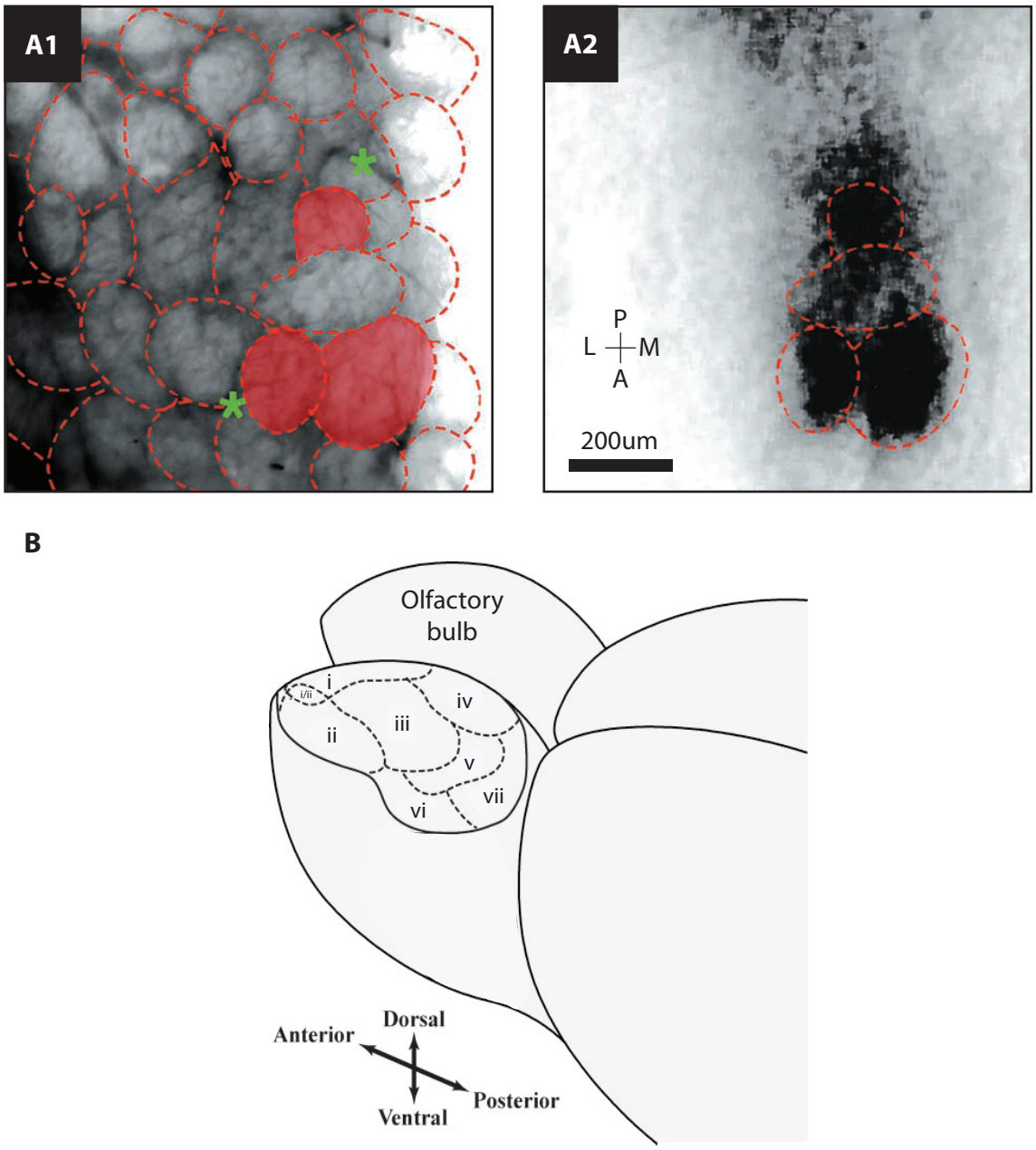

Figure 1.3. Intrinsic signal imaging and chemotopic maps in the OB
A. Intrinsic spots correspond to activity in glomeruli. **A1.** Voltage sensitive dye loading reveals the boundaries of glomeruli (red dashed lines) on the dorsal aspect of the OB **A2.** Overlay of odour-evoked intrinsic signals shows dark spots correspond to activity in glomeruli (From Belluscio and Katz 2001).
B. Diagram of the showing broad chemotopic domains of the dorsal OB. Chemical features that most strongly domains are: i: Anteromedial. Aliphatic acids, aldehydes, esters, diketones. ii: Anterolateral. 6-8 carbon chain aliphatic alcohols, aliphatic ketones, anisole derivatives w/methoxy group. iii: Central, lateral. Phenol family, phenyl ethers. iv: Caudal/Lateral. Broad number of structures, mainly ketones, cyclic ketones, aromatic/ aliphatic ketones, diketones. v: Dorsolateral. No systematic responses identified. vi: Rostroventral aspect of dorsolateral surface. Aliphatic ketones, hydrocarbons, phenyl ethers, diketones, and cyclic ketones. vii, Ventrocaudal aspect of dorsolateral surface: Hydrocarbons, benzene and terpene hydrocarbons. Also phenyl ethers, diketones, small aliphatic ketones, aliphatic ketones, cyclic ketones, and ethers.
(adapted from K. Mori et al. 2006)

Optical techniques have also shown that bulbar representation of enantiomers – chemicals that are mirror-symmetric - may differ by as little as one glomerulus (B. D. Rubin and L. C. Katz, 2001). This suggests that subtle differences in spatial activity maps may support differences in odour object perception (B. A. Johnson and M. Leon, 2007). Furthermore, changes in concentration have also been shown to cause changes in spatial activity maps, (B. D. Rubin and L. C. Katz, 1999; N. Uchida et al., 2000; M. Meister and T. Bonhoeffer, 2001). Maps are thought to change over concentration because each OR subtype has a different affinity for a given odour, thus a different number of ORN populations is recruited at different intensities of that odour (V. Aroniadou-Anderjaska et al., 1997; P. Duchamp-Viret et al., 1999). Therefore, spatial representations may also be crucial to perception of odour concentration.

Projection of ORNs of the same OR type to two distinct glomeruli means that two spatial activity maps in the glomerular layer represent odours (N. Uchida et al., 2000; L. Belluscio and L. C. Katz, 2001; M. Meister and T. Bonhoeffer, 2001). The relevance of these two representations is not yet understood but they have been proposed to perform a number of functions including coincidence detection (T. A. Cleland et al., 2007) and coding of odour concentration (Z. Zhou and L. Belluscio, 2012). They may also be redundant duplications that allow the OB to function if inputs to one of the maps are non-functional due to blockage or injury of one part of the olfactory epithelium (B. M. Slotnick et al., 1997).

.

Intrinsic imaging (B. D. Rubin and L. C. Katz, 1999; L. Belluscio and L. C. Katz, 2001; M. Meister and T. Bonhoeffer, 2001; B. D. Rubin and L. C. Katz, 2001; M. Wachowiak and L. B. Cohen, 2003; R. Vincis et al., 2012) and other optical techniques (R. W. Friedrich and S. I. Korsching, 1997; B. A. Johnson et al., 1999; B. A. Johnson and M. Leon, 2000; C. Linster et al., 2001b; M. Wachowiak and L. B. Cohen, 2001; H. Spors and A. Grinvald, 2002; J. P. McGann et al., 2006; H. Spors et al., 2006) have thus revealed much about bulbar function and have highlighted that even simple monomolecular odorants evoke complex and unique spatial activity patterns of glomeruli that may contribute significantly to the coding of odour identity (B. A. Johnson and M. Leon, 2007; M. Leon and B. A. Johnson, 2009).

As noted earlier, pattern decorrelation of odour maps that depends on centre-surround inhibition would also depend on clustering of glomeruli with similar MRRs (M. Yokoi et al., 1995; K. Mori et al., 2006). However, intrinsic imaging and other optical techniques have shown that chemotopic organisation of glomeruli (L. Belluscio and L. C. Katz, 2001) is not highly precise (E. R. Soucy et al., 2009). The shape and position of chemotopic domains, which typically consist of 10 - 50 glomeruli (L. Belluscio and L. C. Katz, 2001; K. Mori et al., 2006) (see **Figure 1.3B**), vary to some extent from animal to animal, as does the position of glomeruli that express specific ORs (E. R. Soucy et al., 2009; L. Ma et al., 2012). Furthermore, a glomerulus within a domain can be activated by structurally dissimilar odours (B. D. Rubin and L. C. Katz, 2001; T. Bozza et al., 2004; A. L. Fantana et al., 2008). This variability suggests that highly accurate odour representation is possible without precise, stereotyped

glomerular locations (R. W. Friedrich and S. I. Korsching, 1997; B. D. Rubin and L. C. Katz, 1999; L. Belluscio and L. C. Katz, 2001; T. Bozza et al., 2004; D. C. Willhite et al., 2006; I. G. Davison and L. C. Katz, 2007; A. L. Fantana et al., 2008; R. I. Wilson, 2008; E. R. Soucy et al., 2009; V. N. Murthy, 2011; L. Ma et al., 2012). Proposed mechanisms of bulbar function that negate the need for chemotopy thus imply that coding may be more distributed throughout the OB. In this scenario, complete spatial activity maps may not be necessary for accurate odour perception (B. M. Slotnick et al., 1987; B. Slotnick and N. Bodyak, 2002).

1.4. Behavioural tasks for investigating olfactory sensory processing

1.4.1. Overview of olfactory behavioural tasks

Optical and electrophysiological techniques can reveal much about neural processing, but an investigation into the function of a neural network must ultimately demonstrate the impact of its activity, alteration or absence on the system it operates in. Thus, changes in sensory networks should result in measurable alterations in perception. *Psychophysical tests* quantitatively establish the relation between stimulus-evoked activity and alterations in sensory perception (H. Ehrenstein and A. Ehrenstein, 1999). Numerous psychophysical tests have been developed that allow correlates of odour perception to be reported by animals (B. M. Slotnick and H. M. Katz, 1974; B. M. Slotnick and B. J. Nigrosh, 1974; M. Bunsey and H. Eichenbaum, 1996; N. Bodyak and B. Slotnick, 1999; T. A. Cleland et al., 2002; T. A. Cleland and V. A. Narla, 2003; N. M. Abraham et al., 2004; N. Mandairon et al., 2006c; N. Mandairon et al., 2006b; N. Mandairon et al., 2006a; O. Escanilla et al., 2008; T. A. Cleland et al., 2009; O. Escanilla et al., 2010; O. Escanilla et al., 2012) and thus allow the limits of olfactory sensory processing to be probed.

Habituation tasks make use of the innate tendency of rodents to spend more time investigating novel odours than familiar ones (T. A. Cleland et al., 2002; O. Escanilla et al., 2008). Such tasks can be used to probe odour detection thresholds by presenting subthreshold concentrations of odours and increasing concentrations until odours are responded to (O. Escanilla et al., 2008; O.

Escanilla et al., 2010; O. Escanilla et al., 2012). Investigation times decrease after multiple presentations of an odour (O. Escanilla et al., 2008), so habituation can also be used to probe odour recognition whereby familiar, habituated odours are responded to with lower investigation times than novel odours (T. A. Cleland and V. A. Narla, 2003; R. A. Bevins and J. Besheer, 2006).

Cross-habituation tasks first habituate an animal to an odour and then present it with a novel odour. If the novel odour is perceived as similar to the familiar odour, investigation times will be lower than for an odour perceived as different. Thus, these tasks can also be used to probe odour detection, discrimination and recognition (T. A. Cleland et al., 2002).

Operant conditioning tasks use reinforcement or punishment to train animals to respond to specific stimuli with certain prescribed behaviours. For example, in the olfactory *discrimination digging* task, animals learn to dig in one of two scented sand dishes in order to receive a reward. After repeated exposures, the ability to discriminate between the two odours is monitored by the time spent digging in each of the dishes. Once the task is acquired, the ability of the animal to recognise an odour can be probed by removing the reward. The extent to which an animal finds odours similar can be probed by testing discrimination and recognition with subtly different odours (T. A. Cleland et al., 2002).

Go/no-go and *two alternative choice (TAC)* operant conditioning tasks probe the responses of animals conditioned to respond to two or more different stimuli with distinct, prescribed behaviours (B. F. Skinner, 1948; N. Bodyak and B. Slotnick, 1999; N. Uchida and Z. F. Mainen, 2003; N. M. Abraham et al., 2004;

L. M. Kay et al., 2006; D. W. Wesson et al., 2008a). For example, an animal may be rewarded for pushing a lever after sampling stimulus X, and for pushing a different lever after sampling stimulus Y. If the animal pushes the wrong lever after sampling, it receives either no reward or a punishment e.g. footshock (B. F. Skinner, 1948). Correct responses to stimuli can thus be used to determine the ability to discriminate between odours (B. M. Slotnick and B. J. Nigrosh, 1974; N. M. Abraham et al., 2004; L. M. Kay et al., 2006). After the task is acquired, presentation of stimulus in the absence of reward can be used to test recognition (B. Slotnick and N. Bodyak, 2002; B. Slotnick and S. Bisulco, 2003). In these tasks, discrimination between odours and clean air can be used to determine detection thresholds; the concentration of a given odour is incrementally reduced until animals can no longer discriminate it from air above chance levels (B. M. Slotnick and J. E. Ptak, 1977). A *confusion matrix* task also allows the perceived similarities between odours to be assessed. In this task, animals are presented with one of several odours at a sampling port. Rewards are then distributed at the end of one of a number of corridors and each odour is coupled to receipt of a reward in a particular corridor. The frequency with which an animal erroneously travels down a particular corridor allows the perceptual similarity of the sampled odour to be compared to the odour associated with that corridor (S. L. Youngentob et al., 1990; P. F. Kent et al., 1995; P. F. Kent et al., 2003; S. L. Youngentob et al., 2006).

Many of these behavioural tasks have been used to investigate the acuity of olfactory perception in rodents, and thus to provide insight into the coding that underlies it (B. M. Slotnick and H. M. Katz, 1974; B. M. Slotnick and J. E. Ptak,

1977; B. M. Slotnick et al., 1991; T. A. Cleland et al., 2002; T. A. Cleland and V. A. Narla, 2003; N. Mandairon et al., 2006b; N. Mandairon et al., 2006a; O. Escanilla et al., 2008; N. Mandairon et al., 2008; T. A. Cleland et al., 2009; N. Mandairon and C. Linster, 2009; S. Can Guven and M. Laska, 2012; T. A. Cleland et al., 2012).

1.4.2. Olfactory perceptual limits and spatial activity maps

Odour detection thresholds provide one measure of olfactory acuity. Studies using habituation and go/no-go tasks report that rats and mice can detect odour concentrations as low as 0.0001% v/v (B. M. Slotnick et al., 1987; N. Bodyak and B. Slotnick, 1999; O. Escanilla et al., 2010). However, detection thresholds depend on which odour is sampled (M. Laska et al., 2009; L. Larsson and M. Laska, 2011). For example, mice are more sensitive to short- rather than long-chained aliphatic carboxylic acids (S. Can Guven and M. Laska, 2012). This is likely to be because certain groups of odours that are more relevant to the survival of each species are represented with greater with greater acuity by their olfactory systems (S. Can Guven and M. Laska, 2012). The ease with which two odours can be distinguished also allows the acuity of the olfactory system to be evaluated (B. M. Slotnick and J. E. Ptak, 1977; T. A. Cleland et al., 2002; T. A. Cleland and V. A. Narla, 2003; T. A. Cleland et al., 2007). In cross-habituation and operant conditioning tasks, rodents can discriminate between highly similar odours, including those with the same functional group but differing by only one carbon atom in chain length (T. A. Cleland et al., 2002), and enantiomers (C. Linster et al., 2001b; K. McBride and B. Slotnick, 2006).

Furthermore, they can also be trained to discriminate odours that differ in concentration by only 0.001% v/v (B. M. Slotnick et al., 1987).

Behavioural tasks that probe the limits of olfactory perception may offer insight into the importance of spatial activity maps for odour coding. In line with this, odours shown by 2DG imaging to evoke similar bulbar spatial activity patterns were habituated to more quickly than those that evoked more distinct activity patterns (T. A. Cleland et al., 2002; S. L. Ho et al., 2006b; S. L. Ho et al., 2006a). In digging tasks, odours that evoked similar activity maps to odours associated with rewards were responded to with higher digging times than odours that evoked less similar 2DG activity maps (T. A. Cleland et al., 2002; T. A. Cleland and V. A. Narla, 2003). Furthermore, rats took significantly longer to learn to discriminate enantiomers of limonene or terpinen-4-ol, which evoke highly similar 2DG activity patterns, than they did to discriminate carvone enantiomers, which evoke substantially different activity maps (C. Linster et al., 2001b). However, the same deficits were not reported in a go/no-go discrimination task (K. McBride and B. Slotnick, 2006). Confusion matrix tasks indicate that odours that evoke overlapping 2DG representations were confused more frequently than those that evoked highly different patterns (J. E. Schwob et al., 1999). Furthermore, rats with multisite electrodes implanted in the mitral cell layer of their OBs could learn to discriminate between stimulation from two different electrodes 500 m apart but made more mistakes when stimulation came from electrodes spaced 250 m apart (A. M. Mouly et al., 1985). In all, these results suggest that odours that evoke more similar activity maps are

perceived as more similar, implying that spatial activity is crucial for accurate odour perception (B. A. Johnson and M. Leon, 2007).

In operant conditioning paradigms that use automated odour release systems, the time taken to make decisions in discrimination tasks can be accurately recorded (N. M. Abraham et al., 2004) and has been used to determine the upper limits of processing times in the olfactory system (N. Uchida and Z. F. Mainen, 2003; N. M. Abraham et al., 2004; B. Slotnick, 2007a; D. W. Wesson et al., 2008a). Go/no-go and TAC discrimination tasks indicate that odour related decisions can be made within 400ms of odour presentation (N. Uchida and Z. F. Mainen, 2003; N. M. Abraham et al., 2004). Sniffing frequency is known to increase when rodents encounter a novel odour (S. Clarke et al., 1970; D. W. Wesson et al., 2009), and a study that simultaneously monitored sniff patterns and calcium signals in ORNs reported that presentation of a novel odour caused increases in sniffing just 75 ms after onset of ORN activity in glomeruli, suggesting rats can make rapid odour related decisions (D. W. Wesson et al., 2008a). Decisions often occurred tens of ms before glomerular activity had reached peak values, which implies that odour recognition can occur even before complete spatial activity maps are available to the olfactory system (D. W. Wesson et al., 2008a). However, in a different study, mice discriminating highly similar odours needed approximately 100ms longer for accurate decision-making than they did for simpler odour discrimination tasks (N. M. Abraham et al., 2004), implying that a fuller representation may be required for discrimination of more complex odours (A. T. Schaefer and T. W. Margrie, 2012).

In all, these behavioural experiments suggest an important link between spatial activity patterns in the OB and odour perception.

1.4.3. Behavioural investigation of the redundancy of odour-evoked spatial activity maps

Imaging and electrophysiological studies suggest that complex spatiotemporal maps in the OB represent odours (M. Yokoi et al., 1995; M. Wachowiak and L. B. Cohen, 2003; A. T. Schaefer and T. W. Margrie, 2007; E. Yaksi et al., 2007). The spatial component of these maps has been postulated to be crucial for accurate odour perception (B. A. Johnson and M. Leon, 2000, 2007; R. Haddad et al., 2010) and behavioural studies of olfactory acuity largely align with this view (C. Linster et al., 2001b; T. A. Cleland et al., 2002). However, to demonstrate causality between proposed circuit motifs and changes in perception, the impact of manipulation of neural circuits on behaviour must be demonstrated. Pharmacological (O. Escanilla et al., 2008; O. Escanilla et al., 2010; O. Escanilla et al., 2012) or genetic (A. Fleischmann et al., 2008; N. M. Abraham et al., 2010) manipulations of the OB have recently been combined with behavioural tasks to investigate the function of the olfactory system. For example, injections of noradrenaline into the OB have been shown to reduce detection thresholds (O. Escanilla et al., 2010) in rats, while increasing bulbar inhibition by genetic deletion of granule cell AMPA receptor subunits has been shown to significantly reduce odour discrimination times (N. M. Abraham et al., 2010).

One of the simplest manipulations that can be performed on neural circuitry is lesioning of brain areas. The deficits caused by lesions can then be evaluated, allowing the correlation between activity in certain areas and functions to be studied (A. Hendrickson et al., 1977; T. M. Barth et al., 1990; A. Compston, 2011). Studies that used careful psychometric testing with go/no-go tasks, in conjunction with lesions of the OB and post-hoc histology suggest, in stark contrast to imaging and behavioural data, that complex spatial activity maps are not necessary for accurate odour perception (A. Ducray et al., 2002; B. Slotnick and N. Bodyak, 2002; K. McBride and B. Slotnick, 2006; S. L. Youngentob and J. E. Schwob, 2006).

Direct surgical lesions targeted to areas activated by homologous series of fatty acids and aldehydes did not cause deficits in discrimination of those odours (B. Slotnick and N. Bodyak, 2002) and even discrimination of chemically similar enantiomers, which evoke highly similar glomerular activity maps (B. D. Rubin and L. C. Katz, 2001), was not impaired by targeted surgical lesions (B. Slotnick and S. Bisulco, 2003; K. McBride and B. Slotnick, 2006). Indeed, over 90% of OB tissue can be removed before animals suffer deficits in the ability to discriminate between odours (X. C. Lu and B. M. Slotnick, 1998). Animals with substantial lesions of the olfactory epithelium caused by intraperitoneal injection of 3-methylindole (3-MI) reportedly also had no major deficits in either odour detection or discrimination (B. Slotnick, 2007b). Moreover, in extreme cases where rodents had bulbectomies at birth, newly generated ORNs that extended axons through the cribriform plate and formed glomerulus-like structures in the

forebrain were sufficient to support odour detection and discrimination of highly different odorants (B. Slotnick et al., 2004).

This work by the Slotnick group has led to the predominant conclusion that much of the OB circuitry encodes redundant information. Furthermore, direct surgical lesioning implies that odour coding is not reliant on defined, chemotopic spatial activity maps but is distributed more widely throughout bulbar circuitry (B. Slotnick and N. Bodyak, 2002; S. Bisulco and B. Slotnick, 2003; B. Slotnick and S. Bisulco, 2003; K. McBride and B. Slotnick, 2006). However, careful reinterpretation of these studies along with other data implies that lesions may have more impact on odour perception than the Slotnick data suggests.

Rats had increased detection thresholds for odours represented by areas of the bulb targeted by direct surgical lesion (X. C. Lu and B. M. Slotnick, 1998), and also had difficulty discriminating complex odour mixtures (X. C. Lu and B. M. Slotnick, 1998). Mice treated with intranasal irrigation of ZnSO4 had deficits in discrimination despite retaining up to 40% of bulbar inputs (K. McBride et al., 2003). These studies imply that even moderate lesions may cause deficits in odour perception. Furthermore, studies that used focal lesion of the OB are likely to have spared input to at least one of the bulbar regions representing the odours that were used in concomitant discrimination and detection tasks (B. M. Slotnick et al., 1987; B. Slotnick and N. Bodyak, 2002).

Crucially, detection of odours, or discrimination of simple, monomolecular odours is unlikely to require extensive representation in the OB. Odour *quality*

perception and correct identification however, are likely to require more intact representations. Tasks in the lesions studies mentioned above did not satisfactorily probe changes in odour quality perception because detection and discrimination testing used odour stimuli that were rewarded. Mice and rats can learn to discriminate odour pairs after just one stimulus presentation (B. M. Slotnick and H. M. Katz, 1974; C. M. Armstrong et al., 2006), so discrimination and detection trials could theoretically have been performed based on differences between activity patterns elicited in only a handful of neurons (D. P. Wellis et al., 1989). Odour-quality perception is therefore more likely to rely on more intact representations. Thus, in order to determine if spatial activity maps truly are redundant, a behavioural correlate of change in stimulus quality perception after lesion is necessary.

Standard tests of odour recognition pair an odour stimulus with a reward and then probe memory for the stimulus by observing the response to it in the absence of a reward (under extinction) (K. K. Yee and R. M. Costanzo, 1998; T. A. Cleland et al., 2002; B. Slotnick and N. Bodyak, 2002; S. Bisulco and B. Slotnick, 2003). Few behavioural studies in rodents have sought to ascertain changes in perception of odour quality after lesion in this way. Guinea pigs showed marked deficits in discrimination and recognition of odours after full transection of the olfactory nerve, suggesting a marked alteration in odour quality perception (K. K. Yee and R. M. Costanzo, 1998). Observation of changes to bulbar inputs in mice after the same treatment indicated that ORN projections reinnervating the bulb at an equivalent time to the recognition testing in the guinea pig study were in severe disarray, with few defined

glomerular structures (R. M. Costanzo, 2000). This is evidence in favour of the importance of spatial activity maps to odour coding but these studies caused extreme changes to bulbar input and did not confirm the extent of ORN destruction and behaviour in the same animals, or indeed, species.

Only a few studies of change in odour-quality perception after more moderate lesions have been performed. One study investigated the impact of either direct lesion of the OB (after complete contralateral bulbectomy) or 3-MI-induced lesion of the epithelium, on recognition of odours that rats had learned to discriminate before treatment (B. Slotnick and N. Bodyak, 2002). On average, 3-MI lesion of the epithelium caused reductions in recognition scores, while direct lesions had little impact on detection, discrimination or recognition of odours (**Figure 1.4**). In this case, 3-MI may have affected all bulbar odour representations while direct surgical lesions may have affected only one of two bulbar areas activated by odours used in behavioural tasks (B. Slotnick and N. Bodyak, 2002). Another study by the Slotnick group made greater surgical lesions of the OB, which were thought to impact all representations of odours (S. Bisulco and B. Slotnick, 2003). In this case, recognition was significantly impaired, although the authors made little of the significance of this finding. Therefore, tasks that probe odour quality hint that spatial representation of odours may be crucial to accurate odour perception. However, the relevance of spatial activity maps to odour processing is still contested.

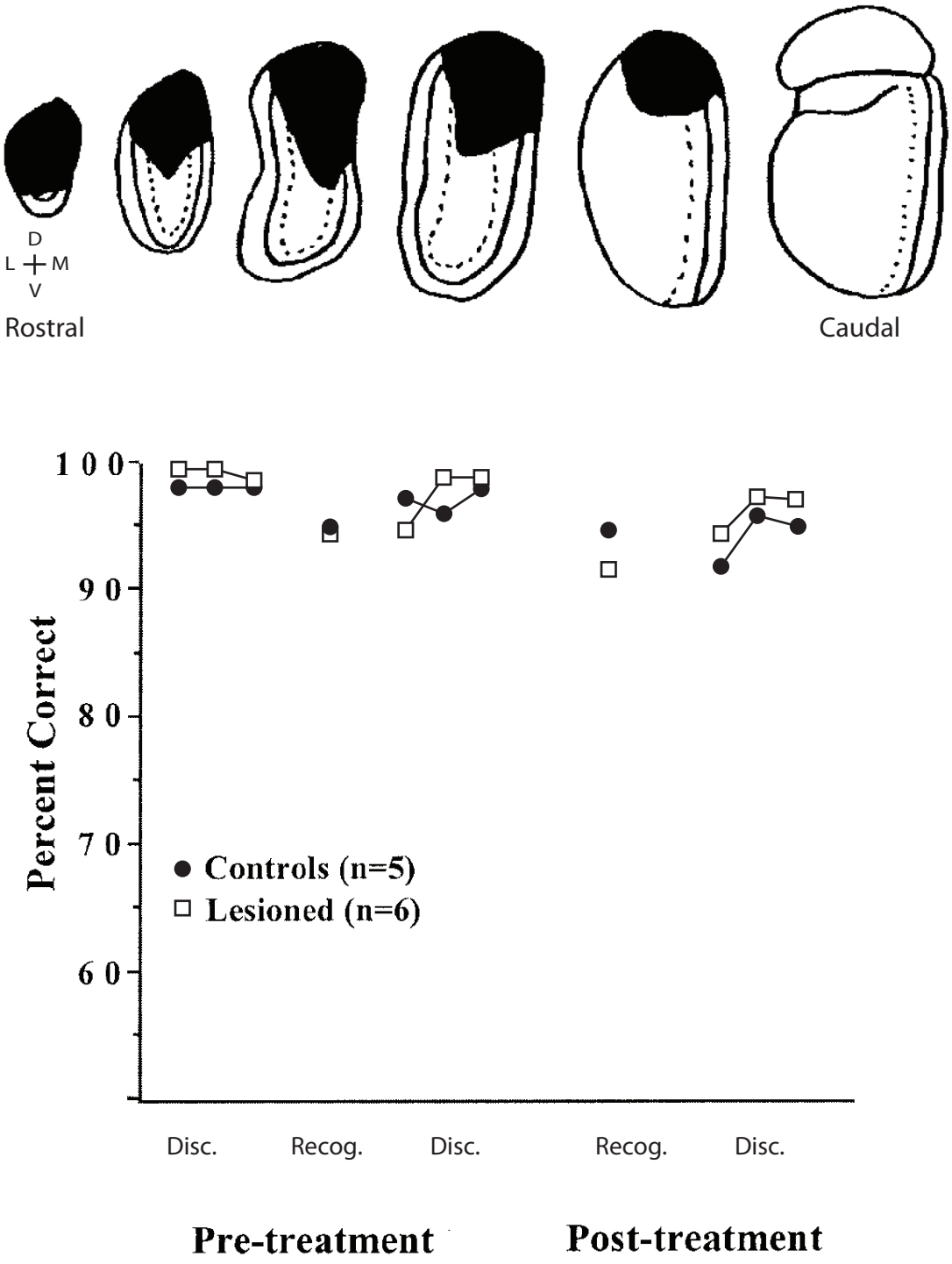

Figure 1.4. Direct surgical lesions of the OB had no impact on odour discrimination or recognition

Top, Example coronal sections of rat OB showing regions of dorsal tissue surgically removed in black. The contralateral OB was fully removed.

Bottom, average discrimination (Disc.) and unrewarded recognition (Recog.) scores from all rats, for odours thought to evoke activity patterns in lesioned areas. Post-treatment recognition score was reduced in lesioned animals, but not significantly different from controls (from B. Slotnick and N. Bodyak 2002).

1.5. Aims of this study

The few studies that combined lesion with testing odour-quality perception had mixed results (B. Slotnick and N. Bodyak, 2002; S. Bisulco and B. Slotnick, 2003). These studies used post-hoc histology to analyse lesions, so they could not verify that lesions effectively removed or altered all bulbar representations of odours that were used to probe behaviour. Furthermore, histological techniques do not allow lesion-induced changes in the same animal to be quantified and neither can they report subtle functional changes in neural activity that may be caused by lesioning. In chapters three and four of this thesis, lesioning studies were re-examined by observing the effects of nasal epithelial lesions on odour-evoked functional activity in the OB, combined with detailed behavioural analysis that included tests of change in odour-quality perception. Lesions were induced by nasal irrigation with $ZnSO_4$, (C. G. Smith, 1938), which has traditionally been used to induce full, but transient anosmia (S. S. Winans and J. B. Powers, 1977; J. W. Harding et al., 1978; A. D. Mayer and J. S. Rosenblatt, 1993; A. Ducray et al., 2002), however, it causes partial reductions in olfactory inputs in smaller doses (B. Slotnick et al., 2000). Functional activity was recorded using intrinsic signals evoked before and after lesion, and behaviour was investigated using a go/no-go discrimination and recognition paradigm.

Previous imaging studies show that large reductions in odour concentration reduce the number of glomeruli activated by an odour (M. Wachowiak and L. B. Cohen, 2003; R. Homma et al., 2009), and lesions of the nasal epithelium may reduce inputs in a similar manner. Thus, in chapters five and six, the effects of

odour concentration on odour-quality perception and intrinsic signals were investigated in order to determine if changes in odour concentration caused deficits in perception that differed from deficits seen after lesioning.

Finally, in chapter seven, the way the olfactory system processes novel and familiar stimuli after lesion was investigated to determine how stored odour-evoked representations are altered by experience.

Chapter Two: Materials and Methods

2.1. Animals

Male C57Bl/6 mice over four weeks old were used in all experiments. Males were used exclusively because olfactory sensitivity in female mice has been shown to fluctuate with the oestrus cycle (K. R. Kumar and G. Archunan, 1999). All procedures were carried out in accordance with Home Office regulations stipulated on project and personal licences.

2.2. Odours

In experiments in chapter three, pair B odours were always ethyl butyrate or pentanal, which consistently evoke dorsal activity in the OB (B. A. Johnson and M. Leon, 1998, 1999, 2000; K. Mori 2006). In chapter five, pair A odours were ethyl butyrate and pentanal. Odours used on other discrimination tasks in all other chapters were randomly assigned from eugenol, 1, 4-cineol, valeric acid, limonene, n-amyl acetate or heptanone. No odour was ever re-assigned to a different pair or reward valency in the course of training an animal. All odours were >97 % purity (Sigma-Aldrich, UK) and all concentrations were diluted volume/volume in mineral oil (Sigma-Aldrich, UK).

2.3. Olfactometers

Olfactometers, based loosely on previous reports (N. Bodyak and B. Slotnick, 1999; N. M. Abraham et al., 2004), (components from Knosys Inc. Fl, USA)

consisted of a Perspex chamber with a sampling port at one end containing an odour outlet and a water dispenser **(Figure 2.1A)**. The water dispenser was gravity fed and gated by a solenoid valve (Biochem Valve inc.). Water-dispenser valve opening times and tube diameter determined the size of the water reward delivered. Valve opening time was calibrated at the start of each pre-training session to dispense 4 - 7 l per opening. Odours were evacuated by an extraction fan at the opposite end of the chamber and by a vent in the sampling port, also attached to an extractor fan.

The odour outlet was supplied by a common channel in turn linked by flexible tubing (Cole Parmer, UK) to eight odour lines, each connected to a 100 ml bottle containing odours dissolved in mineral oil vehicle. System pressure was provided by charcoal-filtered air driven by a pump (APS 300, Tetratec, UK). Solenoid “pinch” valves (ASCO scientific, Inc, USA) gated airflow through each odour channel. Passive one-way check valves (Aquatic design centre, UK) prevented odours flowing back into common lines when pinch valves were open. **(Figure 2.1A)**. In experiments in chapter three, a final valve gated the common line. Odour vapour was allowed to accumulate in the common line, enabling rapid discharge once the final valve was opened. In experiments in chapter five, where different odour concentrations were used, odour lines were kept separate to avoid contamination that can occur when using converging odour lines (B. M. Slotnick and B. J. Nigrosh, 1974). Before the onset of each trial, individual odour lines were aligned to the sampling port by a custom-built rotating turret (**Figure 2.1B** and see **Appendix A**).

Mice initiated *behavioural trials* by placing their heads in the odour sampling

port, interrupting an infra-red (IR) beam. Licking at the water dispenser in the sampling port completed an electrical circuit between the dispenser and a ground plate on the floor of the chamber **(Figure 2.1A)**. This enabled licking behaviour to be monitored (N. Bodyak and B. Slotnick, 1999; N. M. Abraham et al., 2004). The apparatus was controlled and outputs were monitored using custom-built Labview software connected to an analogue-digital/digital-analogue converter (NI USB-6229, Legacy USB DAQ Device, National Instruments). A switch soldered into the valve control circuit board allowed the experimenter to give water rewards manually, independent of the computer software. Odour valves (ASCO Valve, inc) used were alternated every 20 blocks to ensure valve noises or other cues such as minor differences in odour line pressure did not facilitate learning (X. C. Lu et al., 1993; B. Slotnick and N. Bodyak, 2002). Odours were replaced every 20 blocks to ensure no significant run down of concentration over trials occurred.

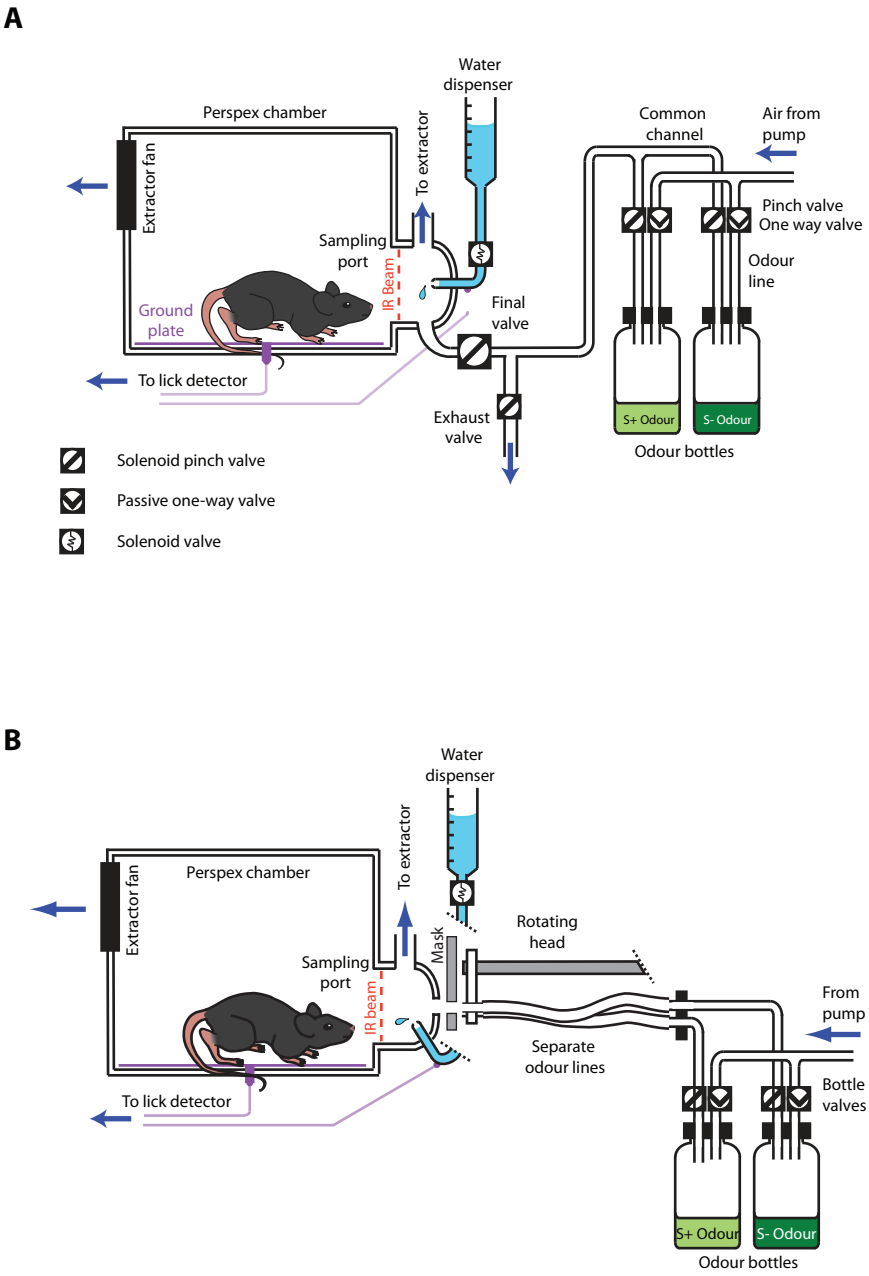

Figure 2.1. Olfactometers

A. Diagram of olfactometer highlighting the Perspex chamber, odour sampling port, odour extraction ports, water dispenser and ground plate.

B. Diagram of olfactometer highlighting the rotating odour turret. Odour lines were rotated by the turret to align them with a hole in the sampling port

(see **Appendix** for more details).

2.4. Behavioural training

In operant conditioning protocols, training procedures began 48 hours after onset of water restriction. During water restriction, mice were allowed access to water for at least five minutes daily, regardless of the number of trials they had completed. They were weighed twice daily and no animal was allowed to drop below 90% of the body weight of age-matched, non-water restricted controls. Changes in noise and light were kept to a minimum. Mice lack the longer wavelength "L" photoreceptor cone and cannot detect red light (P. M. Smallwood et al., 2003), so behavioural rooms were lit with red light when necessary.

2.4.1. Pre-training

Familiarisation

After 48 hours of water restriction, mice were taken from holding cages and placed in the Perspex chamber of the olfactometer. A few water rewards were manually released from the water dispenser to demonstrate the source of water to the naïve animal. Licking responses were measured starting 80ms after IR beam interruption over 1400ms (the '*lick window*'), split into four 350ms bins (**Figure 2.2A**). A behavioural trial was considered the period from onset of IR beam interruption until the lick window expired. Initially, mice received a water reward immediately upon licking at the water dispenser for any portion of the lick window. Over the first few tens of trials, licking criteria were gradually increased until a reward was given only if licking occurred in three or more of the time bins. The inter-trial interval (ITI) was 1s. If the IR beam remained interrupted after a trial was completed, a new trial was automatically initiated.

This training phase served to familiarise mice with the olfactometer environment and ensured they associated licking at the water dispenser for three or more of the four time-window bins with reward. Mice were moved to the next training phase after completing approximately 100 such trials.

Pre-training i

In this training phase, mineral oil vapour was discharged into the sampling port after IR beam interruption for the duration of the lick window. This phase required that the animal associate placing its head in the sampling port with the onset of the carrier stream and that it associate licking for three or more bins during the carrier stream with receiving a water reward. Mice were moved to the next training phase after completing approximately 100 such trials.

Pre-training ii

In this phase, after the IR beam was interrupted, an odour (S+) was delivered from the odour port for the same duration as the lick window and licking at the water dispenser for three or more time bins during odour presentation resulted in delivery of a water reward. The ITI was gradually increased during this phase to 3.5 s - the ITI used in the final discrimination-training paradigm. This phase required the animal to learn to associate licking for three or more bins during presentation of the S+ odour with receipt of a reward. Mice were moved to the next training phase after completing approximately 100 such trials. NB: Mice in chapter three were trained without the pre-training II phase, progressing straight from pre-training i to discrimination training.

2.4.2. Discrimination training

This training phase introduced animals to the discrimination test, and required them to learn that licking for three or more bins during presentation of the S+ odour would result in reward, while licking during the S- odour would not be rewarded.

IR beam interruption triggered presentation of either an S+ (reward coupled) or S- (unrewarded) odour. Lick patterns were recorded for the duration of the stimulus across four 350ms time bins **(Figure 2.2A, top)**. Responses were deemed correct if the mouse licked for three or more time bins during presentation of the S+ odour, or if they licked for two or fewer time bins during the S- odour. Eight to 12 S+ and 12 to eight S- odour trials were presented in a pseudo-random order in blocks of 20 trials. Percentage of correct responses for S+ and S- trials was averaged over 20 trials, giving an overall percentage for each block **(Figure 2.2A, bottom**). Typically, after 200 - 400 trials (10 - 20 blocks), mice learned to withhold licking when the S- odour was presented (**Figure 2.2B**). In cases where mice consistently licked erroneously during the S- odour, ITI could be increased. Alternatively, trials could be triggered only if the IR beam was first resealed, i.e. the mouse had to withdraw its head from the sampling port after each trial. The animal was classed as discriminating correctly (reaching *criterion*) when it performed at ≥ 80 % accuracy for five consecutive blocks **(Figure 2.2B**). On average mice performed approximately 20 blocks per day. Distribution of odour-reward coupling was counterbalanced between animals. This was achieved by alternating attribution of reward to a given odour with increasing animal ID number. Thus in an odour pair consisting of odour X and odour Y, mouse 1 was assigned odour X as S+ and odour Y as

S-, mouse two was assigned, odour X as S-, odour Y as S+, mouse 3 was assigned odour X as S+ and odour Y as S-, and so on.

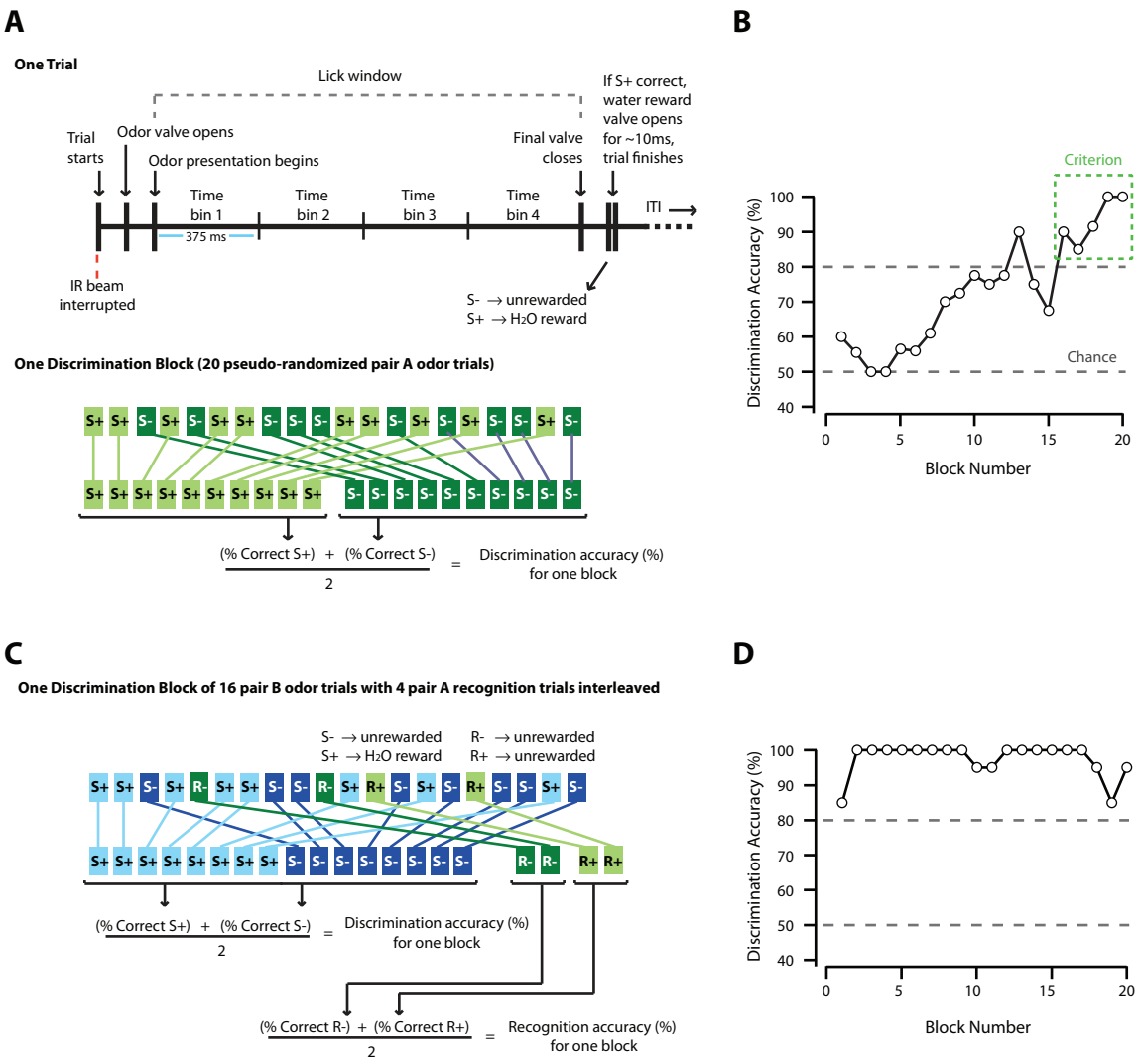

Figure 2.2. Behavioural Paradigms

A. Odour discrimination task. Top, Behavioural trial schematic. When a mouse interrupted the infra-red (IR) beam, a trial was initiated, odours were released from the sampling port and the lick window began. If the mouse licked during three or more of the time bins in the lick window during presentation of the S+ odour, the reward valve opened briefly, releasing a 4 – 7 ul water droplet. Bottom, twenty trials constituting between eight to 12 S+ and 12 to eight S- trials were presented in a pseudorandom order, constituting one block. S+ and S- trials for one block were first averaged separately to give both an S+ and an S- score, before being averaged together to give an overall percentage score for the block.

B. Example discrimination score for one mouse on first exposure to the discrimination task. After around 200 - 400 trials, mice learned to lick during presentation of the S+ odour and withhold licking or remove their head from the sampling port entirely during the S- odour. In this example, criterion - the first block when the average score for 5 consecutive blocks was ≥ 80 % - was reached on the 16th block.

C. Odour recognition test. Two S+ (R+) and two S- (R-) recognition trials were interleaved between 16 S+/S- discrimination trials to form a block. Over five such blocks, 20 recognition trials were recorded and averaged to give an overall block percentage score for recognition. R+ trials were unrewarded.

D. Mice could learn to discriminate a novel odour pair within one block. Having reached criterion on a different odour pair, the mouse was exposed to a novel odour pair for the first time and scored 85 % on the first block.

2.4.3. Concentration training

Mice trained on a range of concentrations were first trained to discriminate pair A odours at a concentration of 1 % v/v. Next, pair A odours at lower concentrations were interleaved among higher concentrations forming pseudo-blocks constituting, e.g. five S+ trials of 0.01 % v/v, five S+ trials of 1 % v/v, five S- 0.01 % v/v trials and five S- 1 v/v % trials. Discrimination accuracy scores for two consecutive blocks were then averaged yielding full blocks (20 trials) of 10 S+ and 10 S- trials for both high (1 % v/v) and low (0.01 % v/v) odours. The same protocol was followed for blocks where the interleaved lower concentrations were 0.1 % and 0.25 % v/v (e.g. **Figures 5.5, 5.8,** chapter five). In total, mice were trained on 0.01 % v/v odours for 30 blocks, 0.1 % v/v odours for 20 blocks and 0.01 % for 20 blocks and 0.25 % v/v odours for seven blocks.

2.4.4. Recognition testing

Mice were trained to discriminate an odour pair (e.g. pair A) until they reached criterion and thereafter for a further 10-20 blocks. They were then trained to discriminate a second odour pair (e.g. pair B) comprising two novel odours. Once they had reached criterion on odour pair B, they were presented with a recognition test consisting of a further five blocks, each comprising 16 pair B odour trials (eight S+ and eight S-) pseudo-randomly interleaved with four pair A odour trials (i.e. recognition test odours; two unrewarded S+ and two S- trials) **(Figure 2.2C**). The recognition test S+ odour was unrewarded to ensure that mice could not rapidly re-learn to discriminate odour pair A (B. M. Slotnick and H. M. Katz, 1974) **(Figure 2.2D)**.

NB: Since none of the $ZnSO_{4\ HD}$-treated mice reached criterion after 30 blocks (600 trials) of pair C discrimination training and exhibited no odour-evoked intrinsic signals (**Figures 3.4, 4.3 - 4.5,** chapters three and four), they were assumed to be anosmic. In a small fraction of $ZnSO_{4\ LD}$-treated mice (2/19) the same phenotype was observed. These mice were therefore excluded from further analysis.

2.5. Chemical lesioning of the olfactory epithelium

Two days after recovery from intrinsic-signal imaging, animals were anaesthetised with isoflurane (Abbott Laboratories, UK) in an isolation chamber for 30 s and each naris was flushed with 3 μl of either NaCl (9 % w/v, 263 mOsm), or low $ZnSO_4$ ($ZnSO_{4\ LD}$, 8.4 % w/v $ZnSO_4$, 275 mOsm) using a micropipette (Gilson, USA). After regaining consciousness, animals were subjected to this procedure twice more, each time after 20 s of anaesthesia. Animals treated with the higher $ZnSO_4$ dosage ($ZnSO_{4\ HD}$) were subjected to another treatment within 24 hours of the first dose. All mice were allowed 12 hours to recover after the last treatment before returning to water restriction.

In all behavioural experiments, assignment of mice to different treatment groups was performed such that an equal number of mice had ethyl butyrate as the S+ odour as had pentanal as the S+ odour in each group. Animals were first separated into two groups; one where odour X was the S+ odour and one where odour Y was S+. Mice within each group were then alternately ascribed a treatment with ascending mouse ID number and the treatment the first animal was given was determined by coin toss. Thus, where treatment group sizes

were odd numbers, assignment of the larger number of S+ or S- to each group was random. This distribution of reward valence ensured that effects of treatment were not due to one odour being over-represented as the S+ or S- within a particular treatment group.

After nasal flush treatment, a colleague switched positions of holding cages and assigned mice different identities such that experiments were performed blind.

2.6. Intrinsic signal imaging

2.6.1. Surgical procedures

Animals were anaesthetised intra-peritoneally with 0.11 mg/g b.w. sodium pentobarbitone (Animalcare Ltd, UK) and placed in a stereotaxic frame. Lignocaine hydrochloride (2 % w/v, Hameln Pharmaceuticals, UK) was administered intradermally to prospective wound sites. The plantar withdrawal reflex and respiration rate were checked regularly and anaesthetic replenished accordingly. Body temperature was held at 36 – 37 º C with a rectal probe and feedback-controlled heating blanket (Watlow, USA). Mice were placed in a stereotaxic frame that could be rotated in all directions (translational, horizontal, vertical) and locked. It was designed to stabilise the head using ear and tooth bars while allowing access to the nose and OB (**Figure 2.3A**). Respiration rate was monitored continuously with a piezo-electric strap (World Precision Instruments, USA) placed under the thorax and was consistently between 0.8 - 2 respiration cycles/s. The scalp was shaved and cleaned using chlorhexidine gluconate (Hibitane, Scientific Laboratory Supplies, UK) in 70% ethanol. The skull over the OBs was exposed with a sagittal incision to the scalp. The bone over both OBs was scraped clean of connective tissue and then either thinned with a dental drill until surface blood vessels (**Figure 2.3B**) could be clearly resolved, or craniotomised.

2.6.2. Image acquisition

The dorsal surface of the bulbs was illuminated as evenly as possible, just below saturation point, using a light source (Hal 100 Zeiss, power source from

Kepco) with a changeable light filter and two flexible delivery arms. To reduce refractory scatter of reflected light caused by drying of the bone, 1 % w/v agar solution (Sigma, UK) was applied to the bulbs and covered with a glass coverslip (Menzel-Glazier, Germany). The stereotaxic frame was rotated until blood vessels on the dorsal surface of one OB were in the same plane of focus. Images were collected with a CCD camera (Adimec, Netherlands) and two AF DC Nikon lenses (Nikon, Japan) in conjunction with an Imager 3001 Lab interface (Optical Imaging Inc. USA) and VDAQ imaging software.

2.6.3. Chronic imaging in anaesthetised animals

Initially, a single image of the blood vessels in the dorsal surface of the OB **(Figure 2.3B)** was recorded using 546 nm (green) light. After this, the camera was focused 150 μm deeper, on the glomerular layer and intrinsic optical signals were recorded for a period of 14.4 s using 630 nm (red) illumination **(Figure 2.3C)**. Imaging trials were triggered from the respiration signal recorded by the piezo-electric strap, and detected using a window discriminator. Intrinsic signals were collected at a frame rate of 25 frames/s for a total of 14.4 s; 30 baseline frames (0 - 3.6 s), 50 stimulus frames (3.6 - 9.6 s), then a further 40 frames (9.6 - 14.4 s) **(Figure 2.3D)** meaning that the stimulus duration used for imaging experiments exceeded the odour sampling times of mice in the behavioral experiments. Individual imaging trials consisted of presentation of either ethyl butyrate or pentanal. An odour-evoked *activity map* contained 20 imaging trials (one block) for one odorant at one concentration that was averaged online. Two to three activity maps of each odour and each concentration were recorded in a given imaging session. After completion of

the first imaging session (session one), the bulbs were covered with Kwik-cast silicone elastomer (World Precision Instruments, USA), the scalp was sewn using non-dissolvable sutures (Ethicon, France) and lignocaine hydrochloride 2 % v/v (Hameln Pharmaceuticals, UK) was applied to the wound at regular intervals. Animals were then placed in a heated recovery chamber, given a dose of the non-steroidal anti-inflammatory drug carprofen (4 g/g body weight) and monitored until fully mobile. After nasal flush and in some cases, further behavioural experiments (seven to 12 days), the animal was re-anaesthetised, replaced in the stereotaxic frame, the skull was re-exposed, and the surface of the OB re-thinned. Surface blood vessel maps recorded in the first session were compared to live images of the blood vessels and used to realign the skull, ensuring that blood vessels were in the same focal plane as the first imaging session. Two or three activity maps for each odour at each concentration were then recorded (session two).

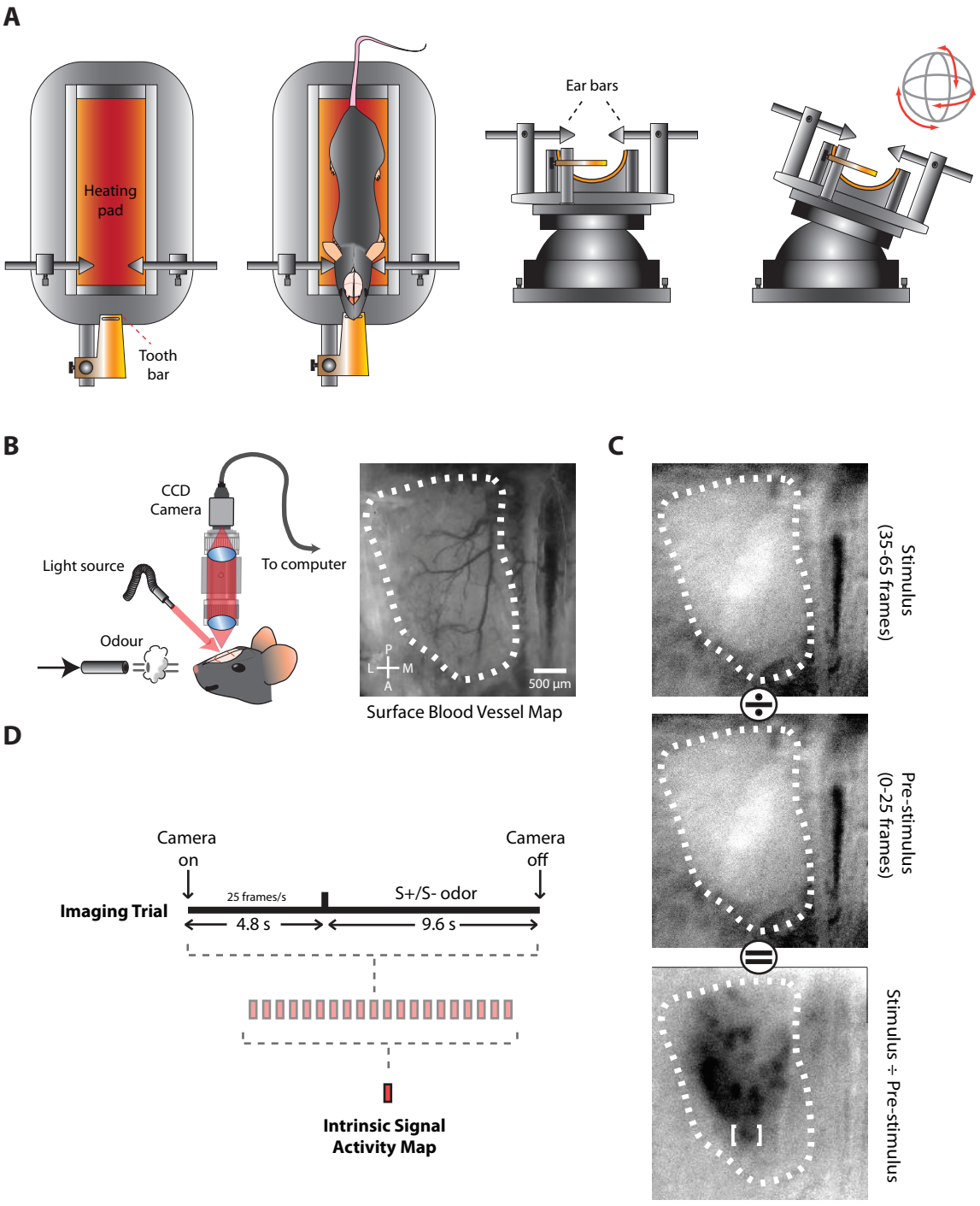

Figure 2.3. Intrinsic optical imaging of the dorsal olfactory bulb (OB)

A. Stereotaxic frame. The stereotaxic frame, bird's eye (left) and front view (right), could be rotated in all directions (translational, horizontal, vertical) and locked. It was designed to stabilise the head using ear and tooth bars while allowing access to the nose and OB.

B. Imaging setup (left) and OB dorsal aspect showing a typical surface blood vessel map (right). Dotted line outlines the thinned region of bone.

C. Red (707 nm) wavelength light reflected from the exposed dorsal surface of the OB was collected before and during odour stimulus presentation. Ratio of during and pre-stimulus images revealed a decrease in absorbance correlated with activity in individual glomeruli (white bracket). This representative example was evoked by 1 % v/v pentanal.

D. Schematic of imaging protocol. Twenty imaging trials (pale red oblongs) were averaged to generate an activity map (red oblong).

2.7. Data analysis

2.7.1. Image alignment and quantification

Images were first converted by averaging 2 x 2 pixels into single bins using the WinMix BlockConverter program (Optical Imaging Ltd, USA). Next, using software custom written in Matlab (Mathworks, USA) and Labview (National Instruments), those frames recorded during stimulus presentation (frames 35 – 65) were divided by the average of pre-stimulus baseline frames (0 - 25), providing image stacks that revealed odour-evoked changes in light reflection **(Figure 2.3C)**, that have been shown to correlate with increases in glomerular activity in the OB (B. D. Rubin and L. C. Katz, 1999; M. Meister and T. Bonhoeffer, 2001; H. Gurden et al., 2006). Image stacks from all activity maps were aligned to the first map recorded in session one using software custom written in Matlab (Mathworks, USA) and Labview (NI) **(Figure 2.4A)**.

Using ImageJ (NIH, Bethesda), circular regions of interest (ROIs) 75 m in diameter (M. Meister and T. Bonhoeffer, 2001, **Figure 2.4B**) were positioned over areas with odour-evoked signal in the first activity map recorded in session one evoked by presentation of 1 % v/v odours. The same set of ROIs was imposed upon aligned images from all activity maps of all sessions and concentrations for a particular odour and for a particular OB **(Figure 2.4B)**. For each image frame, all pixel intensity values were normalised by dividing them by the average pixel intensity of the whole image. The mean normalised pixel value of each ROI was then determined and averaged over 40 stimulus frames (frames 10-50 after odour onset) and subtracted from 1.

2.7.2. Intrinsic signal map correlations and change in relative intensity calculation

Pixel intensity values for each ROI were correlated with the concomitant ROI recorded in other activity maps recorded in the same bulb. All ROI correlations for a given activity map were then averaged, yielding an r- value for each activity map comparison. Across-session correlations were subtracted from within-session correlations, yielding a dissimilarity score whereby high scores indicate large differences between session one and session two odour-evoked activity maps **(Figure 2.4C)**. Dissimilarity scores from intrinsic signals were then averaged across both odours recorded to give average scores for each animal. In some cases, only activity from one odour was recorded, or it was not possible to record signals in both bulbs, either because no signal was evoked in the first session, or because pigment in the dura prevented it being recorded. Thus both the number of animals and activity maps recorded are quoted. For determining relative ROI intensities, activity maps that had within session correlation coefficient r values lower than 0.5 and ROIs whose normalised average pixel intensity did not on average drop below 0.9990 during odour presentation in both sessions one and two, were removed to ensure that only those ROIs that contained signal in both session were included in analysis. After thresholding, intensity values of each ROI were averaged across blocks and then ranked. Session two ROIs were ordered according to their rank in session one. ROI intensity values for session one and two were then normalised to 1 and session two values were subtracted from session one values to determine the extent of change in relative ROI intensity across

sessions for the whole activity map. Subtraction values for all ROIs were then compiled and the population statistics determined. A higher variance of subtraction values indicated a higher change in relative intensity.

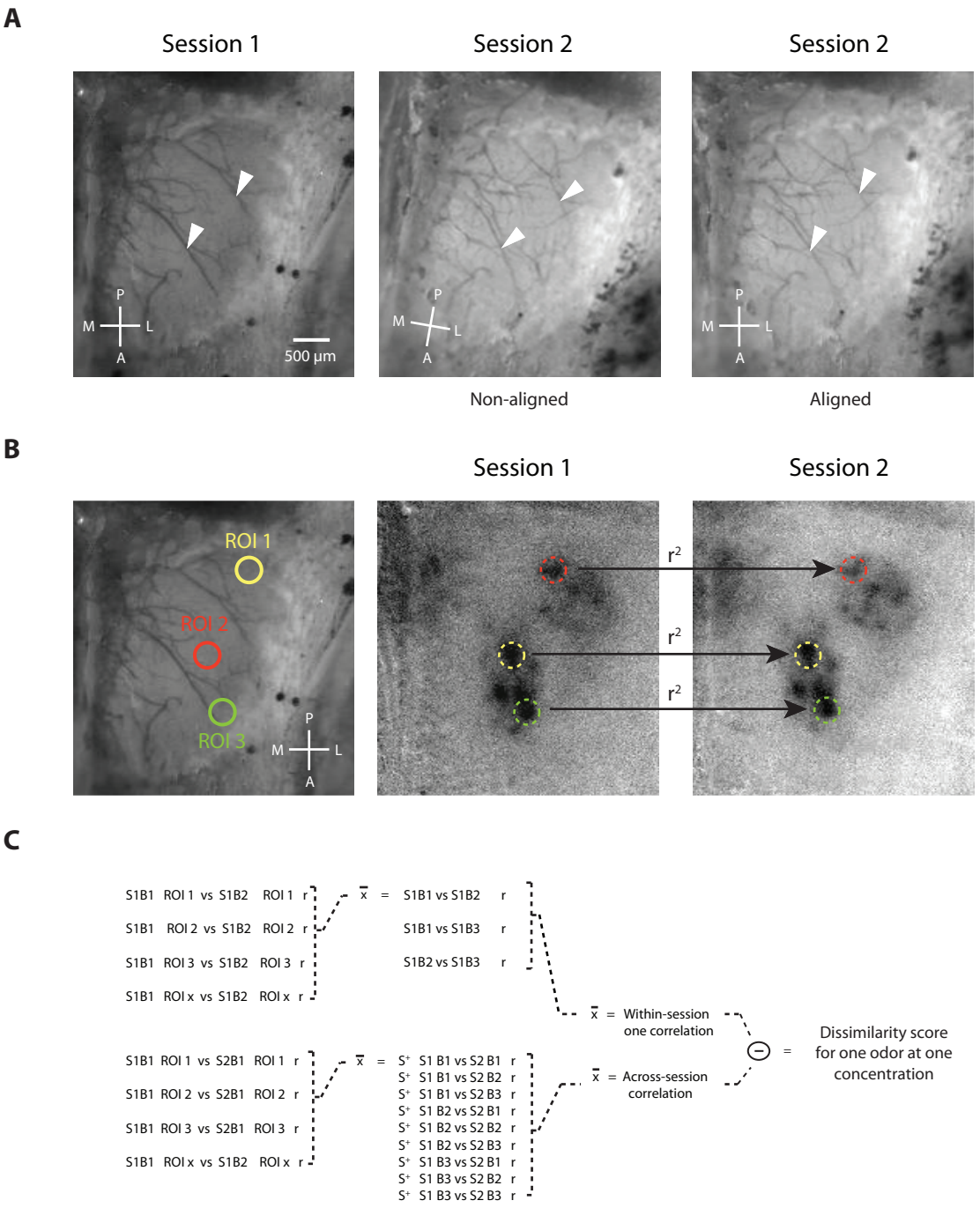

Figure 2.4. Image alignment, region of interest (ROI) selection and correlation
A. Blood vessel maps for all blocks were aligned to the blood vessel map of the first imaging block of session one, evoked by odours of 1 % v/v. Branches in major blood vessels common to all blood vessel maps were used to manually align all blocks to this first block. As each blood vessel map in a block was spatially locked to an intrinsic-signal map, intrinsic images from both session one and session two were consequently aligned with each other.
B. ROIs were selected, again using the first imaging block of session one, evoked by odours of 1 % v/v. Three example ROIs are shown (yellow, red and green circles). Once chosen, ROI templates were imposed upon all intrinsic image blocks for a given animal, for a particular odour. A different set of ROIs was used for each odour imaged.
C. Calculation of dissimilarity score. Within-session correlation refers to correlation between e.g. session one (S1) image blocks (B1,2,3…), while across-session correlation refers to correlation between image blocks recorded in session one and two.

2.8. Statistical Tests

Discrimination, recognition and dissimilarity scores are expressed as the standard error of the mean. ROI intensity subtraction values were compared using Ansari Bradley tests after subtracting medians. Behavioural tests were compared using student's t-tests or one-way ANOVA. Dissimilarity scores were compared using Mann Whitney U tests.

Chapter Three: The effects of $ZnSO_4$ nasal irrigation on odour discrimination and recognition

3.1. Introduction

Partial lesions of the olfactory epithelium or bulb have been suggested to have little impact on behavioural correlates of odour perception in rodents (B. Slotnick et al., 2000; B. Slotnick and N. Bodyak, 2002; B. Slotnick and S. Bisulco, 2003). Lesions targeted to areas of the bulb evoked by highly similar odours do not cause deficits in discrimination of those odours (K. McBride and B. Slotnick, 2006) and even fully bulbectomised rats can learn to discriminate between simple odours when regenerating ORNs from the olfactory epithelium innervate the frontal neocortex or anterior olfactory nucleus (B. Slotnick et al., 2004). The prevailing conclusion of such studies is that much of the bulbar circuitry is redundant and may be removed with little functional consequence for odour perception (B. Slotnick and N. Bodyak, 2002; B. Slotnick et al., 2004; K. McBride and B. Slotnick, 2006). This is ostensibly at odds with functional imaging data which shows that even simple monomolecular odorants evoke complex and unique spatiotemporal activation sequences of glomeruli (R. W. Friedrich and S. I. Korsching, 1997; B. A. Johnson et al., 1999; B. D. Rubin and L. C. Katz, 1999; B. A. Johnson and M. Leon, 2000; C. Linster et al., 2001b; B. D. Rubin and L. C. Katz, 2001; M. Wachowiak and L. B. Cohen, 2001; H. Spors and A. Grinvald, 2002; M. J. Lehmkuhle et al., 2003; M. Wachowiak and L. B.

Cohen, 2003; J. P. McGann et al., 2006; H. Spors et al., 2006; B. A. Johnson and M. Leon, 2007; B. A. Johnson et al., 2007; A. T. Schaefer and T. W. Margrie, 2007).

However, studies that probe only odour detection or discrimination may not be sensitive to subtler changes in olfactory perception. Of the studies that probed odour recognition – which allows odour quality perception to be tested - one observed moderate deficits in odour recognition after large lesions of the OB (S. Bisulco and B. Slotnick, 2003) and the other observed moderate deficits when the OE but not the OB was lesioned (B. Slotnick and N. Bodyak, 2002). The latter study drew conclusions about deficits after OE lesions based on the performance of individual animals and histological analysis that could not confirm if lesions specifically affected odour-evoked activity (B. Slotnick and N. Bodyak, 2002). Thus, the issue of redundancy was re-examined using larger data sets and a detailed analysis of olfactory discrimination and recognition both before and after epithelial lesion with $ZnSO_4$.

3.2. Results

To investigate the impact of lesioning olfactory input on odour-quality perception, the behavioural consequences of flushing the nasal epithelium of mice with zinc sulphate ($ZnSO_4$) were first examined. The ability of mice to discriminate and recognise odours was probed using a go/no-go paradigm (B. Slotnick and N. Bodyak, 2002; N. M. Abraham et al., 2004; D. R. Shimshek et al., 2005) **(Figure 3.1**, and **Figure 2.1, Materials and Methods)**.

After habituation and pre-training (see **Materials and Methods**), mice were trained to discriminate between a pair of odours (pair A, e.g. amyl acetate vs. cineol; pair A discrimination task, 1 % v/v, **Figure 3.2A, B**) in which one odour (S+) was rewarded and the other (S-) was unrewarded. The performance accuracy for discrimination of an odour pair was then calculated from the average responses to S+ and S- trials reported by licking at a water port (see **Figure 2.1, Materials and Methods**). Mice were deemed to discriminate accurately once they reached 'criterion' i.e. performing 80 % accuracy for five consecutive blocks, each block containing twenty trials (consisting of eight to twelve S+ and twelve to eight S- trials per block). This took typically 30 - 50 blocks (600 - 1000 trials) to learn. Mice were trained for a further 60 blocks after reaching criterion. This took approximately 10 days in total. After this, they were trained on a second odour pair (pair B odours, ethyl butyrate versus pentanal) until reaching criterion. This typically took fewer than 10 blocks **Figure 3.2C, D**). Next, to ensure mice could recall previously presented odours, four pair A odour recognition trials were interleaved with sixteen pair B odour discrimination trials (see **Materials and Methods**). Mice were tested for

recognition using an extinction paradigm (to prevent rapid relearning of odours (N. Bodyak and B. Slotnick, 1999), i.e. with the S+ stimulus carrying no water reward. Pair A recognition scores were not significantly different from the average of the last five blocks of pair A discrimination (pair A discrimination, 93.97 ± 0.67 % vs. recognition 92.23 % ± 1.89, $p > 0.19$, n = 14 mice, **Figure 3.3A, B**), demonstrating that mice could perform as well on recognition tests as on discrimination tasks.

After pair A recognition testing, mice were given full access to water for 24 hours, then anaesthetised with sodium Pentobarbitone while odour-evoked intrinsic signals were recorded from the dorsal surface of the OB (B. D. Rubin and L. C. Katz, 1999; M. Wachowiak and L. B. Cohen, 2001; H. Gurden et al., 2006) **(**see **Materials and Methods** and **chapter four)**. After recovery from surgery, mice were briefly re-anaesthetised with isoflurane and given a nasal flush treatment with either 0.9 % w/v NaCl (sham), with a 'low dose' of $ZnSO_4$ (three nasal flushes of 8.4 % w/v $ZnSO_4$ per naris, ***$ZnSO_{4\ LD}$***) or a 'high dose' (2 x three nasal flushes per naris of 8.4 % w/v $ZnSO_4$, ***$ZnSO_{4\ HD}$***) (see **Materials and Methods**). Following a 24-hour recovery period and a further 48 hours of water restriction, mice were trained on a new odour pair (pair C) for 30 blocks (600 trials) **(Figure 3.4A, B)**. None of the $ZnSO_{4\ HD}$-treated mice reached criterion during the 30 blocks tested and neither did they perform significantly better than chance during this time (chi^2 test significance from 50 % for all 30 blocks, 49.93 ± 0.69 %, n = 5 mice, $p > 0.82$, for last five blocks, 49.66 ± 1.31 %, $p > 0.26$, **Figure 3.4A3, B**). As sham-treated mice often started discrimination training of a novel odour pair with discrimination scores around

chance, differences in learning curves were usually only apparent after a few blocks of training (**Figure 3.4).** Thus, discrimination scores were compared after the sham group had on average reached criterion. On average, discrimination scores for the first five blocks after shams had reached criterion were significantly poorer in $ZnSO_{4\ LD}$-treated mice than in shams (ANOVA, $F(1,63) = 17.72$, $P < 0.0001$, **Figure 3.4**).

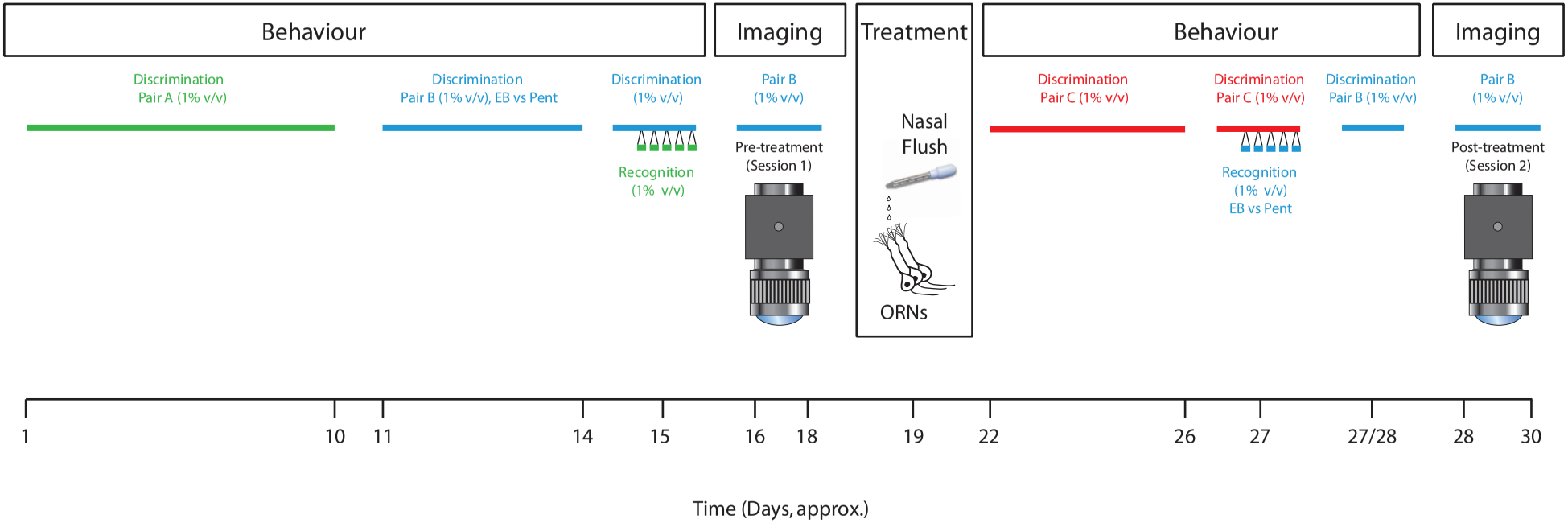

Figure 3.1. Behavioural and imaging protocol

Order of discrimination tasks and recognition tests with approximate timings is shown. Pair A odours (green bars) were amyl acetate, cineol or eugenol. Pair B odours (blue bars) were ethyl butyrate and pentanal. Pair C odours (red bars) were eugenol, limonene, valeric acid, heptanone and cineol. Camera lens shows when, in some cases, intrinsic optical signals evoked by ethyl butyrate (EB) and pentanal (Pent) were recorded.

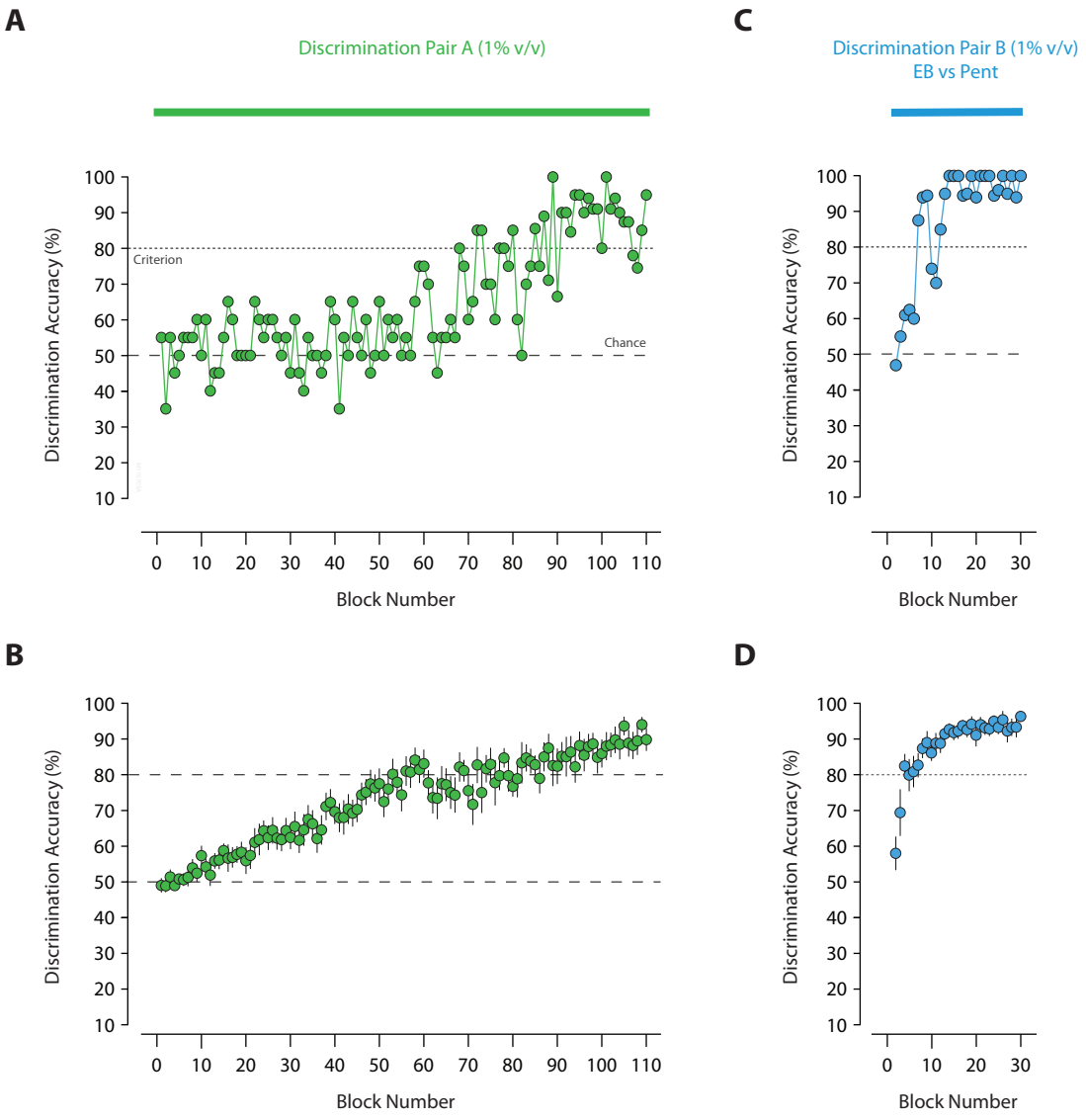

Figure 3.2. Discrimination learning of novel odours

A. Example discrimination scores from one mouse for all blocks of training on pair A odours (green circles).

B. Average discrimination scores for all blocks of pair A odours from all mice (n = 18).

C. Example discrimination scores from one mouse for all blocks of training on pair B odours (blue circles).

D. Average discrimination scores for all blocks of pair B odours from all mice (n = 18).

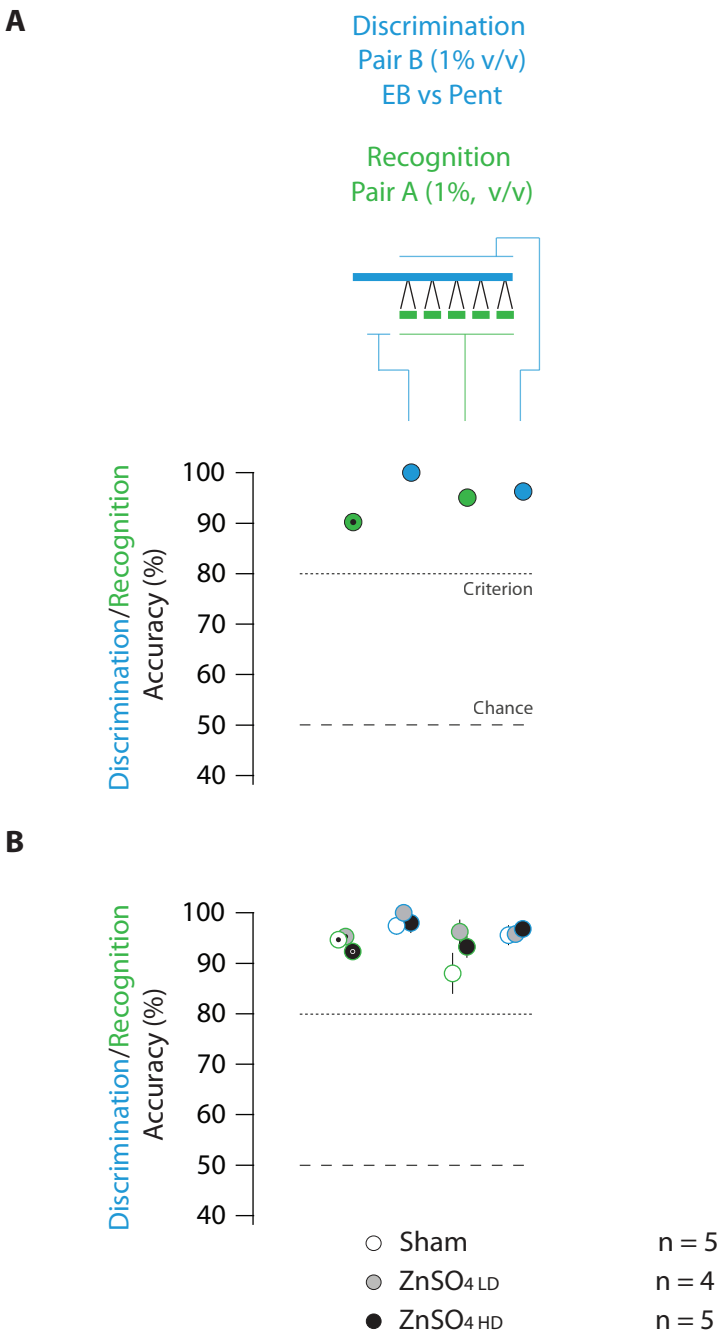

Figure 3.3. Pretreatment odour recognition

A. Example scores obtained from one mouse for recognition of previously experienced pair A odours (green circle, right). Also plotted are the discrimination scores for the average of the last five blocks of pair A odours (dotted green circle, left), discrimination scores for pair B odours for the block of trials immediately prior to (blue circle, left) and those trials presented during recognition testing (blue circle, right), all indicated by thin green and blue lines.

B. As above with averages for mice grouped according to treatment they were later given i.e. sham (open circles), $ZnSO_4$ LD (grey-filled circles) and $ZnSO_4$ HD (black-filled circles).

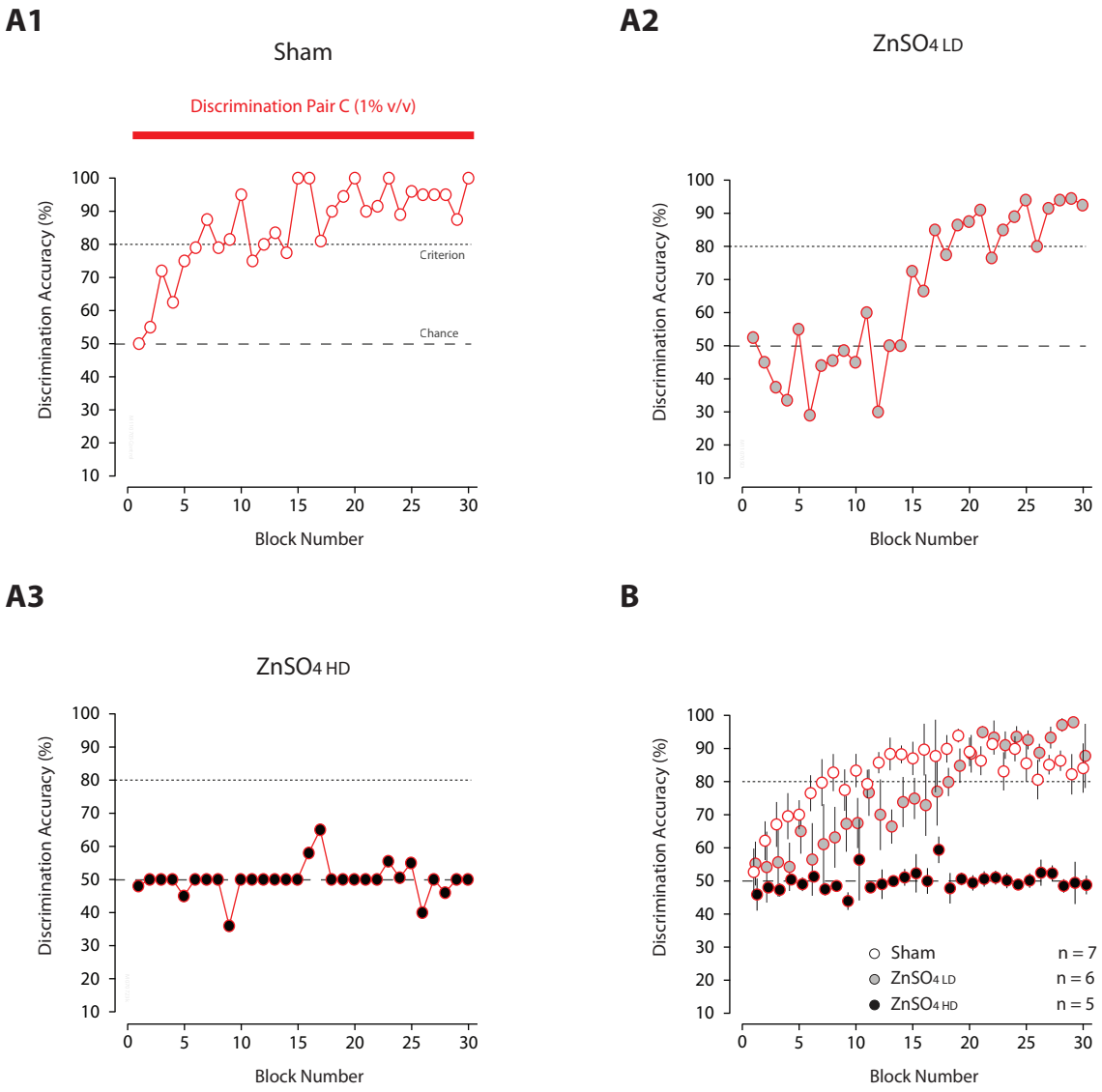

Figure 3.4. Learning of novel odours was impaired by $ZnSO_4$ treatment

A. Example discrimination scores obtained after nasal flush treatment for all 30 blocks of training on novel pair C odours for sham (**A1**, open circles), $ZnSO_4$ LD-treated (**A2**, grey-filled circles) and $ZnSO_4$ HD-treated mice (**A3**, black-filled circles).

B. Average discrimination scores obtained for all 30 blocks of training on novel pair C odours for sham (open circles) low dose $ZnSO_4$ LD-treated (grey-filled circles) and $ZnSO_4$ HD-treated mice (black-filled circles).

After reaching criterion, pair C discrimination scores for $ZnSO_{4\ LD}$-treated mice were not significantly different from shams (ANOVA for first five blocks after shams reached criterion, $F(1,63) = 0.00007$, $P > 0.994$, **Figure 3.4B**). Mice were then tested for recognition of pair B odours. $ZnSO_{4\ HD}$-treated mice continued to perform pair C odour discrimination at chance levels. Recognition scores for pair B odours were not significantly different from chance and were significantly poorer than their own pre-treatment pair B discrimination scores, or those of shams and $ZnSO_{4\ LD}$-treated mice (53.00 ± 1.22 %, n = 5 mice, vs. shams, $p < 0.0001$, vs. $ZnSO_{4\ LD}$-treated, $p < 0.013$ **Figure 3.5A, B**). Despite their accurate discrimination of pair C odours, $ZnSO_{4\ LD}$-treated animals returned sub- criterion recognition scores that were on average significantly lower than shams (shams, 85.7 ± 2.97 %, n = 7, $ZnSO_{4\ LD}$, 70 ± 5.47 %, n = 6, $p < 0.02$, **Figure 3.5A, B).** N.b. Four of the mice included in post treatment pair B recognition tests did not receive pair A recognition tests before nasal flush although all other training was identical. Of these mice, two were ascribed to sham and two to $ZnSO_{4\ LD}$-treatment groups.

Poor recognition of pair B odours was not due to rapid extinction in $ZnSO_{4\ LD}$-treated mice, because the first trials of pair B odour recognition were already significantly lower in $ZnSO_{4\ LD}$-treated mice compared to shams **(**first block, sham, 87,5 ± 5.05 %, n = 7 vs. $ZnSO_{4\ LD}$-treated 70.83 ± 7.68 %, n = 6, $p < 0.04$, **Figure 3.6**).

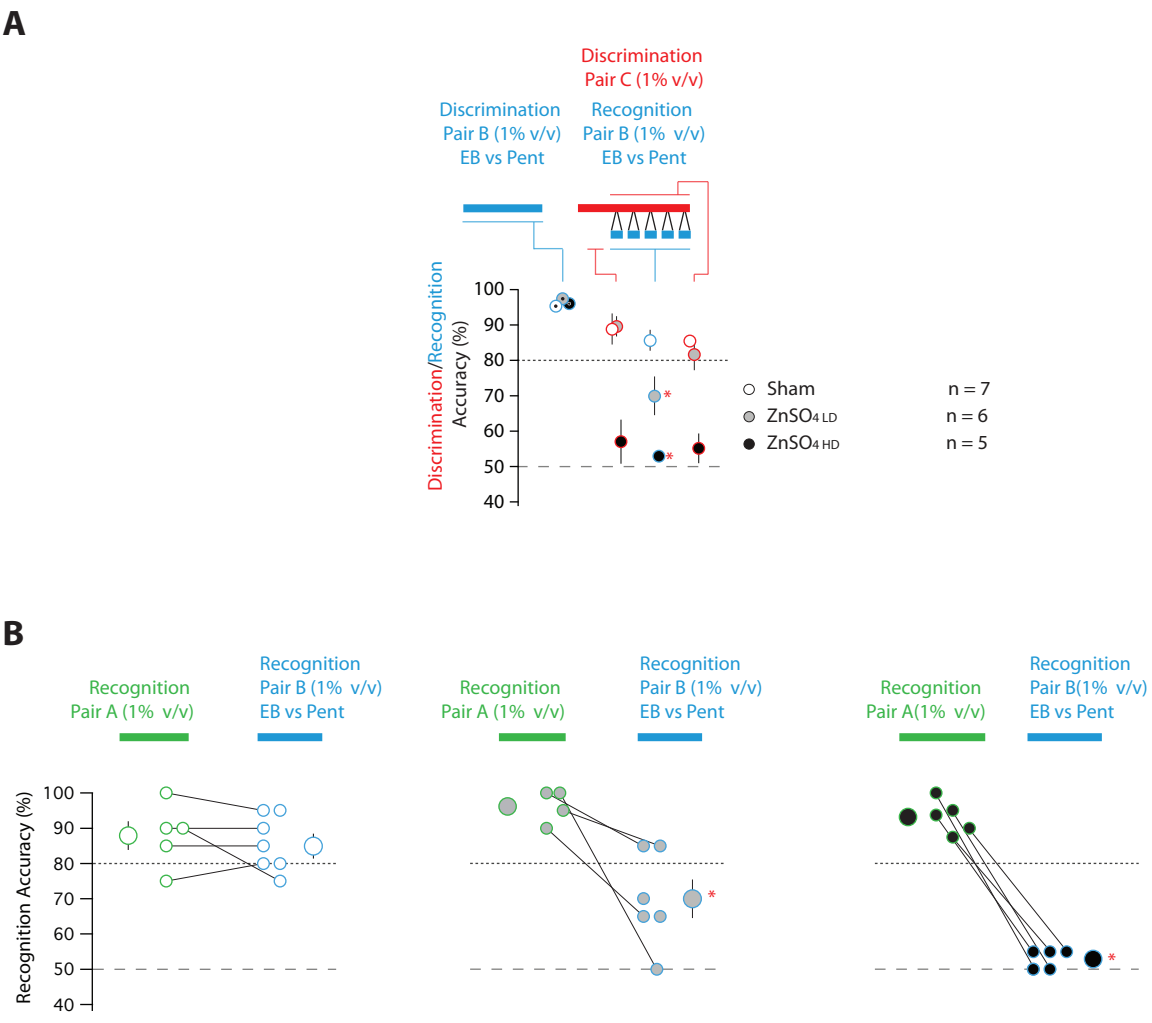

Figure 3.5. Recognition of familiar odours was impaired by $ZnSO_4$ treatment

A. Average recognition scores obtained for familiar pair B odours (blue circles, right). The discrimination scores for the average of the last five blocks of pair B odours (blue circles, left), for pair C odours from the block of trials immediately prior to (red circles, left) and those trials presented during recognition testing (red circles, right), all indicated by thin blue and red lines are also plotted. Sham (open circles) $ZnSO_4$ LD (grey filled circles), and $ZnSO_4$ HD-treated mice (black-filled circles).

B. Individual recognition scores for pair A odours before (green circles) and pair B odours after treatment (blue circles). Large circles are averages. Left, sham (open circles), middle, $ZnSO_4$ LD-treated animals (grey filled circles), right, $ZnSO_4$ HD-treated mice (black-filled circles).

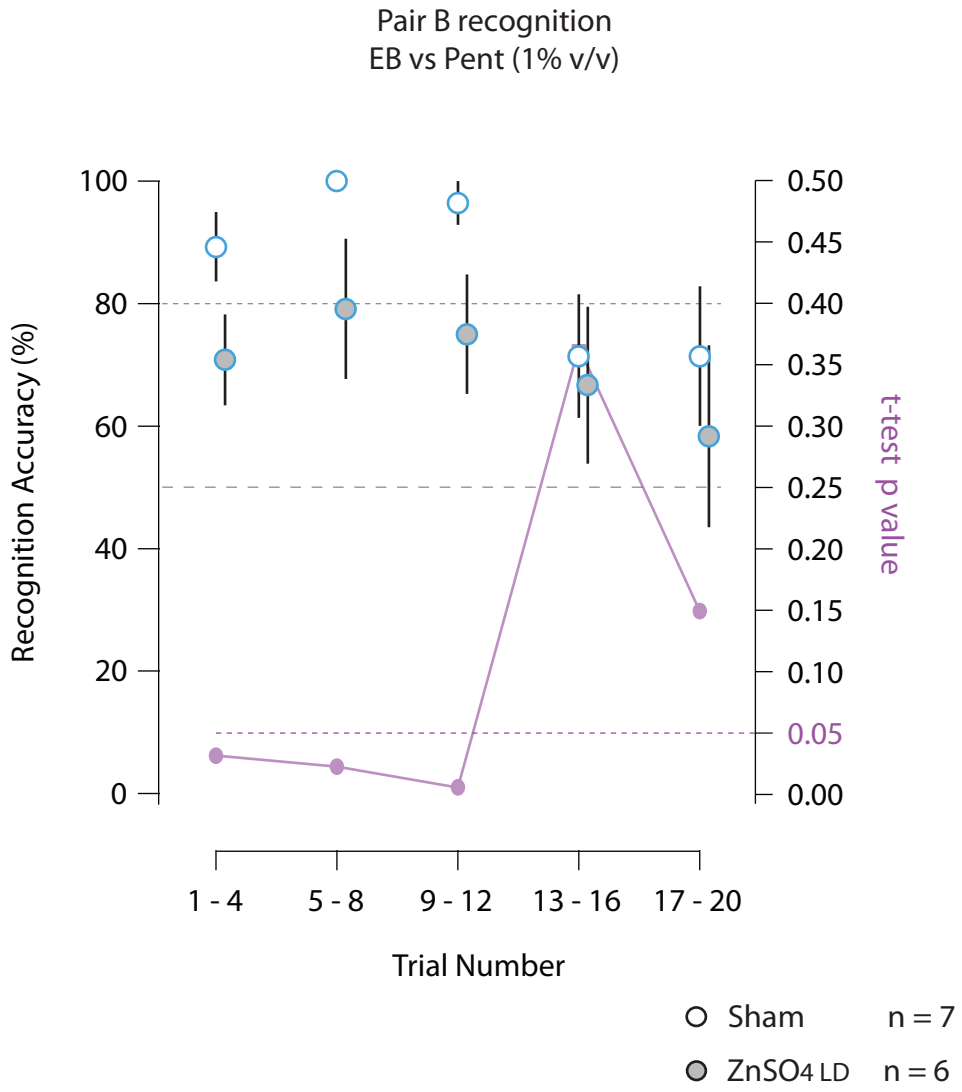

Figure 3.6. Recognition deficit in ZnSO4 LD treated mice was not due to extinction
Odour recognition scores for ethyl butyrate and pentanal for sham (open circles) and ZnSO4 LD-treated mice (grey filled circles). Recognition "mini" blocks consist of two ethyl butyrate and two pentanal trials, indicated by trial number. Purple circles indicate p values for t-tests between shams and ZnSO4 LD-treated groups for each mini block.

This suggests that reduced pair B recognition scores were caused by $ZnSO_{4\ LD}$-treated mice failing to recognise odours from the start of the test period, as opposed to initially recognizing odours, but dissociating them from the reward state more rapidly than shams (D. R. Shimshek et al., 2005). There was no correlation between pair B recognition scores and number of blocks needed to reach criterion on pair C odours (r^2 = 0. 473, n = 5, p > 0.1, **Figure 3.7**) such that some mice with low recognition scores reached criterion in as few blocks as shams while others with high recognition scores required more trials to learn to discriminate pair C odours.

Following recognition testing, mice were retrained on pair B odours (with the S+ odour rewarded again) to ensure that the $ZnSO_{4\ LD}$-treated group could detect previously experienced yet no longer recognised pair B odours. Although $ZnSO_{4\ LD}$-treated mice initially performed significantly worse than shams (first block, sham 87 ± 2.45 %, n = 7 mice vs. $ZnSO_{4\ LD}$-treated, 71.25 ± 6.06 %, n = 6 mice, p < 0.01), they reached criterion on pair B odours within two blocks of retraining (second block, sham, 92.86 ± 3.25 %, n = 7 mice vs. $ZnSO_{4\ LD}$-treated, 92.5 ± 2.92 %, n = 6 mice, p > 0.46, **Figure 3.8A1, A2 & B),** indicating that they could detect and discriminate the previously experienced pre-treatment odours.

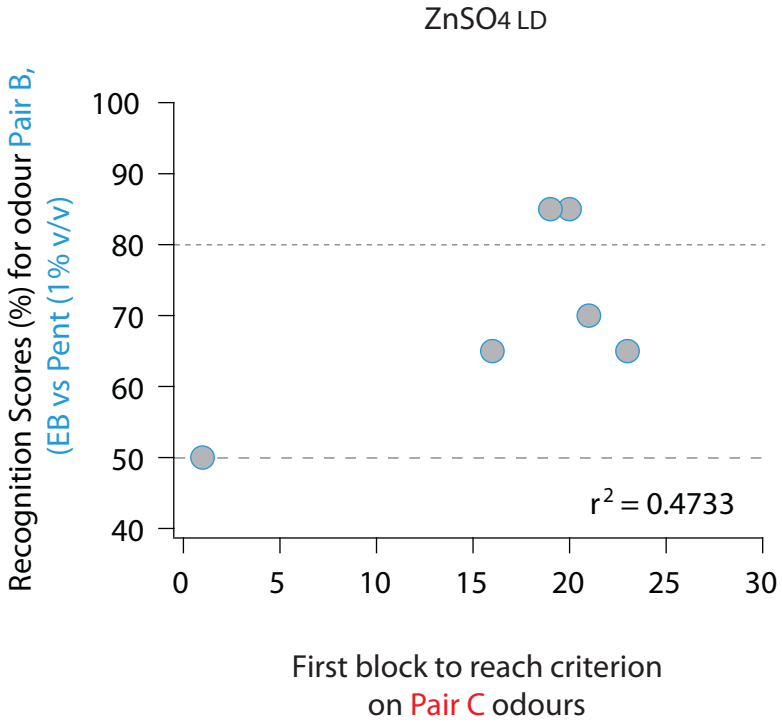

Figure 3.7. Recognition accuracy of a familiar odour was not correlated with number of blocks needed to learn to discriminate a novel odour

Plot showing correlation of pair B recognition score with the number blocks needed to reach criterion on pair C odours for $ZnSO_4$ LD-treated mice.

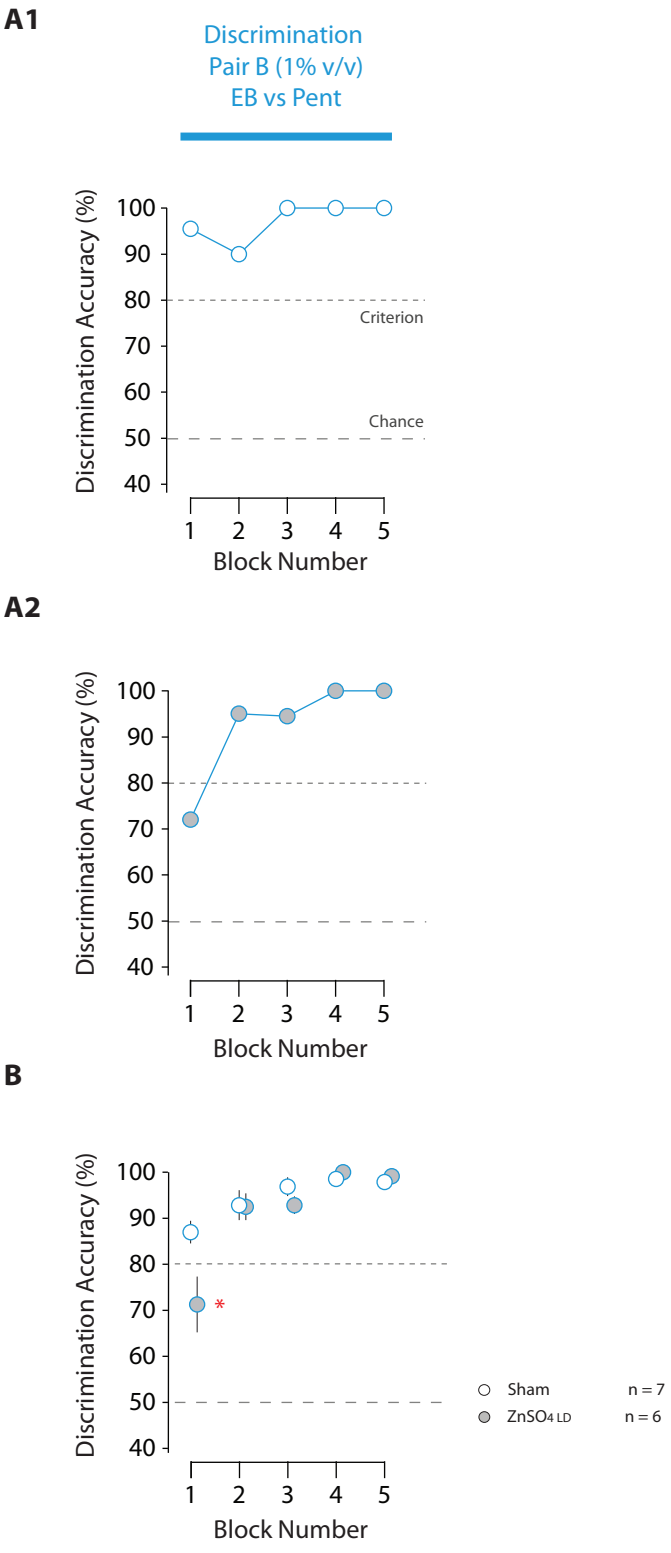

Figure 3.8. Discrimination of previously familiar odours was mildly impaired by $ZnSO_4$ LD treatment

A. Example discrimination scores for previously familiar pair B odours in sham (**A1**, open circles) and $ZnSO_4$ LD-treated mice (**A2**, grey-filled circles) presented after recognition testing. **B.** Average discrimination scores for previously familiar pair B odours in sham (open circles) and $ZnSO_4$ LD-treated mice (grey-filled circles) presented after recognition testing.

NB: After the previous data set was obtained, a rotating odour delivery device was used to improve the reliability of stimulus delivery and reduce contamination (see **Appendix)**. Also, where mice had previously been removed from the olfactometer when they stopped sampling for more than five minutes, they were removed if they failed to lick for three S+ in a row during discrimination training. This was due to natural investigative behaviours in non-motivated mice triggering false S+ responses (N. Bodyak and B. Slotnick, 1999) and accounts for the differences between the number of blocks needed to reach criterion on discrimination tasks in this section and the next.

3.3. Discussion

In summary, these results show that, before treatment, all mice could accurately discriminate and recognise odours in the context of the go/no-go behavioural paradigm. Sham treatment had no adverse effects on either discrimination or recognition of previously experienced odours. Nasal irrigation with $ZnSO_{4\ HD}$ prevented mice either from discriminating novel odours or from recognising previously experienced odours. $ZnSO_{4\ LD}$-treatment did not prevent highly accurate discrimination of novel odours but did impair the ability to learn to discriminate those odours. Furthermore, it caused impairments in both discrimination and recognition of previously experienced odours.

None of the mice treated with $ZnSO_{4\ HD}$ performed significantly differently from chance during either pair C discrimination training or pair B recognition testing, which suggests they were anosmic for these odours at the time of testing. This notion is supported by the absence of detectable odour-evoked signals on the dorsal surface of the OB in all (5/5) $ZnSO_{4\ HD}$-treated mice tested for recognition of pair B odours, determined either qualitatively or quantified using dissimilarity scores (see chapter four, figure 4.4).

Various volumes and concentrations of $ZnSO_4$ have previously been used to induce olfactory impairment. These range from 1 – 800 l of 4 - 10% w/v solution injected into each nasal vault (D. A. Edwards et al., 1972; D. A. Edwards and K. G. Burge, 1973; J. W. Harding et al., 1978; B. K. Gangrade and C. J. Dominic, 1983; G. Archunan and C. J. Dominic, 1990; G. D. Burd, 1993; P. Andine et al., 1995; A. Ducray et al., 2002; K. McBride et al., 2003). Most of

these studies report that while $ZnSO_4$ treatment can be highly effective, even using high volumes expected to fill the nasal cavities several times over is often no guarantee of inducing anosmia (B. Slotnick et al., 2000). A major cause of this variability is likely to be the convoluted nature of the turbinates in the nasal vault, which may obstruct access of irrigants or trap bubbles, stochastically sparing portions of the olfactory epithelium (M. H. Sieck and H. D. Baumbach, 1974; D. H. Matulionis, 1975a, 1975b; B. M. Slotnick and L. A. Gutman, 1977). A number of other factors, such as head position, depth of anaesthesia and exposure time, are also likely to be crucial. In a pilot study for this work, the duration of anesthesia dramatically influenced the extent of ablation. $ZnSO_{4\ LD}$ irrigation under isoflurane caused only mild deficits in odour-evoked intrinsic signals while the same dose administered under prolonged anaesthesia with sodium Pentobarbitone consistently abolished them. Thus, the variability observed in recognition scores after $ZnSO_{4\ LD}$-treatment is likely to be an unavoidable feature of nasal irrigation with substances that interfere with the olfactory epithelium.

The $ZnSO_{4\ HD}$ treatment on the other hand, was apparently consistent, since mice subjected to this dosage were all anosmic when tested on pair C discrimination tasks for at least seven days after treatment. $ZnSO_{4\ HD}$ treatment consisted of two bouts of $ZnSO_{4\ LD}$-treatment (9 l/naris) given on consecutive days, which suggests that the number of doses, as well as concentration, volume of each dose or anaesthesia may be a significant factor in determining the severity of $ZnSO_4$-treatment. Indeed, a number of other studies used multiple applications of $ZnSO_4$ to ensure rigorous disruption of the epithelium (J.

R. Alberts and B. G. Galef, Jr., 1971; D. H. Matulionis, 1975a, 1975b), and two applications of $ZnSO_4$ at 3-hr intervals have been shown to be more effective at disrupting olfaction than one in the rat (D. H. Thor et al., 1976).

$ZnSO_{4\ LD}$-treated mice needed significantly more trials to attain discrimination scores equal to shams and demonstrated significantly reduced recognition of previously familiar odour pairs, suggesting they experienced a significant alteration in their perception of odours. In agreement with these data, moderate lesions of glomerular input have been reported to cause significant deficits in both detection and discrimination of odours in mice (K. McBride et al., 2003). One study using rats also reported similar deficits in recognition after widespread lesions of the olfactory epithelium caused by i.p. injection of 3 methyl-indole (3-MI), but suggested impairments in recognition were secondary to deficits in the ability to discriminate odours (B. Slotnick and N. Bodyak, 2002). Experiments here first confirmed that mice could discriminate a novel odour pair with high accuracy before testing recognition, which allowed the distinction to be drawn between a broader inability to accurately perform the discrimination task and an inability to recognise previously familiar odorants. Other studies in rodents have concluded that extreme reductions of input have little functional consequence for olfactory behaviour (X. C. Lu and B. M. Slotnick, 1998; B. Slotnick et al., 2000; B. Slotnick and N. Bodyak, 2002), in contrast to the data presented here. This will be discussed further in chapter four in the context of the effects of $ZnSO_4$ lesion on odour-evoked intrinsic signals.

Chapter Four: The effects of $ZnSO_4$ irrigation on odour representation in the olfactory bulb

4.1. Introduction

Studies that probed the effects of lesions of the olfactory system used post-hoc histological analysis to determine the extent of neural-tissue damage (B. M. Slotnick and L. A. Gutman, 1977; B. Slotnick and N. Bodyak, 2002). This is advantageous since it allows large portions of the olfactory system to be observed but does not allow lesion-induced changes in the same animal to be quantified and cannot directly report functional changes in neural activity. Functional imaging can overcome these limitations. Intrinsic optical imaging has been extensively used to observe odour-evoked activity in the glomerular layer of the OB, where monomolecular odorants evoke complex and unique spatiotemporal activation sequences of glomeruli (R. W. Friedrich and S. I. Korsching, 1997; B. A. Johnson et al., 1999; B. D. Rubin and L. C. Katz, 1999; B. A. Johnson and M. Leon, 2000; N. Uchida et al., 2000; L. Belluscio and L. C. Katz, 2001; C. Linster et al., 2001b; M. Meister and T. Bonhoeffer, 2001; B. D. Rubin and L. C. Katz, 2001; M. Wachowiak and L. B. Cohen, 2001; H. Spors and A. Grinvald, 2002; M. J. Lehmkuhle et al., 2003; M. Wachowiak and L. B. Cohen, 2003; J. P. McGann et al., 2006; H. Spors et al., 2006; B. A. Johnson and M. Leon, 2007; B. A. Johnson et al., 2007; A. T. Schaefer and T. W. Margrie, 2007; R. Vincis et al., 2012). Both histological studies and calcium imaging show that intrinsic signals evoked by odours reflect glomerular activity

(F. Xu et al., 2000; M. Meister and T. Bonhoeffer, 2001; M. Wachowiak and L. B. Cohen, 2003), which is thought to originate primarily from the release of glutamate from ORN terminals (H. Gurden et al., 2006). Intrinsic imaging is also reasonably non-invasive - requiring neither fluorescent dye loading (A. Grinvald et al., 1986) nor craniotomy, so it causes minimal stress to animals (A. Celerier et al., 2004; R. S. Stawski et al., 2009) and is therefore ideal for chronic use in conjunction with behavioural studies.

To investigate the importance of subtle, odour specific evoked activity to odour quality perception, bulbar intrinsic signals were recorded in mice before and after behavioural training and $ZnSO_4$-induced lesion of the olfactory epithelium.

4.2. Results

Intrinsic signals were analysed to reveal the effect of epithelial lesion on the representation of odours in the glomerular layer of the OB. First, to determine the consistency of intrinsic optical signals across imaging sessions and to evaluate the sensitivity of the analysis program, intrinsic signals evoked by different odours were compared **(Figure 4.1A, B)**. ROIs that contained odour-evoked signals were manually selected and compared with concomitant ROIs from aligned activity maps recorded during presentation of recognition test odours (ethyl butyrate and pentanal) (see **Figures 2.2, 2.3, Materials and Methods**). Pixel intensity values of regions of interest (ROIs) were correlated with the concomitant ROI recorded in activity maps evoked by either the same or different odours in the same OB **(Figure 4.2)**. Correlation coefficients for each ROI were compared between maps recorded in the same session during presentation of the same odour, across sessions with the same odour and across sessions with different odours **(Figure 4.2A, B)**. This generated a within-session and an across-session correlation value for different odours. Across-session correlation values were then subtracted from within-session correlation values, yielding a dissimilarity score where high scores indicate large differences between session one and session two activity maps **(Figure 4.2C, D)**. Comparison of different odours yielded dissimilarity scores on average significantly higher than comparison of the same odour **(Figure 4.2E)**. This established that the imaging techniques and analysis protocols used were sensitive enough to detect differences in odours that evoke distinct but overlapping patterns of activity (L. Belluscio and L. C. Katz, 2001).

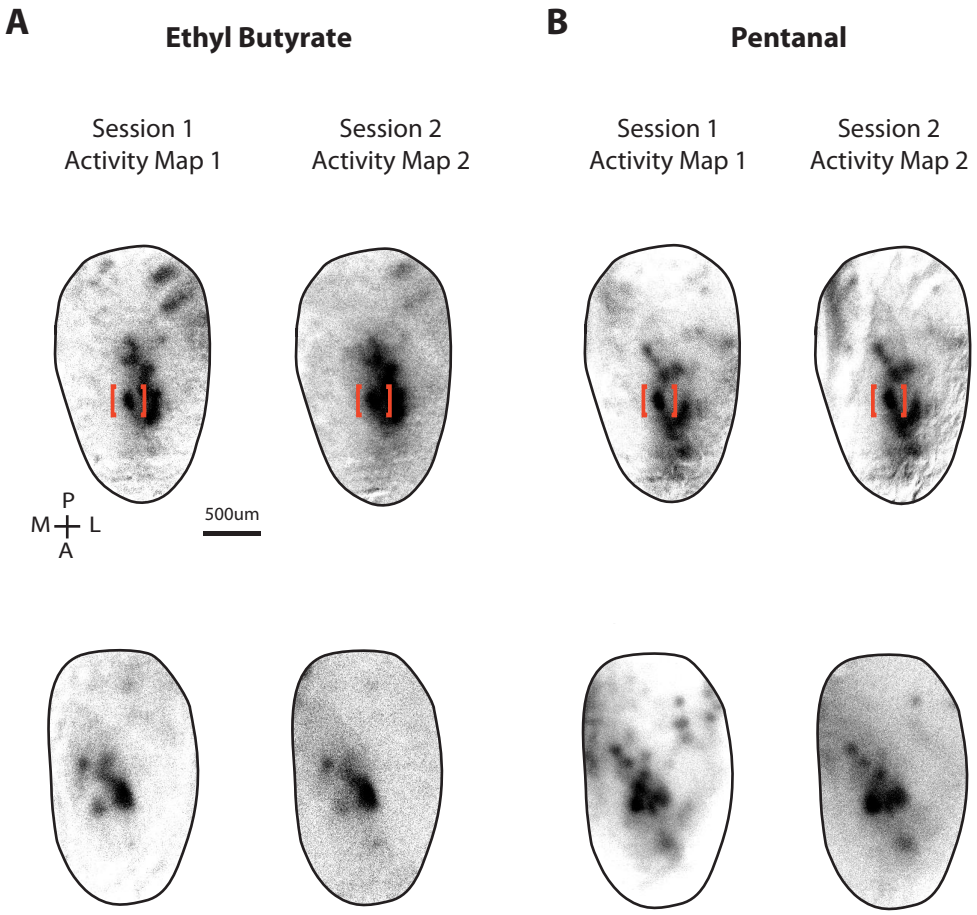

Figure 4.1. Example activity maps recorded in response to recognition test odours
A. Intrinsic signals evoked by ethyl butyrate before (left) and after sham treatment (right). **B.** As in **(A)** for signals evoked by pentanal. Each row corresponds to a different animal. An intrinsic spot that is activated by different odours is indicated with red brackets.

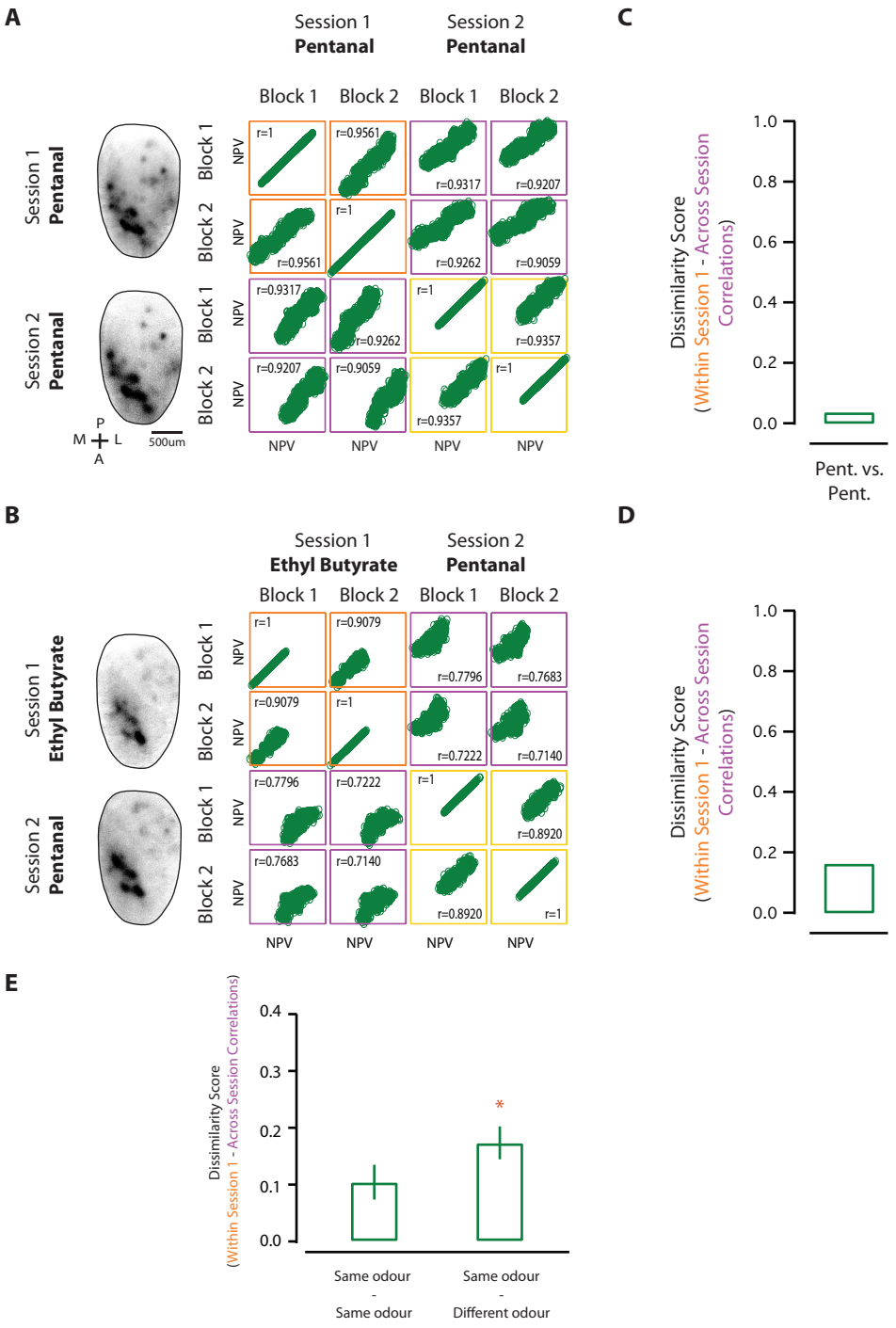

Figure 4.2. Different odours can be distinguished with correlation of spatial activity maps **A.** Example scatter plots of ROI correlations for intrinsic-signal activity maps evoked by the same odour (pentanal). Within session correlations (session one, orange boxes, session two, yellow boxes) and across sessions (purple boxes). Values for each ROI (green clusters) are expressed as normalized pixel value (NPV), r-values displayed are averages of all ROI correlations for each block comparison. The total number of data points plotted correspond to n ROIs x pixels/ROI for one odour. Concomitant activity maps are displayed to the left of NPV correlations. **B.** Example scatter plots as above for intrinsic-signal activity maps evoked by different odours (pentanal vs. ethyl butyrate). **C.** Bar graph showing dissimilarity score of intrinsic-signal activity maps, (evoked from example in **(A)**). **D.** Bar graph showing dissimilarity score of intrinsic-signal activity maps from example in **(B)**. NPV range as follows; same odour 0.9968 - 0.9992, different odours 0.9974 – 1.0005. **E.** Average dissimilarity scores for activity maps evoked by the same (n = 27 activity maps, n = 11 mice) and different odours (n = 14 activity maps, n = 4 mice, $p < 0.04$).

To examine the effects of nasal epithelial lesion on the integrity of odour-evoked spatial activity maps, intrinsic signals were evoked by recognition test odours (ethyl-butyrate and pentanal) from the dorsal surface of the bulb before (imaging session one) and after (imaging session two) nasal flush treatment with either sham, $ZnSO_{4\ LD}$, or $ZnSO_{4\ HD}$. Qualitatively, while the integrity of the odour-evoked glomerular map was maintained for sham-treated mice **(Figure 4.3A)**, $ZnSO_{4\ LD}$-treated mice revealed a phenotype ranging from minor map changes, to an almost complete absence of odour-evoked signals **(Figure 4.3B).** Odour-evoked signals were not detected in mice receiving the $ZnSO_{4\ HD}$-treatment (0/9 mice tested for two odours, **Figure 4.3C)**.

Signals from sham-treated animals had low dissimilarity scores (0.104 ± 0.03, n = 27 activity maps, n = 11 mice, **Figures 4.4A1, B1, 4.5A**), while mice treated with a $ZnSO_{4\ LD}$ showed significantly higher dissimilarity scores (0.340 ± 0.05, n = 32 odour-evoked activity maps, n = 12 mice, $p < 0.0002$, **Figures 4.4A2, B2, 4.5A)**. Mice treated with $ZnSO_{4\ HD}$ showed significantly higher dissimilarity scores than both sham and $ZnSO_{4\ LD}$-treated animals, consistent with the absence of signal in these animals (0.573 ± 0.07, n = 16 odour evoked activity maps, n = 5 mice vs. sham, $p < 0.0001$, vs. $ZnSO_{4\ LD}$, $p < 0.005$, **Figures 4.4A3, B3, 4.5A**).

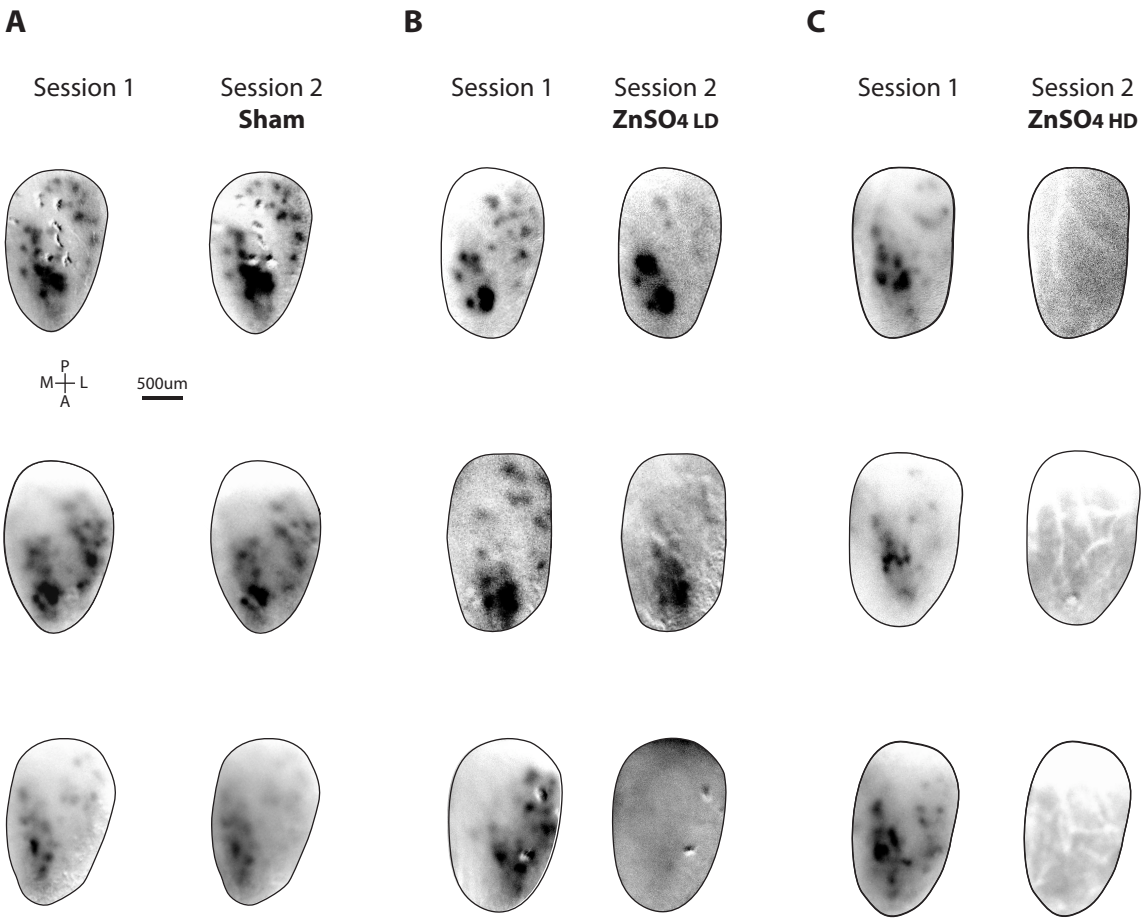

Figure 4.3. Example odour activity maps evoked before and after treatment
Activity maps evoked by the same odours (ethyl butyrate or pentanal) before (left) and after (right) treatment with sham **(A)**, $ZnSO_4$ LD **(B)** and $ZnSO_4$ HD-treatment **(C)**.

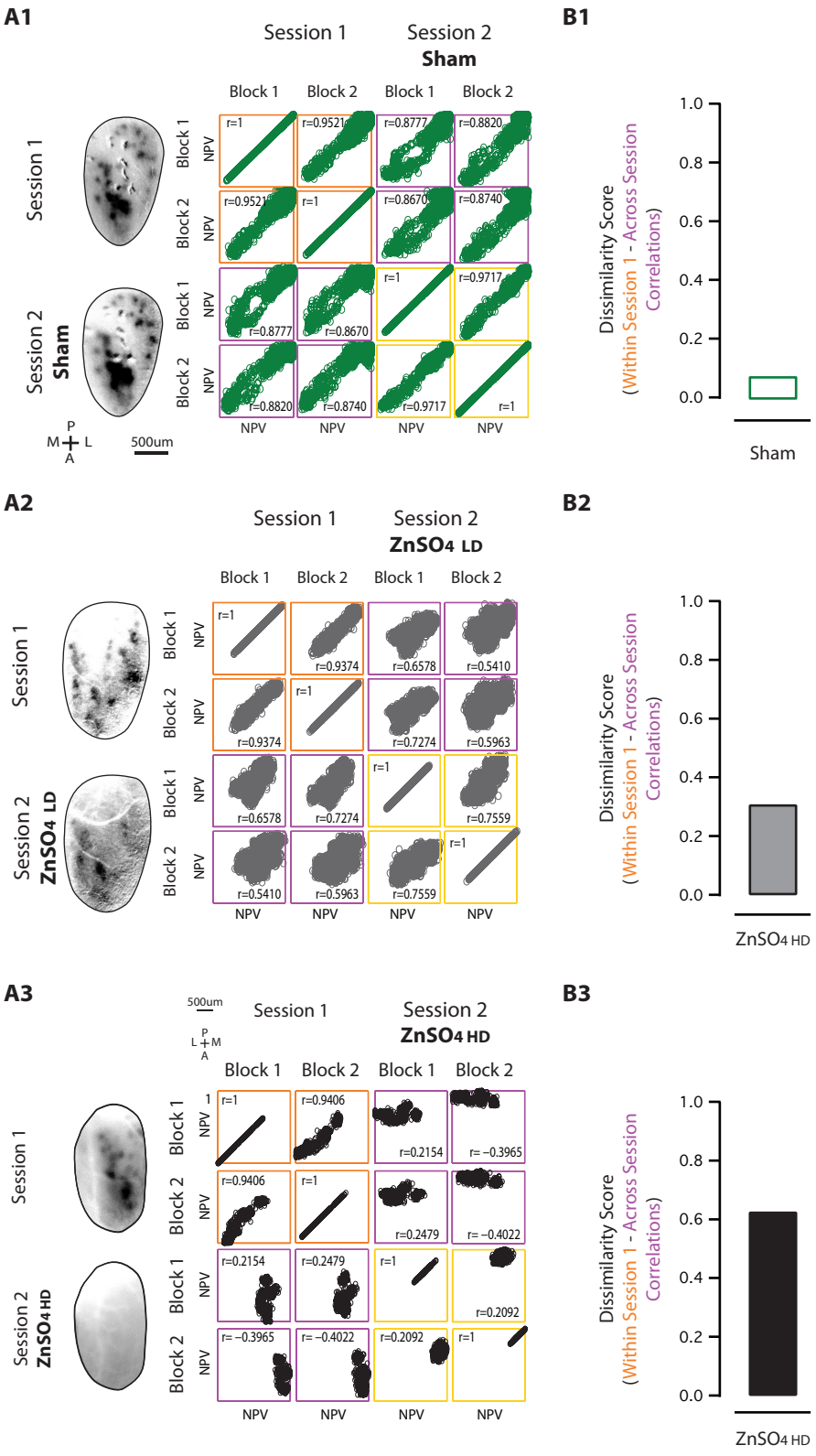

Figure 4.4. $ZnSO_4$ LD treatment significantly altered odour-evoked activity maps while $ZnSO_4$ HD abolishes activity

A. Example scatter plots of ROI correlations for odour-evoked intrinsic-signal activity maps. Within session correlations (session one, orange boxes, session two, yellow boxes) and across sessions (purple boxes) after sham **(A1)**, $ZnSO_4$ LD **(A2)** and $ZnSO_4$ HD treatment **(A3)**. Values for each ROI (sham, green clusters, $ZnSO_4$ LD, grey clusters and $ZnSO_4$ HD, black clusters) are expressed as normalised pixel value (NPV), r-values displayed are averages of ROI correlations for each block comparison. The total number of data points plotted correspond to (contd.)

Figure 4.4. continued
nROIs x pixels/ROI for one odour. Concomitant activity maps are displayed to the left of NPV correlations. **B1.** Bar graph showing example dissimilarity score of intrinsic-signal activity maps for sham treated animal in **(A1)**, **B2-B3** as above for $ZnSO_{4\ LD}$ **(B2)** and $ZnSO_{4\ HD}$–treated animals **(B3)**. NPV ranges are as follows; shams 0.9965 - 1.0027, $ZnSO_{4\ LD}$-treated 0.9956 – 1.0004, $ZnSO_{4\ HD}$-treated, 0.9963 - 1.001.

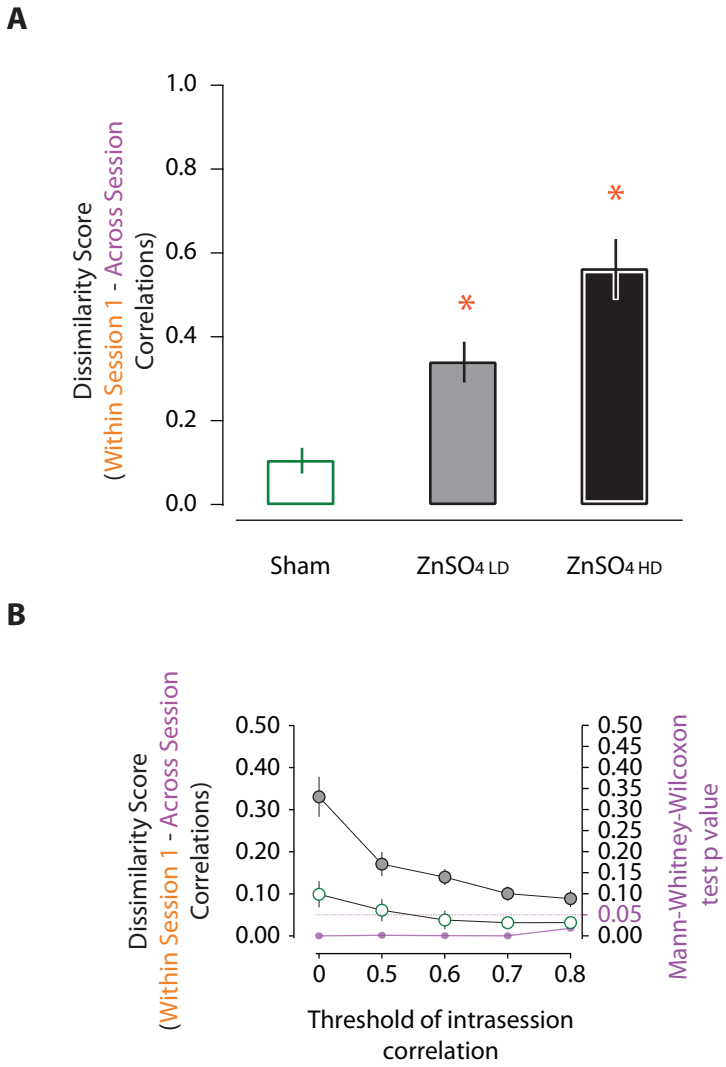

Figure 4.5. $ZnSO_4$ treatment significantly increased dissimilarity scores

A. Average dissimilarity scores for pair B odour-evoked activity maps for sham (green box, n = 27 activity maps, n = 11 mice), $ZnSO_4$ LD (grey box, n = 32 activity maps, n = 12 mice) and $ZnSO_4$ HD–treated animals (black box, n = 16 activity maps, n = 5 mice).

B. Average dissimilarity score for pair B odour-evoked activity maps for sham (open green circles) and $ZnSO_4$ LD (grey-filled circles) after filtering out activity maps with within session correlation scores below various thresholds denoted on the x - axis. Respective p values for Mann-Whitney-Wilcoxon tests performed between shams and $ZnSO_4$ LD-treated groups for each threshold value are shown in purple.

Some bulbs had little odour-evoked signal after $ZnSO_{4\ LD}$-treatment, so activity maps with within-session correlation values below 0.5 were removed from the analysis pool to ensure that differences in dissimilarity scores were not solely due to some bulbs having lost substantial signal. When filtering at 0.5, $ZnSO_{4\ LD}$-treated mice still had significantly higher dissimilarity scores (shams, 0.09 ± 0.03, n = 23 activity maps, n = 11 mice, $ZnSO_{4\ LD}$, 0.20 ± 0.04, n = 20 activity maps, n = 11 mice, $p < 0.002$, **Figure 4.5B**), and this relationship held true with filtering of inter-session correlations of up to 0.8 ($p < 0.02$, **Figure 4.5B)**, suggesting that differences in dissimilarity scores were not solely due to loss of signal but also other alterations of activity maps (see **Figure 6.6**, chapter six).

Behavioural assessment, epithelial lesions and chronic imaging were performed in a subset of mice to determine the relationship between recognition and dissimilarity score. On average, sham-treated mice had both significantly higher recognition scores and significantly lower dissimilarity scores than $ZnSO_{4\ LD}$-treated mice (pair B recognition scores, shams, 86.6 ± 4.41 %, n = 3 vs. $ZnSO_{4\ LD}$-treated, 70.6 ± 4.67 %, n = 8 mice, $p < 0.05$; pair B dissimilarity scores, shams, -0.000378 ± 0.04, vs. $ZnSO_{4\ LD}$-treated, 0.29 ± 0.07, $p < 0.02$, **Figure 4.6A, B**). $ZnSO_{4\ HD}$-treated mice had significantly lower recognition and higher dissimilarity scores than both sham and $ZnSO_{4\ LD}$-treated mice (pair B recognition scores, 53 ± 1.37 %, n = 5, vs. shams, $p < 0.001$, vs. $ZnSO_{4\ LD}$-treated, $p < 0.003$. Pair B dissimilarity scores 0.56 ± 0.07, vs. shams, $p < 0.02$, vs. $ZnSO_{4\ LD}$-treated, $p < 0.02$, **Figure 4.6C**), suggesting a relationship between the integrity of incoming stimulus maps and the capacity to match incoming

odour stimuli to previously learned odours. N.b. of the $ZnSO_{4\ LD}$ treated mice, n = 2 were from the concentration-trained group (see chapter 5, section 5.2.3).

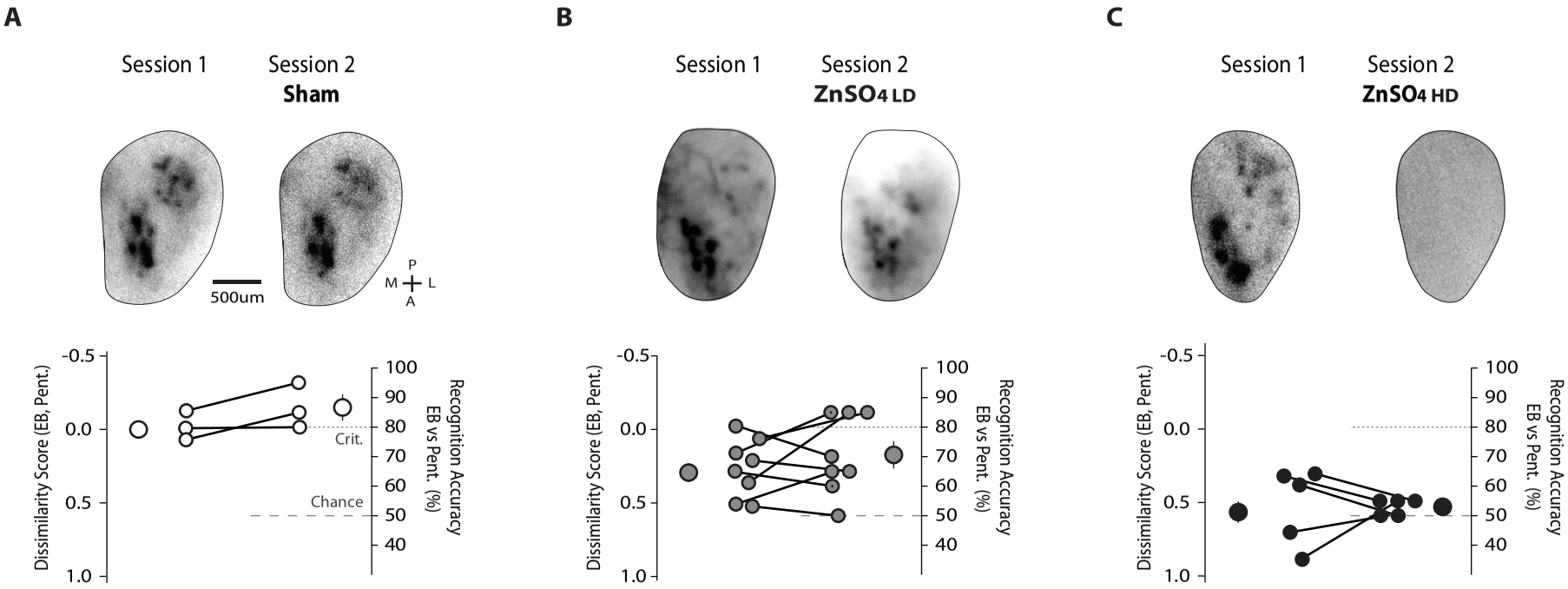

Figure 4.6. Recognition accuracy and activity map integrity are altered after epithelial lesion
A. Top, Example odour-evoked activity maps from before (left, session one) and after (right, session two) nasal flush for sham-treated mice. Bottom, dissimilarity scores for pair B odour-evoked activity maps (left axis) and pair B recognition scores (right axis) for shams. Large circles are averages. **B, C.** As above for $ZnSO_4$ LD- **(B)** and $ZnSO_4$ HD-treated mice **(C)**. Dotted circles in panel **B** are from mice that were also concentration trained (see chapter 5, section 5.2.3).

4.3. Discussion

In summary, these results show that $ZnSO_{4\ HD}$–treatment abolished odour-evoked intrinsic signals, while $ZnSO_{4\ LD}$-treatment caused disruption to bulbar odour representations intermediate between $ZnSO_{4\ HD}$ and sham-treated mice.

In contrast to $ZnSO_{4\ HD}$ treatment, dissimilarity scores from intrinsic-signal imaging data revealed that $ZnSO_{4\ LD}$-treatment on average resulted in a comparatively modest disruption of the glomerular map, indicating that substantial olfactory input was spared in these mice. Despite the presence of odour-evoked intrinsic signals in activity maps from all animals in which both behaviour and imaging were recorded, recognition scores and initial performance on discrimination tasks were significantly poorer in $ZnSO_{4\ LD}$-treated mice than in shams. Recognition test scores were not reduced to chance levels, which suggests that odours may not have been perceived as entirely novel, but significantly altered. Thus, even moderate changes to odour-evoked activity maps can have significant consequences for odour perception. In line with this hypothesis, mice with an estimated 30% of glomerular input spared after lesion also had significant deficits in detection and discrimination of odours (K. McBride et al., 2003). A number of studies in rodents conclude that comparatively extreme lesions have little functional consequence for olfactory behaviour (B. Slotnick et al., 2000; B. Slotnick and N. Bodyak, 2002), in contrast to these data. Up to 90% of olfactory inputs in the rat may apparently be ablated without impairing discrimination of simple odours (X. C. Lu and B. M. Slotnick, 1998). Eradication of bulbar areas activated by enantiomers - which may differ in their spatial activity-patterns by as little as one glomerulus (B. D.

Rubin and L. C. Katz, 2001) and which one would assume were critical for perceptual separation of enantiomer-evoked activity patterns (E. Yaksi et al., 2007; E. Yaksi et al., 2009) - had no effect on the ability of rats to discriminate between those odours (K. McBride and B. Slotnick, 2006). However, more rigorous behavioural studies reveal that lesions may have more impact than hypothesised. Discrimination of simple odours was ostensibly unaffected in rats with direct surgical lesions of the OB, but more errors were made when these animals were challenged with more complex odour mixtures (X. C. Lu and B. M. Slotnick, 1998). Furthermore, stimulus recognition is likely to require comparatively more complex neural representation than discrimination. Thus, studies that probe discrimination alone are unlikely to uncover subtler post-lesion changes in odour perception. A study in rats reported that lesions encompassing approximately a third of the OB had a larger impact on recognition than discrimination (S. Bisulco and B. Slotnick, 2003). Prolonged exposure to methyl bromide gas, which also destroys the olfactory epithelium, caused a reduction in recognition accuracy that correlated to the proportion of spared olfactory epithelium in rats tested in a confusion matrix task (S. L. Youngentob et al., 2006), while intraperitoneal injection with 3-MI significantly affected odour recognition in rats (B. Slotnick and N. Bodyak, 2002). Direct surgical lesion of the OB, ablating areas thought from 2-DG uptake to be activated by specific odours was reported to have little impact on recognition of those odours in rats (B. Slotnick and N. Bodyak, 2002), while another study by the same authors observed significant deficits in odour recognition and subtler changes to detection and discrimination when up to one third of the bulb was aspirated (S. Bisulco and B. Slotnick, 2003). This suggests that few input

channels to the OB are necessary for highly accurate discrimination of simple odours (B. Slotnick and N. Bodyak, 2002), but highlight that accurate recognition of a stimulus is likely to require comparatively more input signal. In line with this, there was no correlation between performance on pair B recognition tests and the number of blocks needed to achieve criterion on pair C odours in $ZnSO_{4\ LD}$-treated mice. Indeed, in some individual cases, mice learnt to discriminate pair C odours as quickly as shams but later showed profound deficits in pair B recognition.

In conclusion, combined imaging and behavioural data suggests that even relatively modest deviations from representations of familiar stimuli can cause odour stimuli not to be recognised. In contrast to a number of other studies, this suggests that coding in the OB of the mouse is non-redundant and that all available information may be required to enable rapid and accurate olfactory judgements.

Chapter Five: The effects of concentration reduction on odour recognition

5.1. Introduction

One possible alternative explanation for the inability of $ZnSO_4$-treated mice to recognise previously presented odours as shown in chapter three, is that treatment induced a homogeneous reduction in ORN input, resulting in an odorant being perceived at an apparent lower concentration during post-treatment recognition testing. If so, the lesion-induced behaviour and map changes described in chapters three and four might simply reflect a change in odour representation caused by an apparent reduction in stimulus concentration.

Rodents have been shown to extrapolate odour identity over at least tenfold changes in concentration but larger changes can cause them to respond as though odours appear in some way novel (N. Uchida and Z. F. Mainen, 2008; T. A. Cleland et al., 2012). Thus, a naïve group of mice was tested to see if they performed in the context of the go/no-go behavioural paradigm in the same way as rodents reported in other studies - namely, with reduced recognition scores when challenged with familiar odours presented at novel concentrations. In a different group of mice, intrinsic-optical signals evoked by a range of odour concentrations were obtained to compare signals with those recorded after $ZnSO_{4\ LD}$-treatment.

5.2. Results

5.2.1. The effects of reduction of concentration on odour discrimination and recognition behaviour in mice

First, a group of naïve mice was trained on 1 % v/v pair A and then on 1 % v/v pair B odours **(Figure 5.1A - C)**. Lower concentrations (0.05 % or 0.01 % v/v) of pair A odours were presented for the recognition test **(Figure 5.2A, B)**. Mice performed significantly worse on recognition tasks where odours were reduced 20 - 100 fold from the concentrations they had been trained on (1 % v/v, 92.14 ± 4.06 %, n = 7 vs. 0.05 % v/v, 78.13± 7.64 %, n = 8, $p < 0.047$. 0.01 % v/v, 68.3 ± 11.37, n = 3, $p < 0.01$, **Figure 5.2A, B**) and also performed significantly worse than their own previous pair A discrimination score (last five blocks of pair A discrimination, 1 % v/v, $p > 0.21$, 0.05 % v/v, $p < 0.006$ and 0.01% v/v, $p < 0.04$, **Figure 5.2B**).

To ensure they could detect the low concentration recognition test odours, mice were trained to discriminate pair A odours at the same reduced concentrations **(Figure 5.3A1-3, B)**. The first and second blocks of pair A discrimination scores were significantly lower in mice presented with 0.01 % v/v (second block, 1 % v/v, 98.33 ± 1.83 %, n = 7 vs. 0.01 % v/v, 73.33 ± 13.39 %, n = 3, $p < 0.007$) but were then indistinguishable from mice tested with 1% v/v thereafter (third block, 1 % v/v, 96.67 ± 2.71 % vs. 0.01 % v/v, 88.33 ± 11.37 %, $p > 0.13$). Discrimination scores for odours presented at 0.05 % v/v were not significantly different from 1 % v/v on the first block of discrimination training trials (1 % v/v, 85 ± 8.94 % vs. 0.05 % v/v, 75.63 ± 6.94 %, $p > 0.17$). These data suggest

that, mice trained on this go/no-go task to discriminate monomolecular odorants presented at 1% v/v perceive the same odours to be in some way distinct if presented at detectable 20-100 fold lower concentrations (T. A. Cleland 2012).

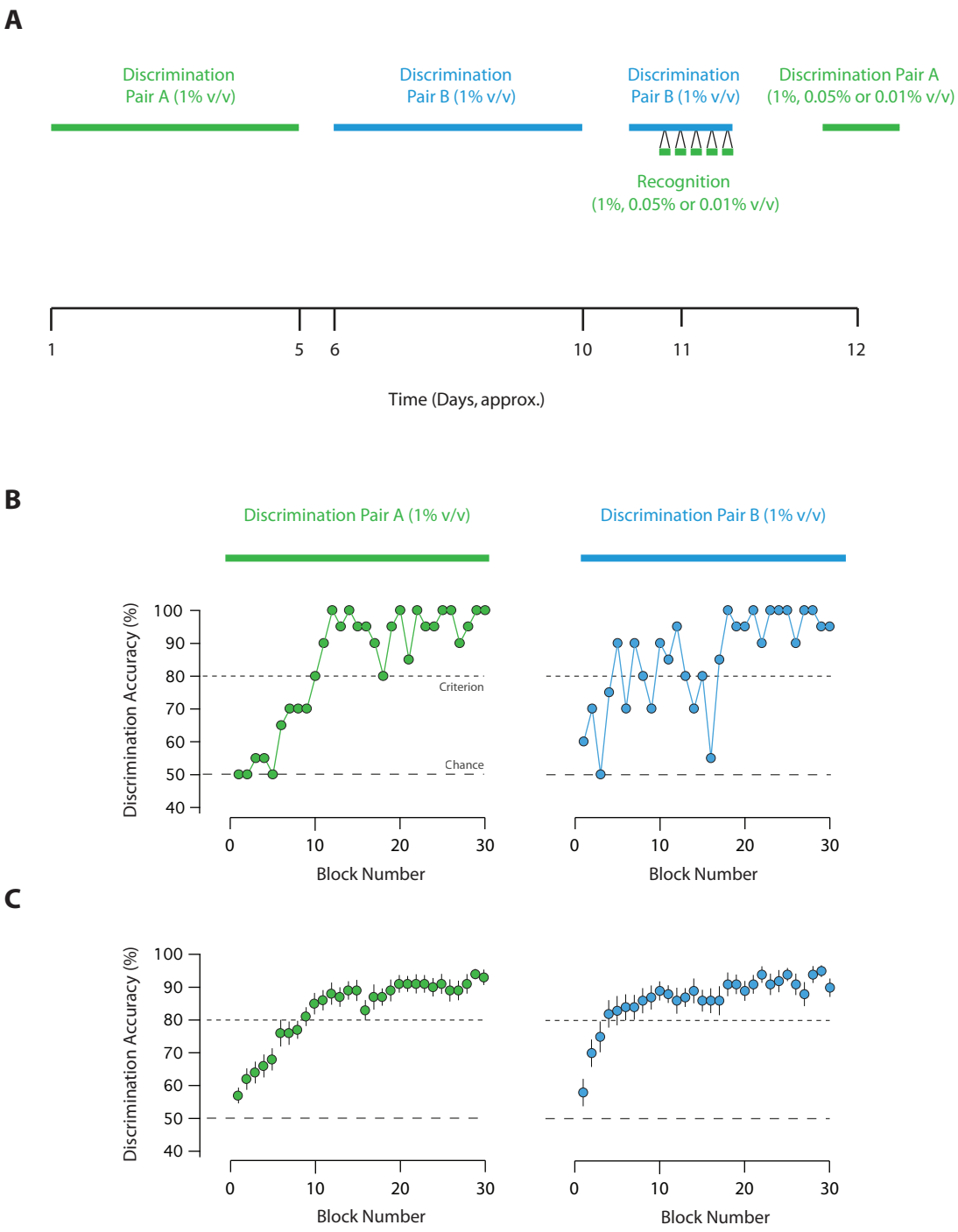

Figure 5.1. Behavioural protocol and discrimination learning of novel odours

A. Order of discrimination tasks and recognition tests with approximate timings is shown. Pair A odours (green bars) were amyl acetate, cineol, ethyl butyrate, pentanal or eugenol. Pair B odours were ethyl butyrate, pentanal, amyl acetate or cineol (blue bars).

B. Left, example discrimination scores obtained from one mouse for all blocks of training on pair A odours 1 % v/v (green circles) and right, pair B odours 1 % v/v (blue circles).

C. Left, average discrimination scores for all blocks of training on pair A odours obtained from all mice (green circles, n = 18 mice), right, for pair B odours obtained from all mice (blue circles, n = 18 mice).

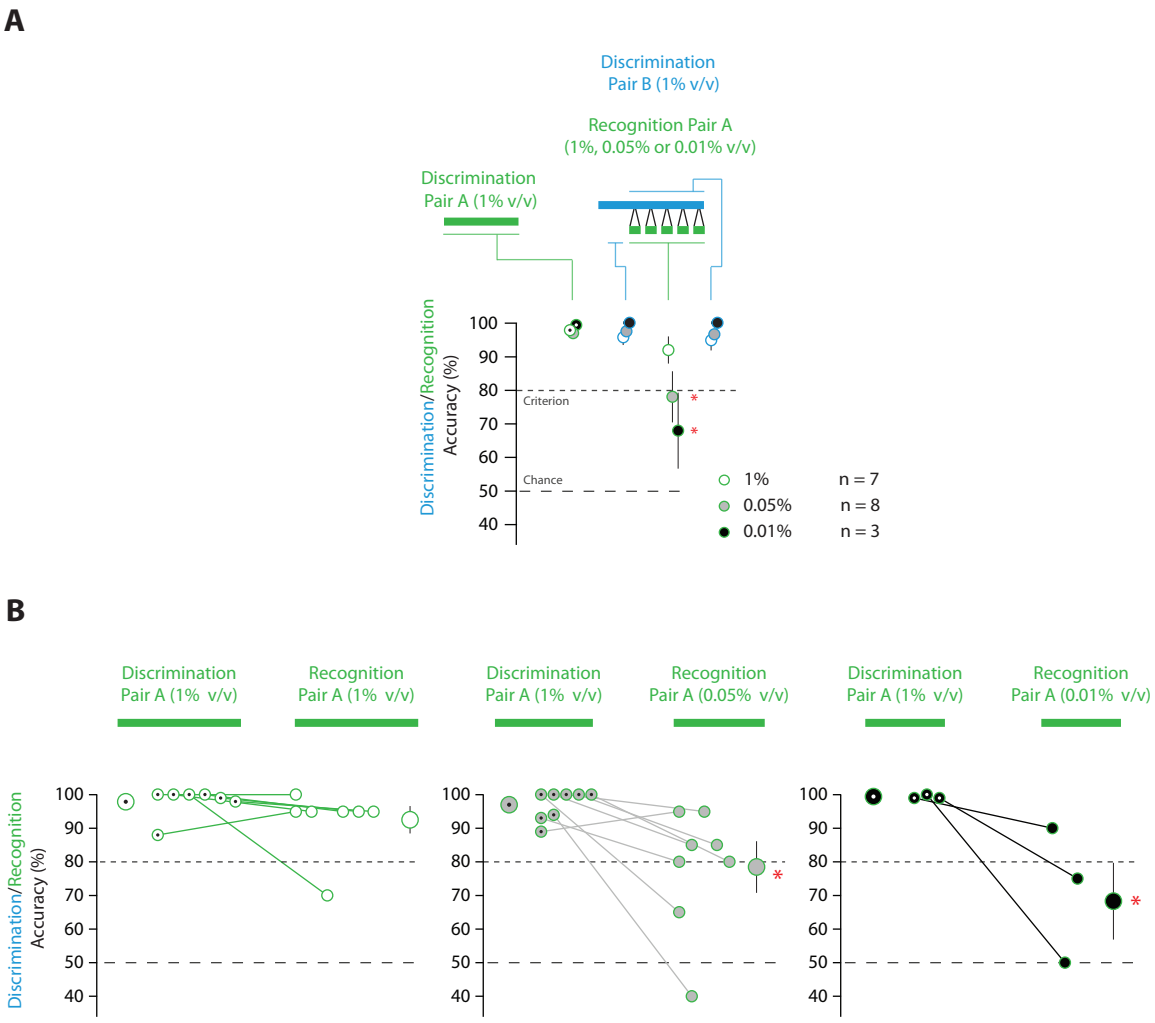

Figure 5.2. Presentation of familiar odours at unfamiliar concentrations caused reduction in recognition scores

A. Average scores obtained for recognition of previously-presented pair A odours at either the familiar concentration of 1 % v/v (green, open circles, right) or novel concentrations of 0.05% v/v (green, grey-filled circles, right) or 0.01 % v/v (green, black-filled circles, right). Discrimination scores for the average of the last five blocks of pair A odours (dotted green circles, left), discrimination scores for pair B odours for the block of trials immediately prior to (blue circles, left) and those trials presented during recognition testing (blue circles, right), all indicated by thin green and blue lines, are also plotted.

B. Individual scores for pair A discrimination (dotted green circles on left of plots) and pair A recognition (green circles on right of plots). Large circles are averages. Left, mice presented with 1 % v/v (open circles), middle, 0.05 % v/v (grey filled circles) and right, 0.01 % v/v (black-filled circles) odours for recognition testing.

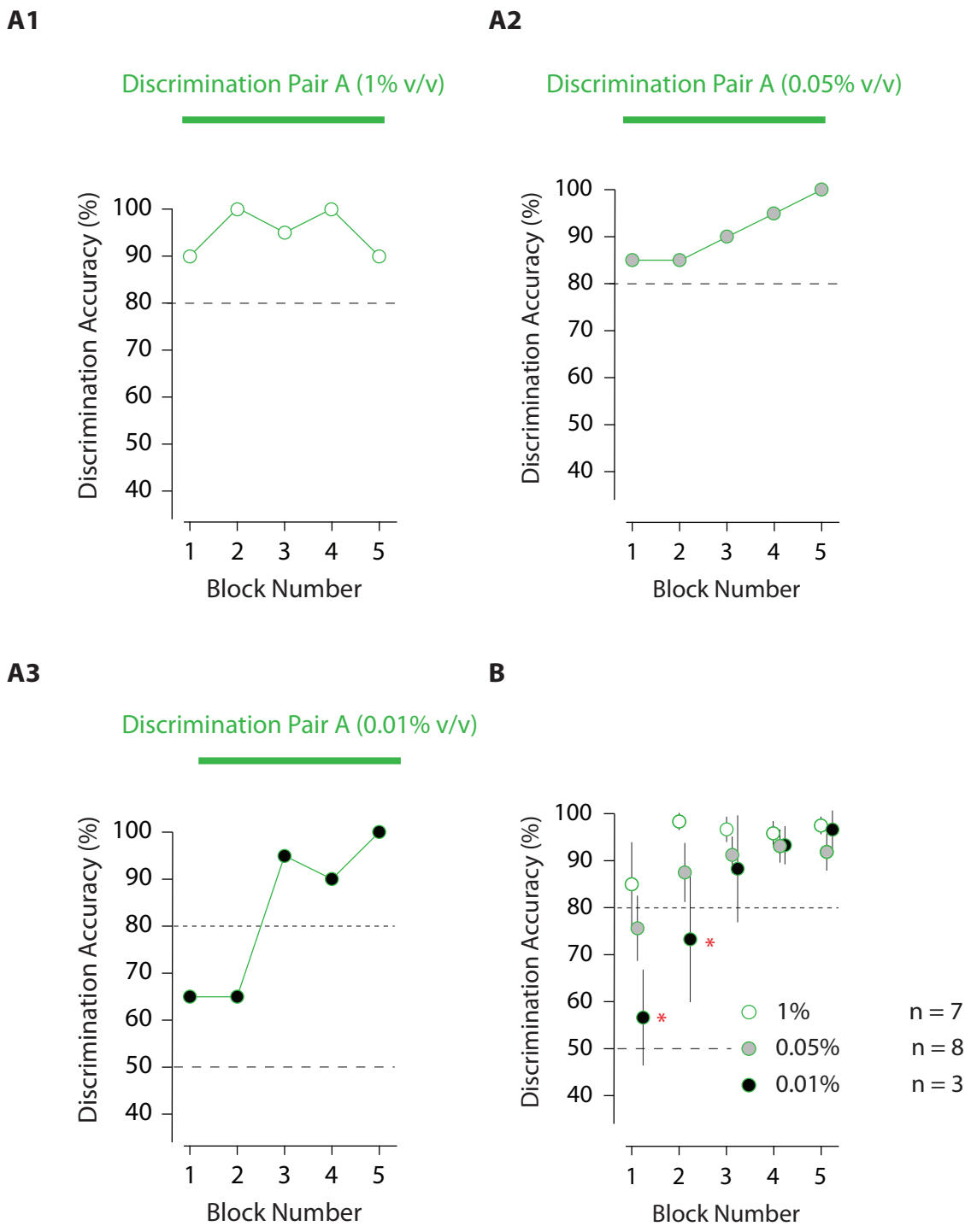

Figure 5.3. Odours presented at reduced concentrations were detectable

A. Example discrimination scores for previously presented pair A odours in mice presented with 1 % v/v (**A1**, open circles), 0.05 % v/v (**A2**, grey-filled circles) and 0.01 % v/v odours (**A3**, black-filled circles) immediately after recognition testing.

B. Average discrimination scores for pair A odours presented at 1 % v/v (open circles), 0.05 % v/v (grey-filled circles) and 0.01 % v/v odours (black-filled circles) immediately after recognition testing.

5.2.2. The effects of concentration training on recognition of familiar odours presented at novel, reduced concentrations

Both $ZnSO_{4\ LD}$-treatment and presenting mice with familiar odours at novel concentrations caused them to respond with reduced recognition scores. However, it was not possible to determine definitively if this behavioural phenotype originated from the same change in perception. Thus, mice were first trained to generalise across a range of odour concentrations so that presentation of the same odour at a novel concentration would be responded to with a high recognition score, i.e. as if responding to a familiar odour (T. A. Cleland et al., 2012).

To enable mice to generalise across a range of concentrations in the context of the go/no-go behavioural paradigm, they were trained to discriminate ethyl butyrate and pentanal at a number of fixed concentrations namely; 0.01, 0.1, 0.25 and 1 % v/v (pair A odours). Odours of different concentrations were interleaved throughout the training protocol **(Figure 5.4)**. Mice were first trained to discriminate pair A odours at a high concentration (1 % v/v) before interleaving odours of lower concentrations (0.25, 0.1 and 0.01 % v/v) in discrimination tasks. Mice performed with high accuracy on discrimination tasks for all concentrations trained **(Figure 5.5A, B).** They were next trained to discriminate pair B odours at 1 % v/v **(Figure 5.5C, D)**. Once they reached criterion on pair B odours, they were probed with a recognition test comprising familiar pair A odours (ethyl butyrate and pentanal) at a novel concentration of 0.05 % v/v. Concentration trained mice achieved above criterion recognition scores when challenged with unfamiliar concentrations of ethyl butyrate and

pentanal, indistinguishable from those scores obtained from mice presented with the familiar 1 % v/v concentration for recognition testing (1 % v/v, 91.67 ± 2.79 %, n = 6 vs. 0.05 % v/v, 97.14 ± 2.14 %, n = 7, $p > 0.07$, **Figure 5.6A, B**). Recognition of 0.05 % v/v odours following concentration training was significantly higher than for recognition of 0.05 % v/v odours in mice without concentration training (0.05 %, v/v, without training, 78.13 ± 7.07 %, n = 8, 0.05 % v/v, trained, 97.14 ± 2.14 %, n = 7, $p < 0.01$). Mice also showed no deficits in discrimination of pair A odours presented at reduced concentrations (first block, 1% v/v, 88.33 ± 7.92 %, n = 6, 85.71 ± 6.12 %, n = 7, $p > 0.39$).

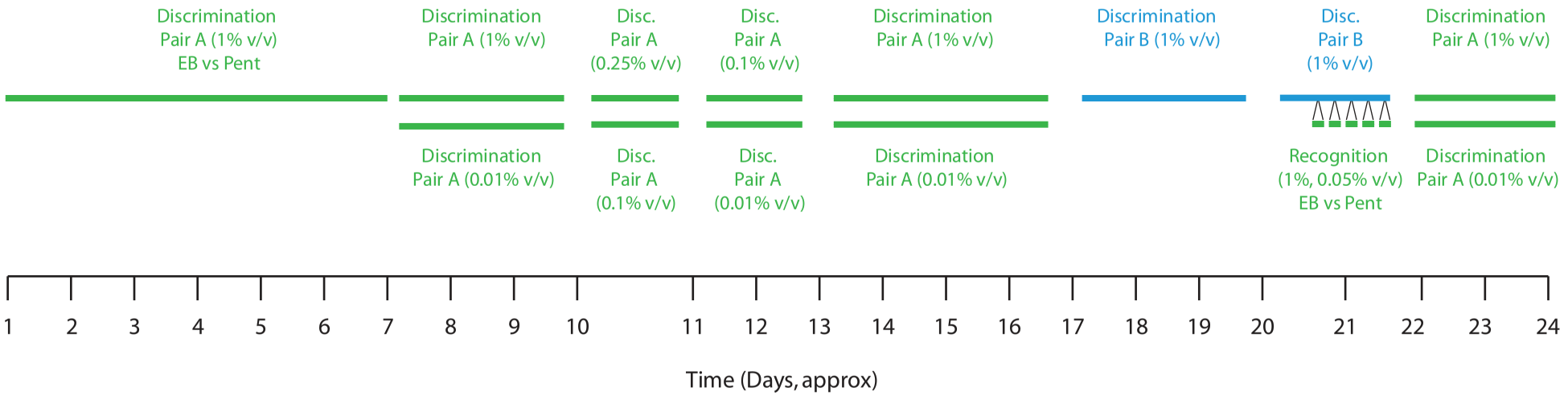

Figure 5.4. Behavioural protocol for concentration training

Order of discrimination tasks and recognition tests with approximate timing is shown. Pair A odours were ethyl butyrate and pentanal (green bars), pair B odours were eugenol and cineol (blue bars).

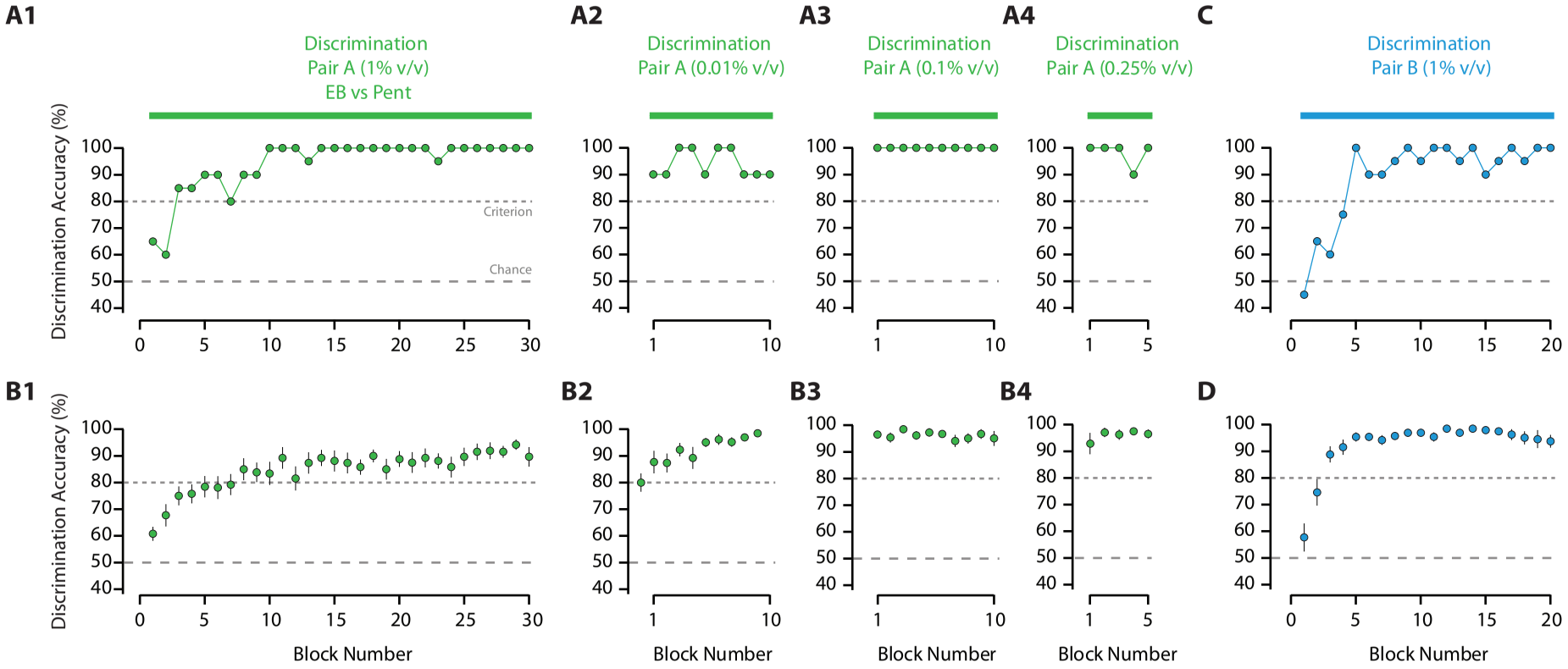

Figure 5.5. Discrimination learning for odours of various concentrations

A1-A4. Example discrimination scores from one mouse obtained for 30 blocks of training on pair A odours at 1 % v/v **(A1)**. Example discrimination scores obtained for the first 10 blocks of training on pair A odours at concentrations of 0.01 % v/v **(A2)**, 0.1 % v/v **(A3)** and first five blocks of 0.25 % v/v **(A4)**.

B1-B4. Average discrimination scores (n = 13 mice) obtained for 30 blocks of training on pair A odours at 1 % v/v **(B1)**. Average discrimination scores obtained for the first 10 blocks of training on pair A odours at concentrations of 0.01 % v/v **(B2)**, 0.1 % v/v **(B3)** and first five blocks of 0.25 % v/v **(B4)**.

C. Example discrimination scores obtained for 20 blocks of training on pair B odours at 1 % v/v.

D. Average discrimination scores obtained for 20 blocks of training on pair B odours at 1 % v/v.

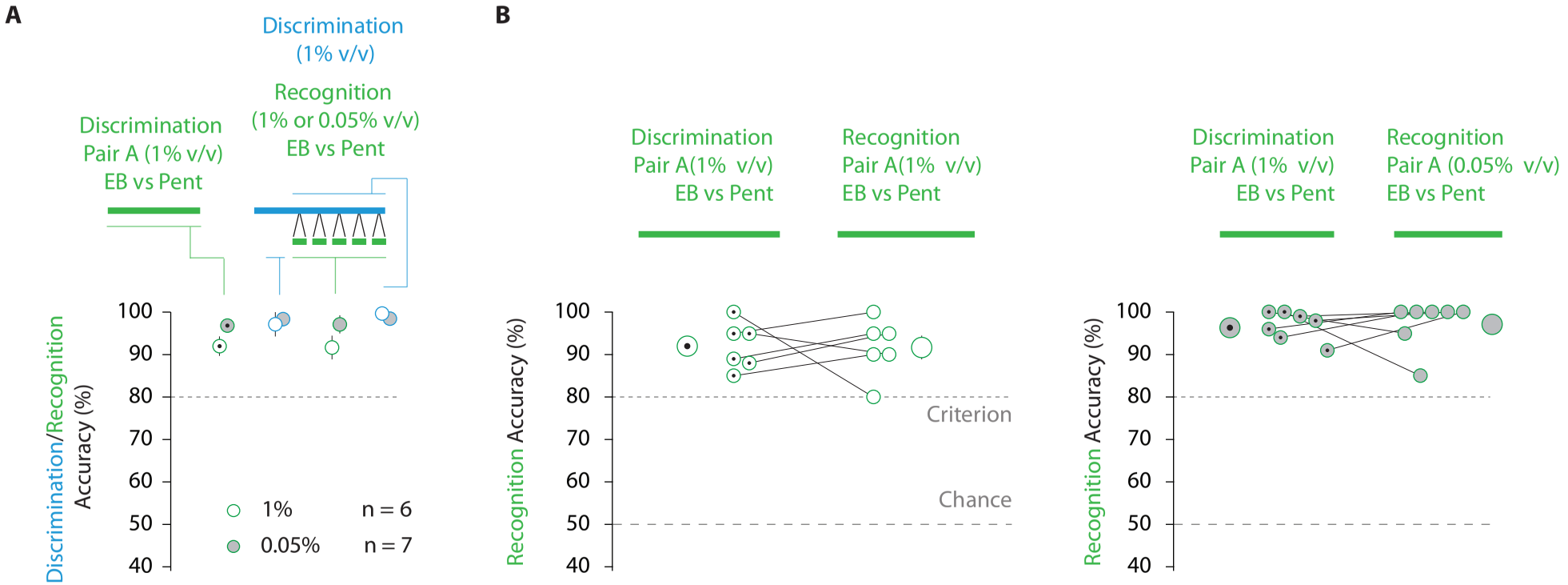

Figure 5.6. Concentration training allowed mice to generalise across odour concentrations

A. Average recognition scores for concentration-trained mice obtained for recognition of familiar pair A odours at either the familiar concentration of 1 % v/v (green, open circles, n = 6) or novel concentrations of 0.05% v/v (green, grey-filled circles, n = 7). Discrimination scores for the average of the last five blocks of pair A odours at 1% v/v (dotted green circles), discrimination scores for pair B odours for the block of trials immediately prior to (blue circles, left) and those trials presented during recognition testing (blue circles, right), indicated by thin green and blue lines, are also plotted.

B. Left, individual recognition scores for pair A discrimination (dotted, open green circles) and pair A recognition (open green circles) for mice presented with 1 % v/v odours in recognition tests. Larger circles are averages. Left, as above for mice presented with 0.05 % v/v odours in recognition tests (grey-filled circles).

5.2.3. The effects of concentration training on odour recognition in sham- and $ZnSO_4$-treated mice

If $ZnSO_{4\ LD}$-treatment resulted in recognition test odours being perceived as though presented at a reduced concentration, then pre-training $ZnSO_{4\ LD}$-treated mice on a range of concentrations would be expected to improve recognition scores, as demonstrated above (Figure 5.6). Thus, a subset of mice from section 5.2.2 that had been trained to generalise across odours were treated with nasal flush **(Figure 5.7)**. Recalculation of learning curves for this subset of mice showed that they all learned to discriminate pair A odours at a range of concentrations with high accuracy (**Figure 5.8A, B**) as well as pair B odours at 1 % v/v **(Figure 5.8C, D)**. After training on pair B odours and testing for pair A recognition, all (6/6) mice previously tested for recognition of familiar, high concentration odours (1% v/v) were treated with $ZnSO_{4\ LD}$, while 5/7 mice tested for recognition of familiar odours of reduced concentration (0.05% v/v) were assigned to the sham treatment group. Mice were trained on novel pair C odours after treatment.

Despite concentration training, $ZnSO_{4\ LD}$-treated mice still performed significantly worse than shams in the first five blocks of training after shams had reached criterion (ANOVA, first five blocks, $F(1, 53) = 21.09$, $P < 0.00003$, **Figure 5.9A, B**). However, after reaching criterion, they performed no differently from shams (ANOVA, first five blocks after $ZnSO_{4\ LD}$-treated mice reached criterion, $F(1, 53) = 2.01$, $P > 0.16$, **Figure 5.10A**). $ZnSO_{4\ LD}$-treated animals also performed below criterion for recognition of pair A odours (ethyl-butyrate and pentanal presented at 1 % v/v) and were significantly worse than

shams (sham, 1 % v/v, 96.00 ± 1.87 %, n = 5 vs. $ZnSO_{4\ LD}$, 1 % v/v, 65.00 ± 8.56 %, n = 6, $p < 0.008$, **Figure 5.10A, B**), or their own pre-treatment pair A recognition scores ($ZnSO_{4\ LD}$ pre-treatment pair A recognition, 95.83 ± 3.27 %, $p < 0.004$).

To confirm that $ZnSO_{4\ LD}$-treated mice retained the ability to detect previously familiar but no longer recognised odours, mice were retrained on the pair A discrimination task (1 % v/v). Again, concentration trained mice performed similarly to non concentration trained mice (chapter three) with $ZnSO_{4\ LD}$-treated animals initially performing significantly worse than shams, but quickly learning to discriminate previously familiar odours after the first block of retraining (first block, sham, 93.00 ± 4.18 % vs. $ZnSO_{4\ LD}$-treated, 69.17 ± 11.26 %, $p < 0.04$; second block, sham, 94.00 ± 4.18 % vs. $ZnSO_{4\ LD}$-treated, 84.17 ± 8.42 %, $p > 0.13$, **Figure 5.11**).

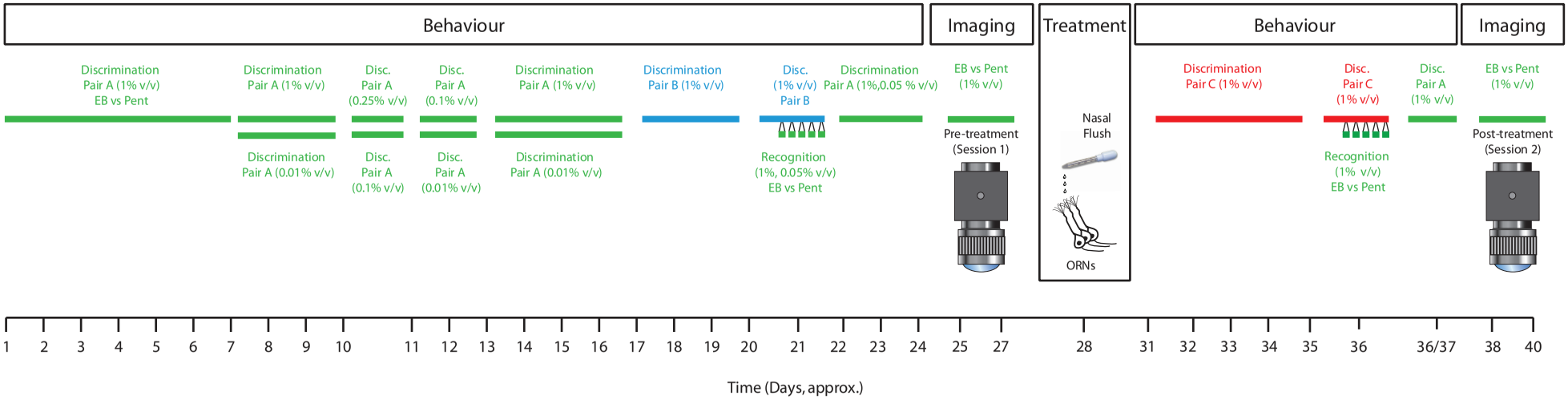

Figure 5.7. Behavioural protocol for concentration training and nasal flush

Order of discrimination tasks and recognition tests with approximate timing is shown. Pair A odours were ethyl butyrate and pentanal, pair B odours were eugenol and cineol, pair C odours were amyl acetate and limonene. Camera lens icon shows when, in some cases, intrinsic optical signals evoked by ethyl butyrate and pentanal were also recorded. N.b. these data are taken from a subset of mice from section 5.2.2 that had been trained to generalise across odours; all (6/6) mice previously tested for recognition of familiar, high concentration odours (1% v/v) were treated with $ZnSO_4$ LD, while 5/7 mice tested for recognition of familiar odours of reduced concentration (0.05% v/v) were assigned to the sham treatment group.

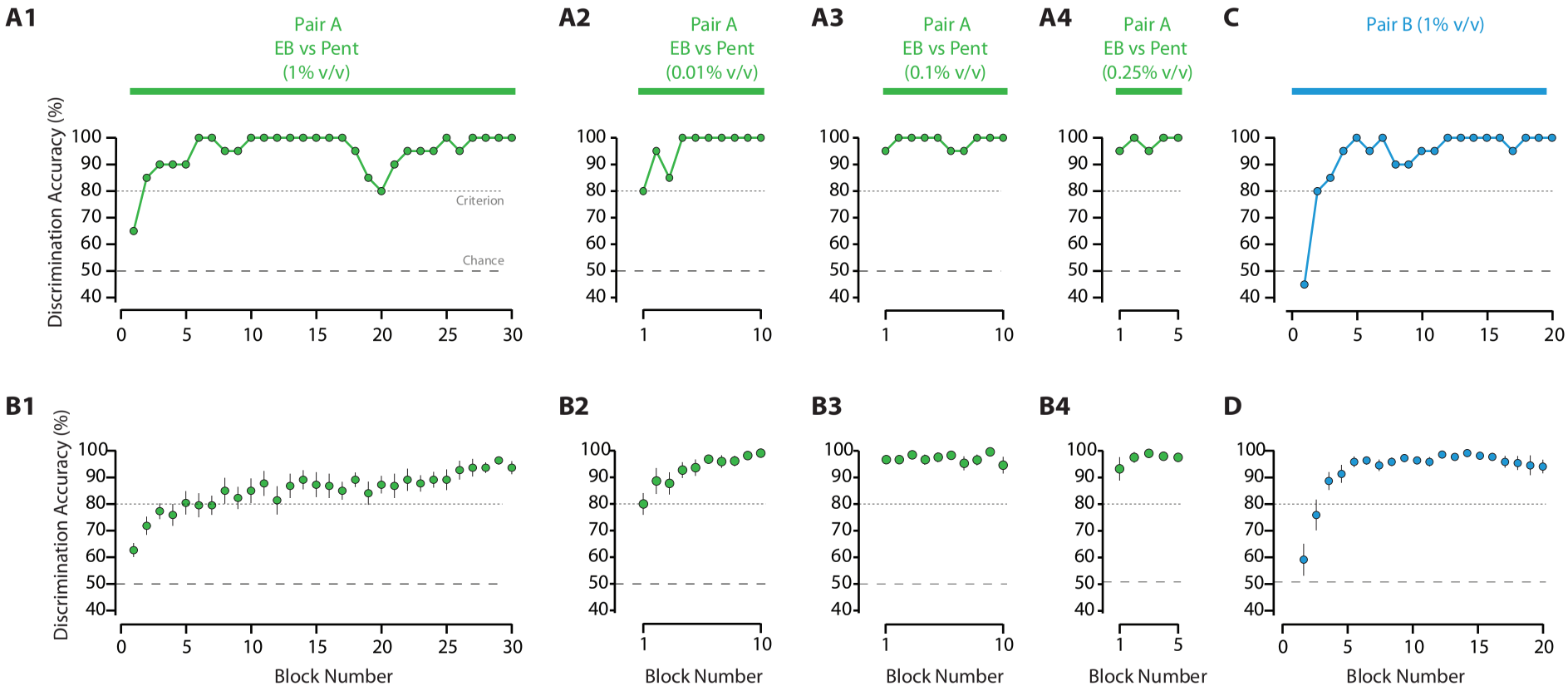

Figure 5.8. Discrimination learning for odours of various concentrations

A1-A4. Example discrimination scores from one mouse obtained for 30 blocks of training on pair A odours at 1 % v/v **(A1)**. Example discrimination scores obtained for the first 10 blocks of training on pair A odours at concentrations of 0.01 % v/v **(A2)**, 0.1 % v/v **(A3)** and first five blocks for 0.25 % v/v **(A4)**.

B1-B4. Average discrimination scores for all mice (n = 11) obtained for 30 blocks of training on pair A odours at 1 % v/v **(B1)**. Average discrimination scores obtained for the first 10 blocks of training on pair A odours at concentrations of 0.01 % v/v **(B2)**, 0.1 % v/v **(B3)** and first five blocks for 0.25 % v/v **(B4)**.

C. Example discrimination scores obtained for 20 blocks of training on pair B odours at 1 % v/v.

D. Average discrimination scores for all mice (n = 11) obtained for 20 blocks of training on pair B odours at 1 % v/v.

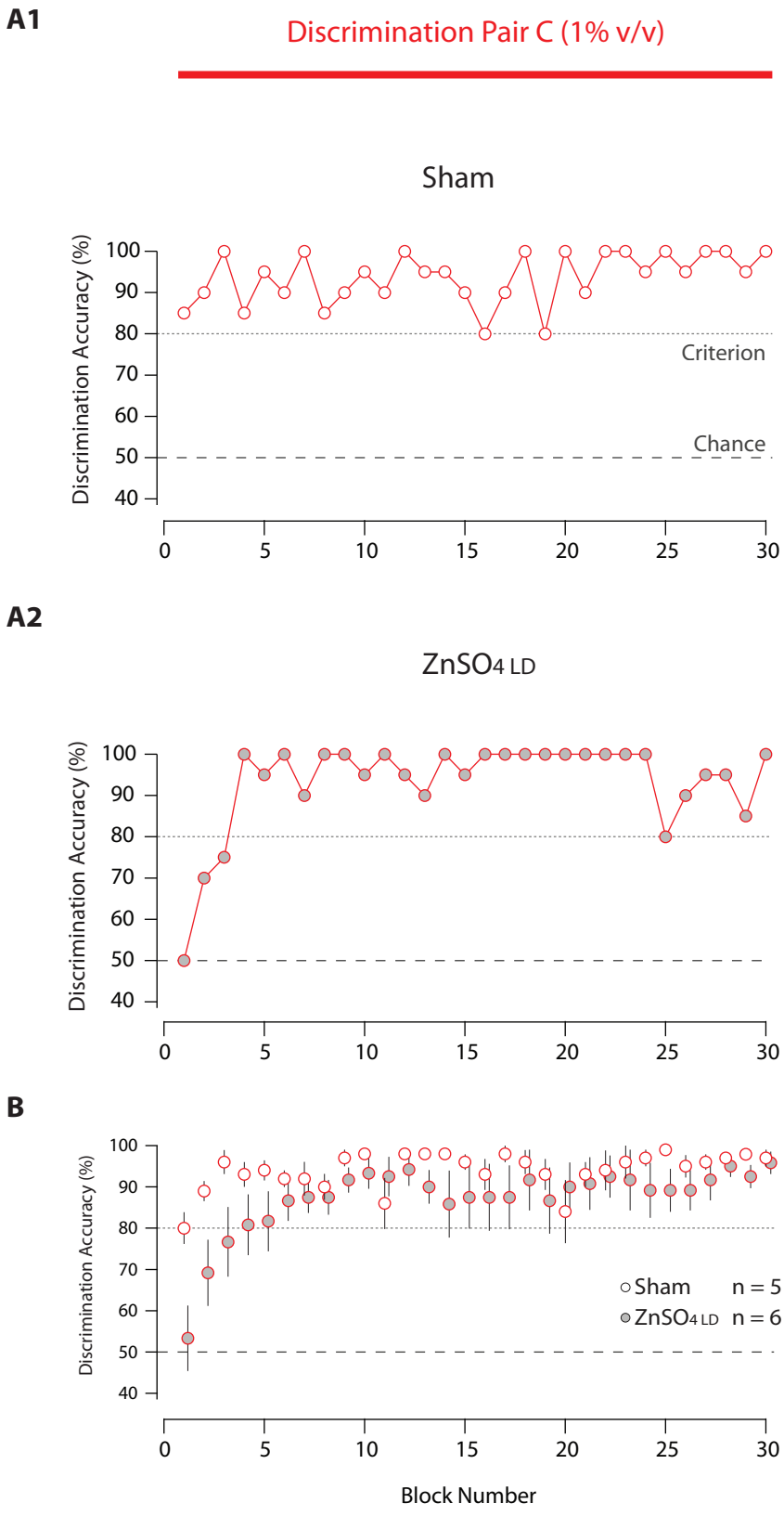

Figure 5.9. Learning of novel odour pairs was impaired by $ZnSO_4$ LD treatment
A. Example discrimination scores obtained for all 30 blocks of training on novel pair C odours for sham (**A1**, open circles) and $ZnSO_4$ LD-treated (**A2**, grey-filled circles) concentration trained mice.
B. Average discrimination scores obtained for all 30 blocks of training on novel pair C odours for sham (open circles) and $ZnSO_4$ LD-treated (grey-filled circles) concentration-trained mice.

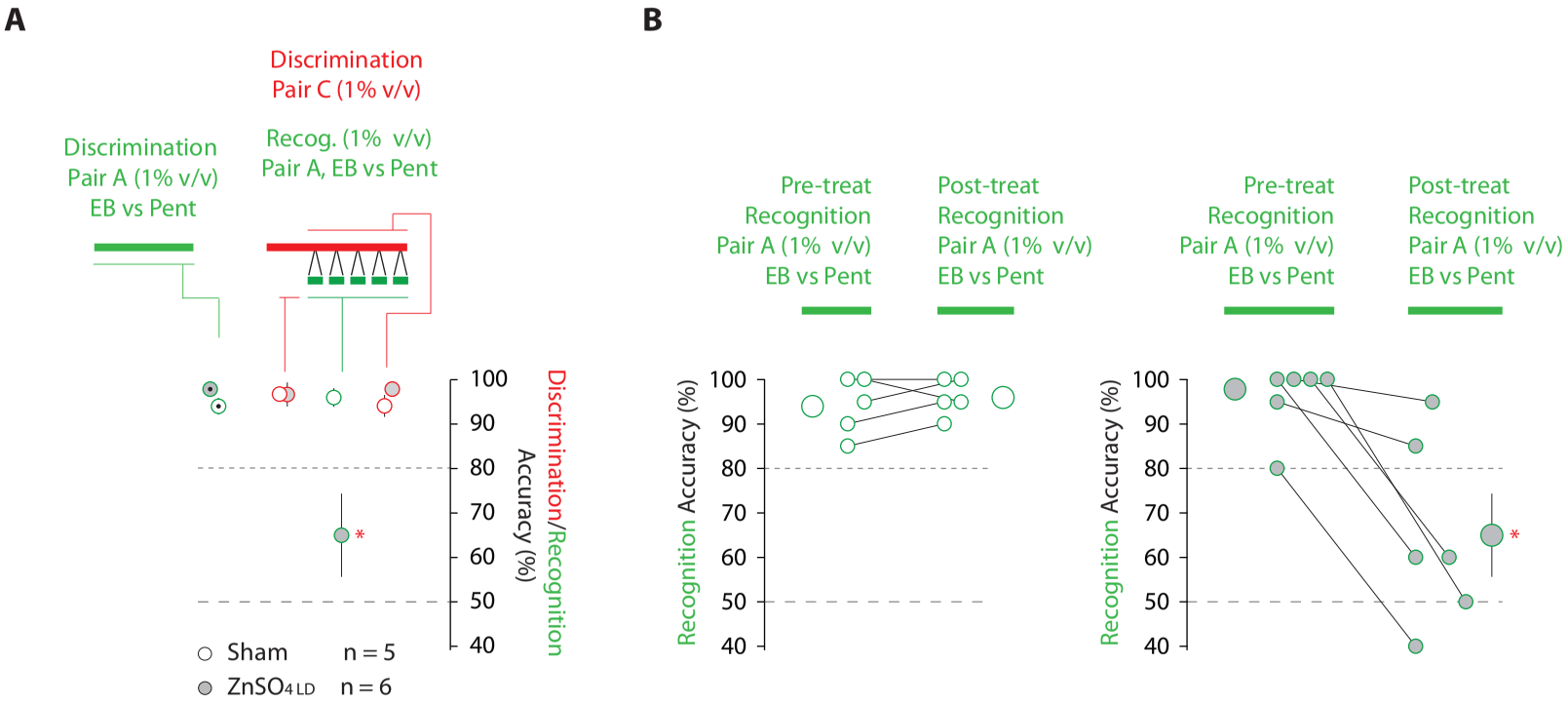

Figure 5.10. $ZnSO_4$ LD treatment caused reductions in recognition score despite concentration training

A. Average recognition scores obtained for familiar pair A odours (green circles, right) in concentration trained mice. Discrimination scores for the average of the last five blocks of pair A odours (dotted green circles), discrimination scores for pair C odours for the block immediately prior to (red circles, left) and those trials presented during recognition testing (red circles, right), all indicated by thin red and green lines. Sham (open circles, n = 5) and $ZnSO_4$ LD-treated animals (grey-filled circles, n = 6), are also plotted.

B. Left, individual recognition scores for pair A odours before (open green circles, left) and after sham treatment (open green circles, right) from concentration trained mice. Large circles are averages. Right, as above for $ZnSO_4$ LD-treated concentration trained mice (grey-filled circles).

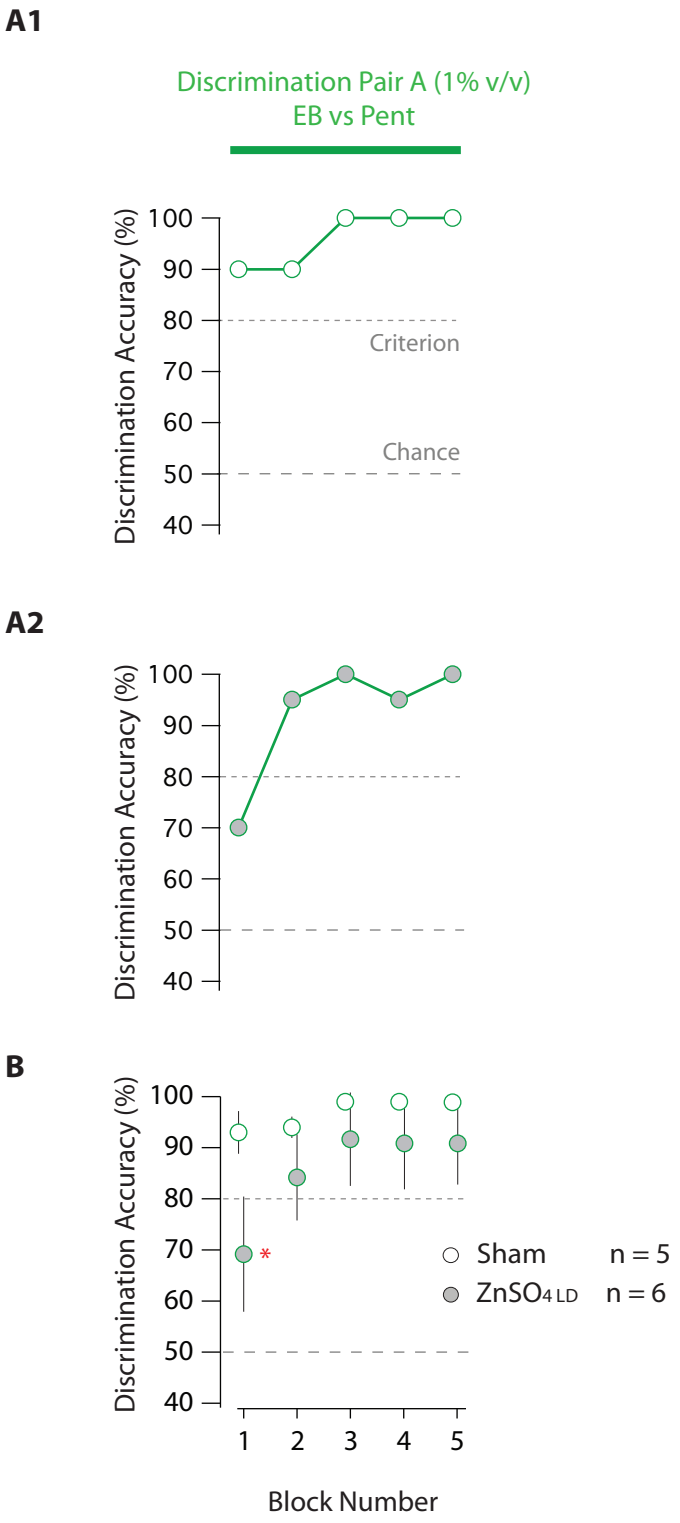

Figure 5.11. $ZnSO_4$ LD treatment caused mild impairments in ability to discriminate previously experienced odours

A. Example discrimination scores for previously familiar 1% v/v pair A odours in concentration-trained mice treated with either sham (**A1**, green, open circles) or $ZnSO_4$ LD (**A2**, grey-filled circles).

B. Average discrimination scores for previously presented 1% v/v pair A odours in concentration-trained mice treated with either sham (green, open circles) or $ZnSO_4$ LD (grey-filled circles).

Thus, concentration training did not allow mice to generalise across changes to incoming odour representations caused by $ZnSO_{4\ LD}$-treatment. This suggests that $ZnSO_{4\ LD}$-treatment significantly altered the perception of incoming odour stimuli, and that it alters apparent odour quality rather than apparent odour concentration.

5.3. Discussion

5.3.1. The effects of reduction of odour concentration on odour discrimination and recognition behaviour in mice

A parsimonious alternative explanation for impairments in recognition and discrimination after $ZnSO_{4\ LD}$-treatment could be that nasal irrigation resulted in a homogenous loss in the number of functional ORNs innervating glomeruli. In this scenario, $ZnSO_{4\ LD}$-treatment may impair recognition by causing familiar odours to be perceived at a novel, reduced concentration. In order to test this hypothesis, it first needed to be determined if presenting odours at concentrations substantially lower than concentrations mice had been trained on also reduced recognition score in the context of the go/no-go behavioural paradigm. Results indeed showed that training mice to discriminate an odour pair at one concentration, then testing their ability to recognise the same odour pair at a concentration reduced 20 - 100 fold from the trained concentration resulted in a significant reduction in recognition score. Reduced concentrations were not below detection thresholds because, when previously familiar odours presented at reduced concentrations were rewarded, mice rapidly learned to discriminate between them. This is in line with others studies, which found that mice can detect odours at least two orders of magnitude lower than the lowest concentration of ethyl butyrate and pentanal used here (B. M. Slotnick et al., 1989; N. Bodyak and B. Slotnick, 1999).

This suggests that, at concentrations 20 - 100 fold lower than an entrained odour, perception of that stimulus is significantly altered. In agreement with these data, rodents have been reported not to automatically generalise across

concentrations that deviate more than tenfold from an entrained odour (N. Uchida and Z. F. Mainen, 2008; R. Homma et al., 2009; T. A. Cleland et al., 2012). This suggests that the identity of some odorants is not necessarily inherently encoded by the olfactory system over their full range of detectable concentrations and may have to be learned.

Thus, presenting odours of reduced concentration during recognition testing was a crucial control to demonstrate that mice responded to odours differently after large changes in concentrations in the context of the go/no-go behavioural paradigm. However, it was not possible to determine definitively from these olfactory tests, whether the alteration in input caused by $ZnSO_{4\ LD}$ caused a change in odour perception comparable to reduction of odour concentration.

5.3.2. The effects of concentration training on recognition of familiar odours presented at novel, reduced concentrations

Concentration-trained mice responded with high recognition scores when presented with a familiar odour presented at an unfamiliar concentration, suggesting they could generalise across a larger range of odour concentrations than non-concentration-trained mice. This supports observations that representations of entrained odours are labile and can be expanded or perhaps fused with other representations depending on conditioning or experience (T. A. Cleland et al., 2012).

5.3.3. The effects of concentration training on odour recognition sham- and $ZnSO_4$-treated mice

It was not possible to determine definitively from the tests used in chapter three and section 5.2.1 of this chapter whether the alteration in input caused by $ZnSO_{4\ LD}$ caused a change in odour perception comparable to reduction of odour concentration. However, concentration-trained mice generalised when presented with odours of reduced concentrations before lesion, but not after lesion, when presented with familiar odours at familiar concentrations (1 % v/v), which suggests that $ZnSO_{4\ LD}$-treatment did not cause a change in perception equivalent to reducing odours more than 100-fold. Therefore, lesions caused by $ZnSO_{4\ LD}$ probably changes aspects of odour quality rather than apparent concentration.

Chapter Six: The effect of concentration reduction on odour-evoked glomerular activity maps

6.1. Introduction

Differences in perception should arise from observable differences in neural activity. If $ZnSO_{4\ LD}$-treatment resulted in a previously-presented odorant being perceived as novel and not merely reduced in concentration, one would expect the glomerular activity map altered by $ZnSO_{4\ LD}$-treatment to be changed in a manner that did not reflect map changes observed by varying odour concentrations. As a test of this assumption, intrinsic signals evoked by various concentrations of the recognition test odours were recorded in a group of naïve mice.

6.2. Results

6.2.1. The effects of concentration reduction on odour-evoked glomerular activity maps

Intrinsic signal maps evoked by ethyl butyrate and pentanal presented at varying concentrations were recorded from a group of naïve mice distinct from those used in previous chapters **(Figures 6.1, 6.2A - D)**. Intrinsic-signal activity maps recorded at 1 % v/v odour concentrations in session one were correlated with activity maps evoked by various concentrations recorded in session two **(Figure 6.3A - D)**. Over the range of concentrations recorded, dissimilarity scores for maps evoked by 1 % v/v odours in session one and those evoked by varying odour concentrations in session two were not significantly different from dissimilarity scores for maps evoked by 1 % v/v odour presentation in both sessions (session one 1 % v/v vs. session two 1 % v/v, 0.08 ± 0.05, n = 8; session one 1 % v/v vs. session two 0.1 % v/v, 0.20 ± 0.11, n = 6, $p > 0.206$; session one 1 % v/v vs. session two 0.05 % v/v, 0.155 ± 0.09, n = 8, $p > 0.677$. Session one 1 % v/v vs. session two 0.01 % v/v, 0.23 ± 0.11, n = 8, $p > 0.902$, **Figures 6.3A - D, 6.4**). This suggests that intrinsic signals did not change substantially over this range of concentrations.

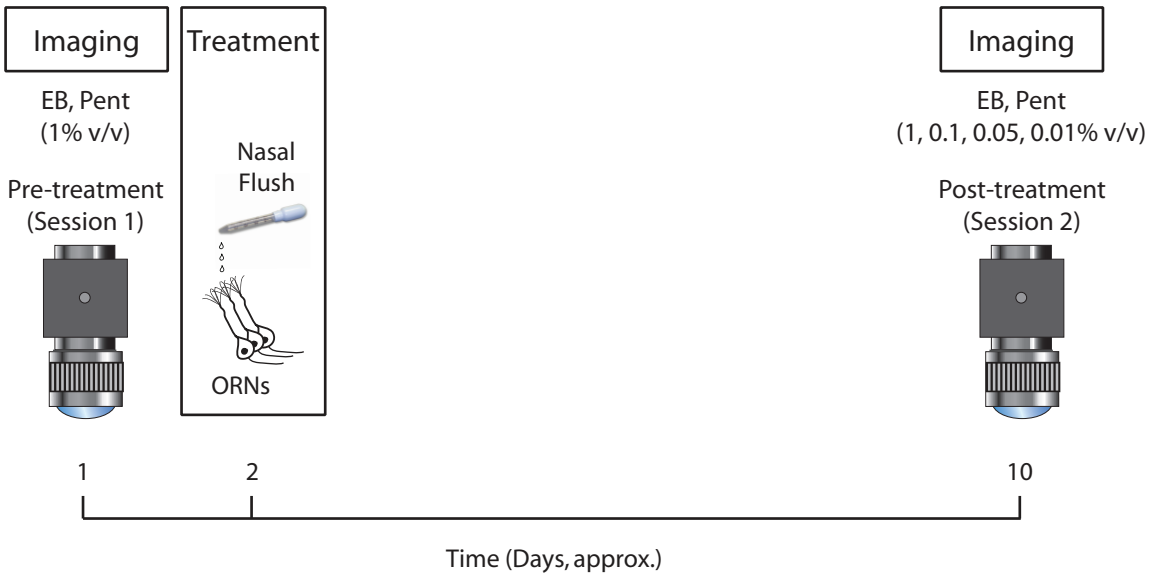

Figure 6.1. Imaging protocol for odours of various concentrations
Approximate timing of imaging protocol in mice in which intrinsic signals were evoked by odours of different concentrations is shown. Odours used were ethyl butyrate and pentanal at concentrations of 1 % v/v in session one and 1%, 0.1 %, 0.05 % and 0.01 % v/v in session two.

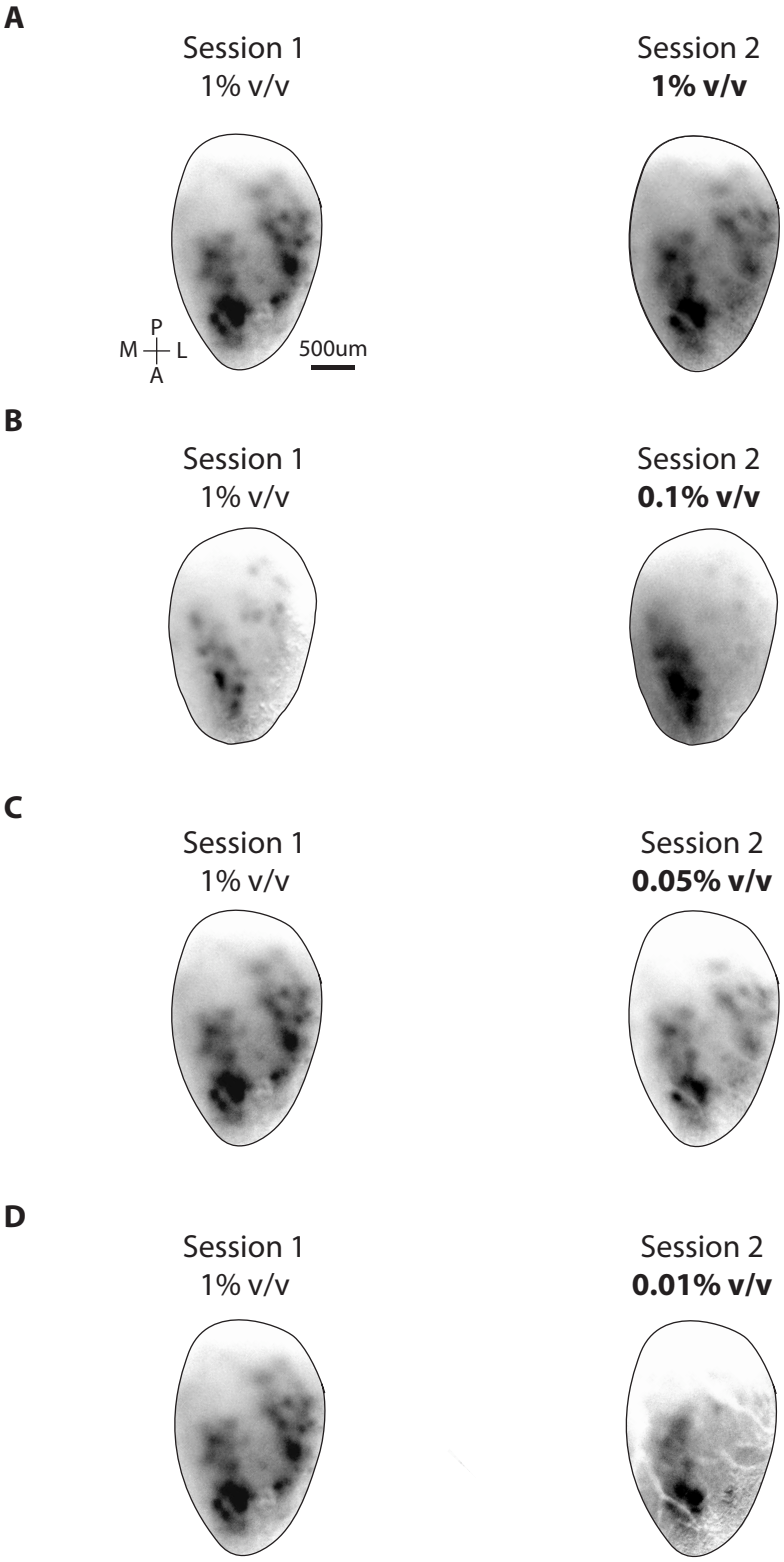

Figure 6.2. Example activity maps evoked by different odour concentrations
A. Maps evoked before sham treatment by 1% v/v odours in session one (left) and by 1% v/v odours in session two (right), after sham treatment.
B-D. As in **A**, where odours in session two were 0.1% **(B)**, 0.05% **(C)** and 0.01% v/v **(D).** Maps in panel **B** were recorded from a different animal than those in **A**, **C** and **D**.

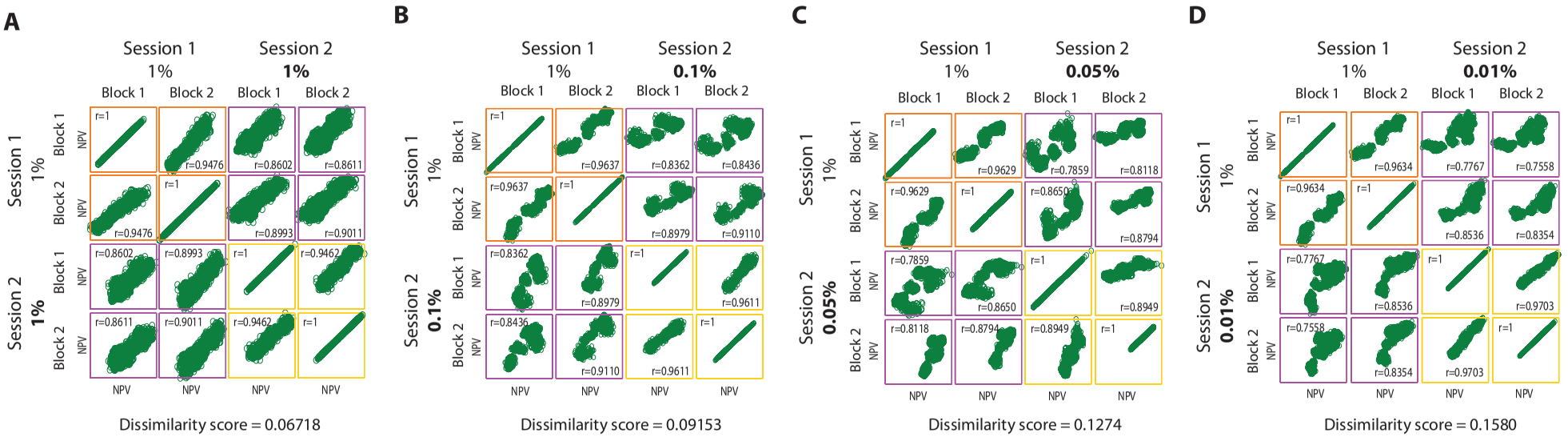

Figure 6.3. Reduction in concentration did not significantly alter activity maps

A. Example scatter plots of ROI correlations from odour-evoked activity maps recorded where odours used to evoke activity in session one were 1 % v/v, and in session two were 1 % v/v. Within session one correlations (orange boxes), within session two correlations (yellow boxes), across session correlations (purple boxes). Values for each ROI (green clusters) are expressed as normalized pixel value (NPV), r-values displayed are averages of all ROI correlations for each block comparison. NPV range; 0.9962483 - 1.000171. **B - D.** As above for activity maps evoked in session one by 1 % v/v odours and in session two by 0.1 % **(B)**, 0.05 % **(C)** and 0.01 % v/v **(D)** odours. NPV range as follows; 0.1 %, 0.9907591–0.9993034, 0.05 %, 0.9954119 - 1.001823, 0.01 % 0.9907591 – 1.000166.

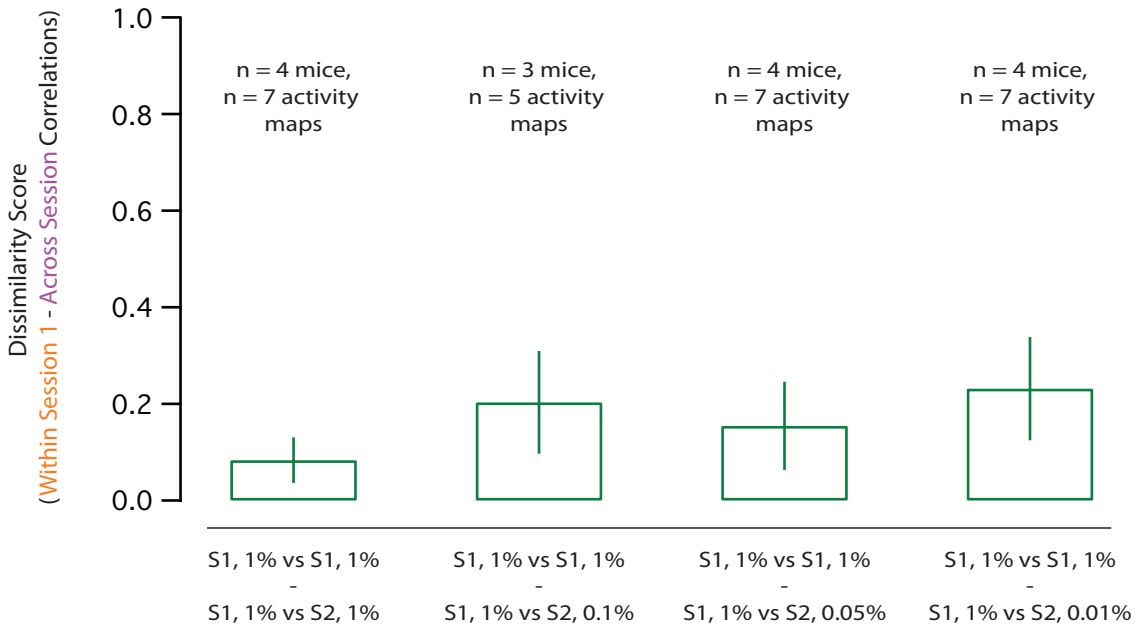

Figure 6.4. Reduction in concentration did not significantly alter dissimilarity score
Average dissimilarity scores for activity maps evoked by 1 % v/v odours in session one (S1) and 1 %, 0.1 %, 0.05 % and 0.01 % v/v odours in session two (S2).

6.2.2. The effects of change in concentration and $ZnSO_{4\ LD}$ treatment on relative glomerular intensity

Changes in correlation may originate from a loss of activity, a change in activity patterns, or a combination of the two. Reduction in dissimilarity scores after filtering out within session correlations lower than 0.5 (Figure 4.5B) suggested that there was a significant reduction in signal after $ZnSO_{4\ LD}$-treatment. However, changes in correlation may also have originated from changes in the relative levels of glomerular input. To determine if $ZnSO_{4\ LD}$-treatment also caused a major change in relative levels of glomerular activity, ROIs from all activity maps recorded in treated animals (chapter 4, section 4.2) were thresholded so that only those containing signal in both session one and two remained (see materials and methods). The intensity value of each ROI was then averaged across blocks within session one, normalised to 1 and rank ordered. Session two ROIs were then plotted in the order determined by the rank in session one and normalised to 1 **(Figure 6.5A1)**. Session two values were then subtracted from session one values to yield a *subtraction value* which represented the extent of change in relative intensity across sessions for the entire activity map **(Figure 6.5A2)**. ROI pixel intensity maps were also generated to emphasise the change in rank between session one and session two, indicated by the change of size and colour of an ROI-related spot **(Figure 6.5A3)**. Subtraction values for all ROIs were then compiled and the population statistics determined **(Figure 6.5B)**. In this analysis, a larger variance reflected a larger change in relative ROI intensity across sessions. For all odour-evoked activity maps that contained ROI activity, no reliable changes in the relative intensities of ROIs across concentrations were observed (1 % v/v session one -

1 % v/v session two, inter-quartile range, 0.20, n = 7; session two, 0.1 % v/v, 0.17, n = 5, p > 0.60; session two, 0.05 % v/v, 0.19, n = 7, p > 0.97; session two, 0.01 % v/v, 0.25, n = 7 p > 0.83, **Figure 6.5A, B)**. This is consistent with experiments that show that relative glomerular intensity remains constant over a moderate range of concentrations (M. Wachowiak et al., 2000; M. Wachowiak et al., 2002). In contrast, $ZnSO_{4\ LD}$-treatment produced a marked change in relative ROI intensity across sessions compared to shams (sham, inter-quartile range, Q1 – Q3, 0.24, n = 15, vs. $ZnSO_{4\ LD}$-treatment, 0.48, n = 9, p < 0.0004, **Figure 6.6A - C)**. N.b. Activity maps from mice evoked by different odour concentrations were naïve, those evoked before and after $ZnSO_{4\ LD}$ or sham treatment were taken from the same group containing both naïve and trained animals used to determine dissimilarity scores in section 4.2, figure 4.4.

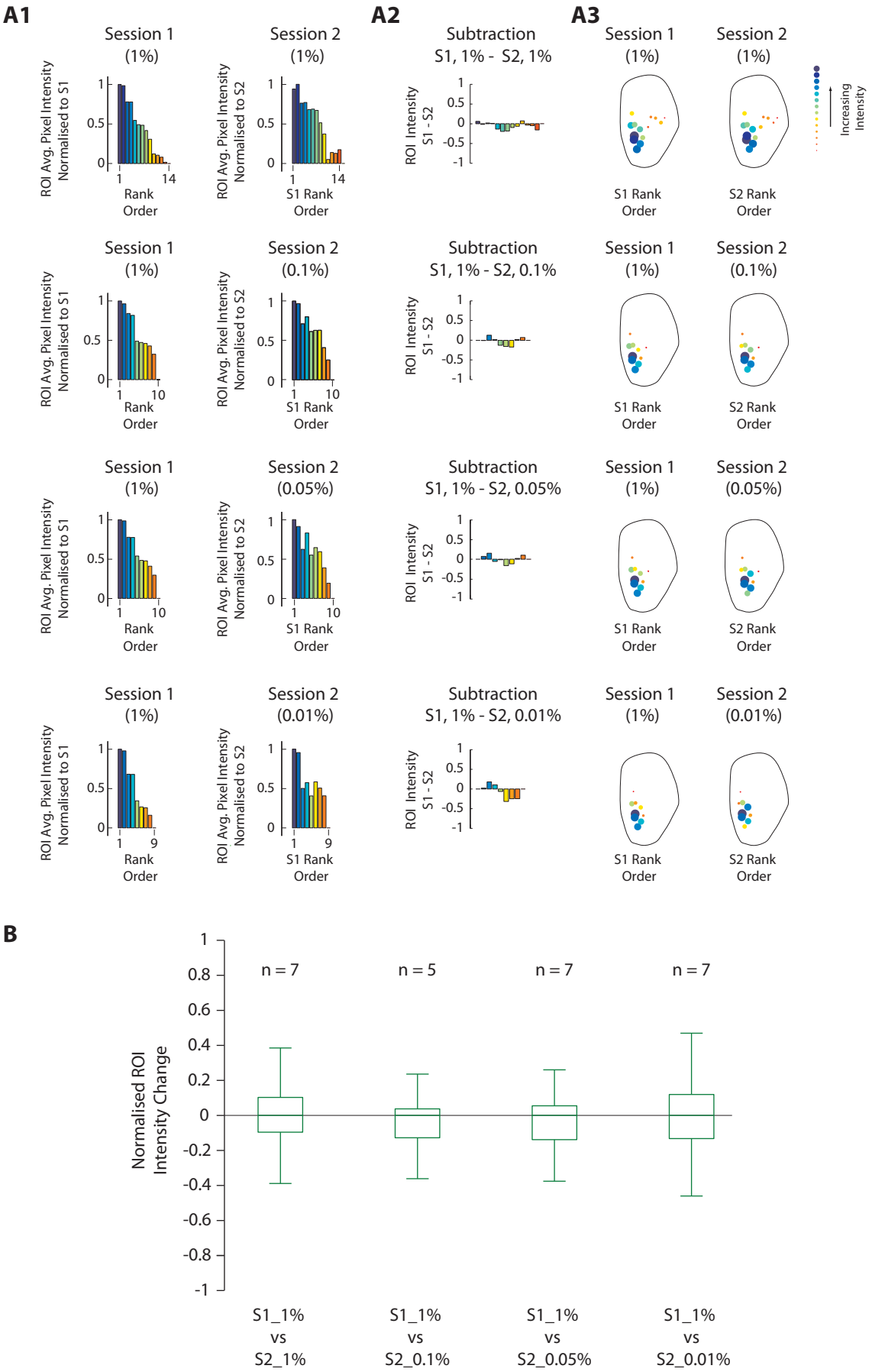

Figure 6.5. Reduction of concentration did not significantly alter relative glomerular intensity (continued overleaf)

Figure 6.5. Reduction of concentration did not significantly alter relative glomerular intensity (Continued)

A1. Left, Example bar graphs of ranked average pixel intensity for each ROI evoked in session one (S1) by 1 % v/v odours. ROI intensity is normalised to the maximum ROI in session one. Right, Example bar graph of ranked average pixel intensity for each ROI evoked in session two (S2) by either 1 %, 0.1 %, 0.05 % or 0.01 % v/v odours. ROI intensity is normalised to the maximum ROI from session two.

A2. Subtraction of session two ROI intensity values from session one values.

A3. Average ROI pixel intensity map; large blue spots have the highest average pixel intensity, small, orange spots have the lowest average pixel intensity. Change in average pixel intensity rank between session one (left) and session two (right) is indicated by change of size and colour of an ROI spot.

B. Normalized ROI intensity change for subtraction values of all ROIs. Medians have been normalised to 0. Boxes indicate the first (bottom) and third (top) quartile. Whiskers extend to the most extreme data values within the range q1 – 1.5 x (q3 – q1) to q3 + 1.5 x (q3 – q1), where q1 and q3 are the 25th and 75th percentiles, respectively.

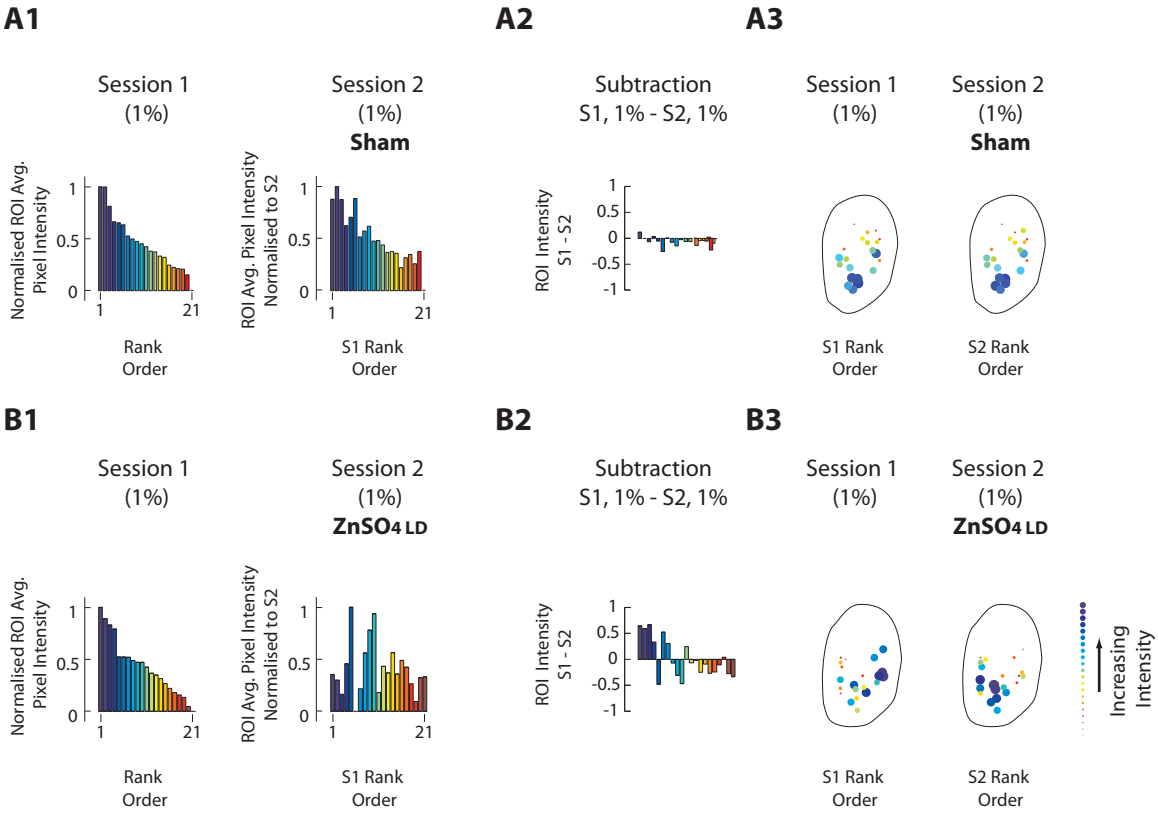

Figure 6.6. $ZnSO_4$ LD treatment significantly altered relative glomerular intensity

A1. Left, Example bar graph of ranked average pixel intensity for each ROI evoked in session one (S1). ROI intensity is normalised to the maximum ROI in session one by 1% v/v odours. Right, Example bar graph of ranked average pixel intensity for each ROI evoked after sham treatment in session two (S2) by 1% v/v odours. ROI intensity is normalised to the maximum ROI from session two.

A2. Subtraction of session two ROI intensity values from session one values from sham-treated animals.

A3. Average ROI pixel intensity map; large blue spots have the highest average pixel intensity, small, orange spots have the lowest average pixel intensity. Change in average pixel intensity rank between session one (left) and session two (right) is indicated by change of size and colour of an ROI spot.

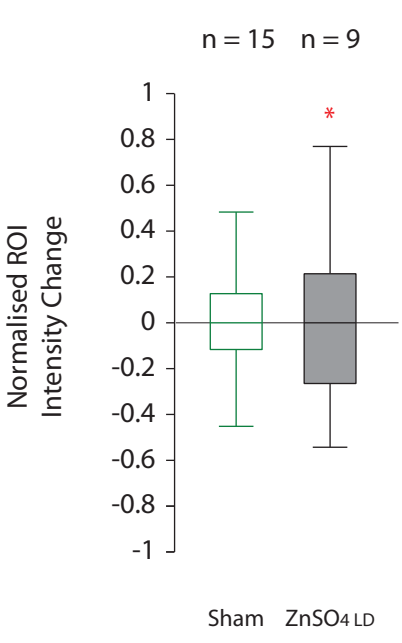

B1-B3. Example as above for activity maps recorded in sessions 1 and 2 from a $ZnSO_4$ LD-treated animal.

C. Normalised ROI intensity change for subtraction values of all ROIs for sham (green box) and $ZnSO_4$ LD-treated animals (grey-filled box). Medians have been normalised to 0. Boxes indicate the first (bottom) and third (top) quartile. Whiskers extend to the most extreme data values within the range q1 – 1.5 x (q3 – q1) to q3 + 1.5 x (q3 – q1), where q1 and q3 are the 25th and 75th percentiles, respectively.

6.3. Discussion

6.3.1. The effects of concentration reduction on odour-evoked glomerular activity maps

Qualitatively, changes were observed in intrinsic-optical signals over the range of concentrations recorded as glomerular responses became more pronounced at higher concentrations. Despite this, changes were not great enough to cause a significant change in dissimilarity score for any of the concentrations tested. Map similarity between imaging blocks of different concentrations was not caused by contamination, because entirely separate odour lines were used to deliver odours (**Materials and Methods, Figure 2.1B, Appendix**). Odour maps are thought to change with increasing concentration as some olfactory receptor populations with lower affinities for odorants are recruited and others respond more intensely (B. A. Johnson et al., 1999; B. D. Rubin and L. C. Katz, 1999; M. Meister and T. Bonhoeffer, 2001; H. U. Fried et al., 2002; H. Spors and A. Grinvald, 2002; H. Spors et al., 2006; R. M. Carey et al., 2009; M. L. Fletcher et al., 2009; R. Homma et al., 2009). One might expect slightly larger variations in dissimilarity scores over 100 – fold changes in concentration However, odour maps remain moderately stable over 10 – 100 - fold changes in concentration, similar to the range used in the data presented here (0.01% -5%: (B. D. Rubin and L. C. Katz, 1999; N. Uchida et al., 2000; M. Wachowiak et al., 2000; H. U. Fried et al., 2002; M. Wachowiak et al., 2002).

Recordings based on calcium sensitive dyes are thought to reflect neural activity more faithfully than intrinsic imaging, as fluorescent probes can be

loaded specifically into ORNs by perfusion of the naris (D. W. Wesson et al., 2008a, 2008a). When intrinsic signals and calcium signals were compared in the same bulb, intrinsic optical signals had a smaller dynamic range over concentration changes than calcium signals and saturated at comparatively lower concentrations (M. Wachowiak and L. B. Cohen, 2003). This discrepancy is thought to be due to intrinsic signals reporting activity in second order neurons (E. Chaigneau et al., 2007) and from neural activity at higher concentrations becoming uncoupled from the haemodynamic changes that are thought to underlie the signal. This may account to some extent for the lack of difference in dissimilarity score between different concentrations. At the lowest concentration recorded (0.01% v/v), dissimilarity scores were high compared to the highest concentration (1 %v/) although not significantly different, suggesting that if signals recorded at even lower concentrations had been recorded, dissimilarity scores would have reached significance.

Dissimilarity scores were not altered dramatically over concentration, but recognition scores were significantly impaired when mice were challenged with unfamiliar concentrations of familiar odours reduced 100-fold. This may in part be due to the relative insensitivity of intrinsic imaging to smaller changes in concentration however, increasing the number of exposures to conditioned stimuli is known to reduce generalisation in rodents (T. A. Cleland et al., 2007). Thus, after over 600 exposures to pair A odours, highly trained mice may have been less likely to extrapolate over large changes in concentration than naïve mice.

6.3.2. The effects of change in concentration and $ZnSO_{4\ LD}$ treatment on relative glomerular intensity

Comparison of the relative intensity of glomerular activity revealed significant differences between activity maps from $ZnSO_{4\ LD}$-treated animals and those recorded in shams or evoked by different concentrations. Relative glomerular intensity is known to change over large concentration ranges (M. Meister and T. Bonhoeffer, 2001; H. U. Fried et al., 2002; H. Spors and A. Grinvald, 2002), but presynaptic readouts of ORN activity show that it is reasonably stable across the 10-100 fold changes in concentration similar to those used in both imaging and behavioural experiments (B. D. Rubin and L. C. Katz, 1999; M. Meister and T. Bonhoeffer, 2001; H. U. Fried et al., 2002; M. Wachowiak et al., 2002; T. A. Cleland et al., 2007).

Conversely, axon tracing studies in the rat show that moderate nasal $ZnSO_4$ irrigation results in irregular sparing of glomerular innervation by ORNs, with glomeruli that contain substantial spared axons often intermingled with glomeruli receiving sparse or no innervation (B. Slotnick et al., 2000). This is likely to alter relative glomerular intensity dramatically. Thus, substantial differences in dissimilarity scores between $ZnSO_{4\ LD}$-treated activity maps and changes in concentration may in part be explained by differences in relative glomerular intensity.

As $ZnSO_{4\ LD}$-treatment significantly altered relative glomerular intensity, maintenance of comparative levels of glomerular activity may be a crucial factor for determining the stability of perceived odour identity. This is in agreement

with processing steps thought to occur in the OB, which may maintain relative levels of glomerular activity even after widespread normalisation of glomerular outputs (J. L. Aungst et al., 2003; T. A. Cleland et al., 2007; T. A. Cleland et al., 2012).

Chapter Seven: Comparison of discrimination of novel and previously experienced odours after $ZnSO_4$ treatment

7.1. Introduction

Results from discrimination tasks showed that $ZnSO_{4\ LD}$-treatment not only altered the recognition of previously familiar odours but also the ability to learn to discriminate novel odours. Thus, in this chapter, data from concentration and non-concentration trained mice were pooled to compare the overall impact of $ZnSO_{4\ LD}$-treatment on the time-course of discrimination learning for novel (pair C) odours after treatment, and previously experienced but no longer recognised odours after treatment (pair A or B odours; ethyl butyrate vs. pentanal).

7.2. Results

Learning curve data obtained from concentration trained and non-concentration trained mice in chapters 3 and 4 was first pooled. As sham-treated mice often started discrimination training of a novel odour pair with reduced discrimination scores, differences in learning curves were usually only apparent after a few blocks of training (e.g. **Figure 3.4,** chapter three). Thus, learning curves were plotted to align both concentration trained and non-concentration trained groups to the first block when shams from both groups reached criterion on average (**Figure 7.1A - C**). There was no significant difference between sham and $ZnSO_{4\ LD}$-treated mice on pair B odours before treatment (ANOVA, first five blocks, $F(1, 118) = 0.52$, $P > 0.47$, n = 12 shams, n = 12 $ZnSO_{4\ LD}$-treated mice, and see **Figure 7.1A** for block by block t-test comparisons). After treatment, $ZnSO_{4\ LD}$-treated mice performed significantly worse than shams on novel pair C odours (ANOVA, first five blocks, $F(1, 118) = 9.07$, $P < 0.004$, **Figure 7.1B**) corroborating earlier observations that the ability to discern odours was initially impaired in these animals. Discrimination of previously experienced (pair A/B, ethyl butyrate vs. pentanal) odours by $ZnSO_{4\ LD}$-treated animals was also initially impaired compared to shams but improved far more quickly than novel (pair C) odours (pair A/B post-lesion first block, shams, 89.5 ± 2.20 %, n = 12, $ZnSO_{4\ LD}$-treated, 70.21 ± 5.54 %, n = 12, $p < 0.002$, second block, shams, 93.33 ± 1.98 %, $ZnSO_{4\ LD}$-treated, 88.33 ± 4.37 %, $p > 0.15$,

Figure 7.1C).

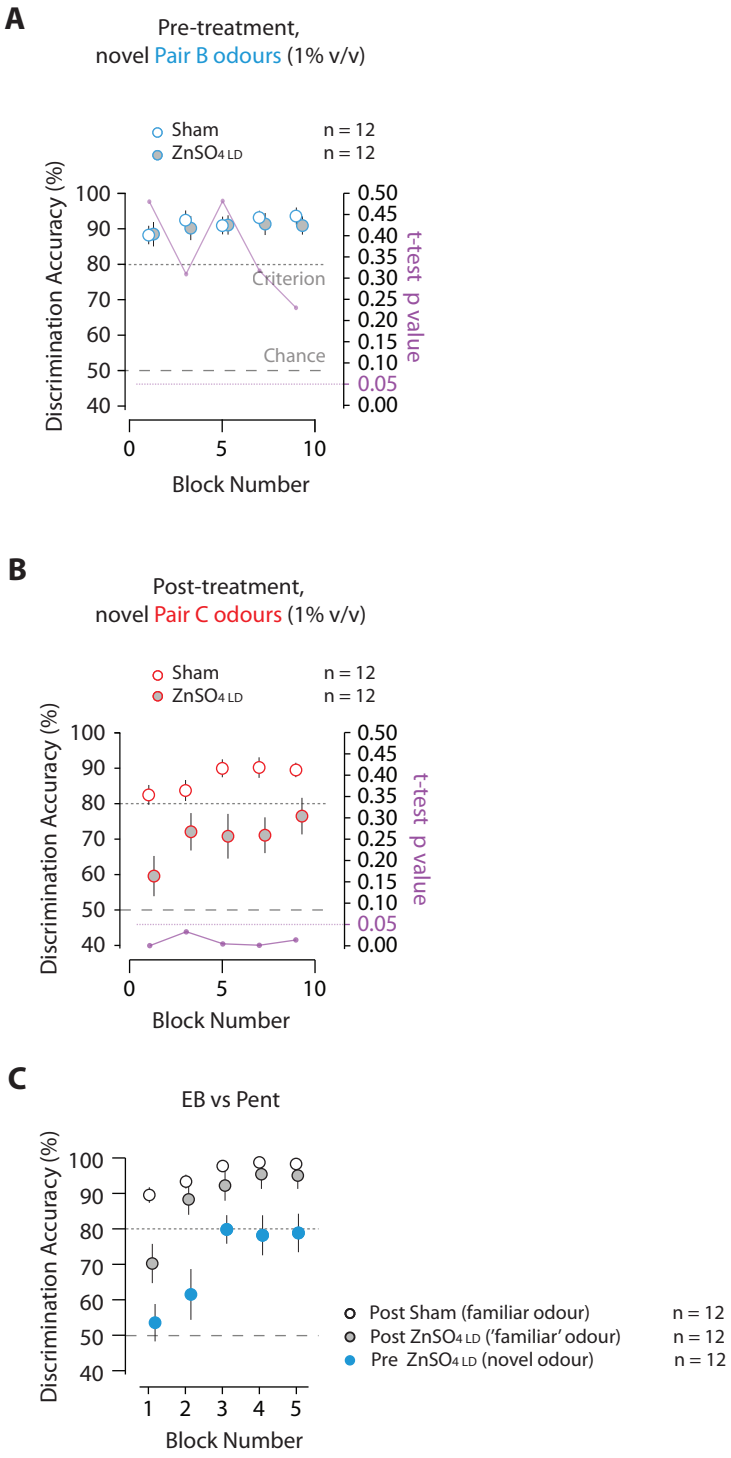

Figure 7.1. Mice responded to previously experienced and novel odours differently after lesion

A. Pre-treatment discrimination learning for the first five blocks of pair B odours plotted according to the first block when shams reached criterion. Purple circles indicate p values for t-tests between sham and $ZnSO_4$ LD-treated groups for each block.

B. Post-treatment discrimination learning for first five blocks of pair C odors plotted according to the first block when shams reached criterion. Purple circles indicate p values for t-tests performed between sham and $ZnSO_4$ LD-treated groups for each block.

C. Post-treatment discrimination learning scores for ethyl butyrate and pentanal for $ZnSO_4$-LD treated (grey-filled circles) and shams (open circles). Also plotted are discrimination learning scores for novel (1 % v/v) ethyl butyrate and pentanal presented prior to lesioning (blue-filled circles).

Discrimination scores for the first five blocks of discrimination training on previously experienced odours (ethyl butyrate vs. pentanal) after $ZnSO_{4\ LD}$-treatment were also significantly higher than for discrimination of the same odour pair before treatment (ANOVA, $F(1,118) = 12.68$, $P < 0.0005$, **Figure 7.1C**). This reflects the notion that pair B odours were perceived as partially familiar after treatment rather than being perceived as completely novel but being rapidly learnt.

These data support evidence presented in previous chapters that $ZnSO_{4\ LD}$-lesion of the epithelium causes maps to be altered such that previously experienced odours are no longer recognised. Furthermore, $ZnSO_4$-treatment prolonged discrimination learning for both novel and previously experienced odour pairs. However, discrimination learning of previously experienced odours after treatment was more rapid than for the same odours before treatment. This suggests that, despite being altered, odour maps representing ethyl butyrate and pentanal remained similar enough to pre-treatment maps such that discrimination of previously encountered odours could be 'relearned' more quickly than genuinely novel odours.

7.3. Discussion

As noted in both concentration and non-concentration trained mice, learning to discriminate novel odour pairs both before and after lesioning took significantly longer than "relearning" to discriminate once familiar odours which appeared altered by lesioning. This suggests that, while incoming representations of previously familiar odours are adjusted enough by lesioning such that they are no longer recognised, they may not be perceived as entirely novel either. Thus, quicker relearning of previously familiar odours after lesion may reflect the rapid incorporation of the lesion-altered stimulus maps into an odour template previously established during initial conditioning with the stimulus (T. A. Cleland et al., 2012).

An alternative explanation for quicker pair B learning after treatment could be that lesioning caused pair B odours to be perceived as completely novel but mice somehow learnt to discriminate between them far more quickly than they did pair C odours. However, it is unlikely that pair B odours were perceived as entirely novel because pair B recognition scores were significantly higher than chance.

This implies that $ZnSO_{4\ LD}$-treatment alters incoming odour representations so that they do not quite match stored templates of those odours. A recent study in humans has implicated the piriform cortex in the process of pattern matching (C. Zelano et al., 2011). Human participants were primed to expect a particular odour stimulus, which induced activity in the posterior piriform cortex similar to activity seen when sampling an actual odour stimulus. Thus, pre-stimulus

activity was suggestive of a stored stimulus template. If an unexpected odour stimulus was presented, activity in the posterior piriform cortex became more similar to the actual incoming stimulus, suggesting the piriform cortex is the locus of matching incoming stimuli with stored odour templates (C. Zelano et al., 2011). This study, and the data presented here suggest that, the olfactory system develops prescribed representations of odours during conditioning. Incoming odour stimuli may then be matched to stored templates in the piriform cortex. If these stimuli are altered slightly by lesion, the stored template can be modified with further conditioning to incorporate the incoming odour stimulus.

Chapter Eight: General discussion

8.1. Redundancy of bulbar circuitry

Identifying the functions of neural networks is fundamental to understanding how the brain allows us to perceive our world. The prevailing view, based on lesioning studies, is that the olfactory system requires surprisingly little input to support odour perception (B. Slotnick et al., 2000; B. Slotnick and N. Bodyak, 2002; B. Slotnick et al., 2004; K. McBride and B. Slotnick, 2006). In contrast to these studies, the data presented here in chapters three and four suggest that even moderate disruption of odour representation can cause a marked change in odour-quality perception.

Comparing intrinsic signals evoked by odours of reduced concentrations with those altered by lesion showed that $ZnSO_{4\ LD}$-treatment did not homogenously reduce inputs, but significantly altered relative glomerular intensity. The combinatorial nature of olfactory representation in the OB suggests that relative glomerular activity levels may be a crucial coding motif (T. W. Margrie and A. T. Schaefer, 2003; V. N. Murthy, 2011). In line with this, global normalisation of activity maps across large changes in concentration has been suggested to preserve relative activity (T. A. Cleland et al., 2007), allowing downstream centres to identify odours based on relative ORN responses (R. J. O'Connell and M. M. Mozell, 1969; M. Wachowiak et al., 2002; R. I. Wilson and Z. F. Mainen, 2006; T. A. Cleland et al., 2007). Furthermore, rats are known to

categorise odour mixtures according to the molar ratios of their components over a range of concentrations, implying that comparison of relative levels of activity within the bulb is an important coding feature (N. Uchida and Z. F. Mainen, 2008).

Chemotopic organisation has been proposed to allow local lateral connections in the OB to alter activity of glomeruli with similar MRRs (M. Yokoi 1995; K. Mori 2006). However, the fractured chemotopic representation of odours in the bulb, and lesion studies that remove chemotopic foci (B. M. Slotnick et al., 1987; X. C. Lu and B. M. Slotnick, 1994; B. Slotnick and N. Bodyak, 2002), suggest that lateral inhibition may act via more specific connections with other glomeruli that are not distance dependent (D. C. Willhite et al., 2006; A. L. Fantana et al., 2008; E. R. Soucy et al., 2009). The relevance of chemotopic odour representation was not directly examined here but the reliance of the olfactory system on spatial activity map integrity implies that chemotopic organisation of glomeruli is a crucial component of odour coding. Imprecise chemotopy may still play a role in distance-dependent lateral inhibition if glomeruli within chemotopic domains are more strongly connected than those in different domains (V. N. Murthy, 2011).

In studies where recognition scores were significantly reduced but significantly above chance after lesion, it was argued that perception of familiar stimuli was not significantly altered (S. Bisulco and B. Slotnick, 2003; S. L. Youngentob et al., 2006). However, any significant deficit in recognition score, even if significantly above chance, implies that alteration in odour representation had

some perceptual effect and therefore that the missing pieces of the incoming stimulus puzzle were not redundant. This implies that sensory systems use all the information afforded them by intricate and unique activity patterns.

In all, this implies that the integrity of odour-evoked spatial activity maps is as important as their subtle, complex nature suggests (B.A. Johnson and M. Leon, 2007). Modelling suggests that at least 50% of the OB circuitry is required for accurate discrimination of complex odour mixtures (A. T. Schaefer and T. W. Margrie, 2012). In line with this, it is probable that lesion studies that found no alterations in olfactory behaviour would have uncovered significant deficits if subjects were; challenged with tests that probed changes in odour recognition, treated with lesions that affect all representations of odours in the OB (B. A. Johnson and M. Leon, 2007), and perception was probed using odours representative of those found in the natural environment, which are not only complex, but are presented in the context of thousands of other complex background odours.

8.2. Perceptual correlates of concentration change

Sensory systems must maintain stimulus identity despite incomplete information or large changes in intensity (G. A. Wright et al., 2005; G. Wallis et al., 2009; D. L. Barbour, 2011; T. A. Cleland et al., 2012). In olfaction, stimulus identity is known to be maintained to some extent across changes in odour concentration (R. Gross-Isseroff and D. Lancet, 1988; N. Uchida and Z. F. Mainen, 2008; R. Homma et al., 2009; T. A. Cleland et al., 2012). The deficit in recognition

scores caused by presenting familiar odours at reduced concentrations observed in chapter five and in other studies (N. Uchida and Z. F. Mainen, 2008; T. A. Cleland et al., 2012) suggests that odours were perceived differently at lower concentrations. However, in human studies, the quality of odours such as benzaldehyde is altered substantially over a range of concentrations (R. Gross-Isseroff and D. Lancet, 1988) while the perceived quality of others such as peppermint is more resistant to changes in intensity (D. Krone et al., 2001). Reduction in recognition scores in mice suggests that the same odour may be perceived as two distinct entities at different concentrations. In this scenario, stored odour templates in the olfactory system encode a discrete range of odour features, including intensity information (T. A. Cleland et al., 2012). Even odours of the same molecular structure are perceived as distinct entities if concentration falls outside this range (R. N. Shepard and J. J. Chang, 1963; R. N. Shepard, 1987; H. J. Duncan et al., 1992; T. A. Cleland et al., 2002; M. L. Fletcher and D. A. Wilson, 2002; C. Linster and T. A. Cleland, 2002; T. A. Cleland and V. A. Narla, 2003; L. M. Kay et al., 2006; N. Mandairon et al., 2006a; T. A. Cleland et al., 2009; M. Leon and B. A. Johnson, 2009; T. A. Cleland, 2010; V. N. Murthy, 2011; T. A. Cleland et al., 2012; O. Escanilla et al., 2012; K. N. Wu et al., 2012).

A number of mechanisms have been proposed to underlie the ability of the olfactory system to generalise across subtle changes in odour stimulus. In the case of concentration invariance, normalisation of ORN inputs by inhibitory interneurons in the glomerular layer is thought to play a role (M. Bonino et al., 1999; V. Aroniadou-Anderjaska et al., 2000; A. Hayar et al., 2005; D. De Saint

Jan et al., 2009). However, M/T cell tuft responses vary more widely than those in their somas over large changes in concentration, (M. Chalansonnet and M. A. Chaput, 1998; M. L. Fletcher et al., 2009; J. Niessing and R. W. Friedrich, 2010), which suggests that normalisation may also occur in the EPL. In agreement with this, global, non-specific lateral inhibition has also been proposed to contribute to concentration-invariant odour representation in the OB (B. A. Johnson and M. Leon, 2000; M. Wachowiak et al., 2002; T. A. Cleland et al., 2007). Proposed mechanisms of pattern decorrelation that rely on lateral inhibition would be likely to alter relative glomerular intensity (M. Yokoi et al., 1995; A. L. Fantana et al., 2008). Imaging data in chapter six suggests that relative glomerular intensity is maintained over a 100 - fold concentration change so it may be important for maintenance of odour identity over changes in intensity (N. Uchida and Z. F. Mainen, 2008). Thus, there may be a trade-off between discriminating highly similar odours, which requires enhancement of differences between glomeruli by pattern decorrelation, and odour identification over changes in intensity mediated by global normalisation, which maintains relative glomerular intensity levels.

8.3. Alteration of stored stimulus templates

Recognition scores for previously familiar pair B odours were significantly decreased after $ZnSO_{4\ LD}$ treatment, which suggests that incoming odour stimuli were significantly altered compared with stored stimulus templates. However, data in chapter seven showed that relearning of pair B odours after $ZnSO_4$ lesion was faster than learning of a novel odour before lesion, suggesting

alterations by $ZnSO_4$ did not cause the odour to be perceived as entirely dissimilar from its pre-treatment identity. This process was most likely to be due to an adaptive mechanism because it did not occur in the absence of reinforcement i.e. during recognition tests. Enantiomers, odour mixtures, odours that evoke similar activity maps and odours of similar concentration are not initially distinguished by rodents in non-associative tasks, (C. Linster et al., 2001b; T. A. Cleland et al., 2002; M. L. Fletcher and D. A. Wilson, 2002; C. Linster et al., 2002; N. Mandairon et al., 2006b; N. Mandairon et al., 2006a; T. A. Cleland et al., 2012) but can be distinguished after discrimination training with reinforcement (B. M. Slotnick and J. E. Ptak, 1977; T. A. Cleland et al., 2002). Furthermore, increasing the number of odour-reward pairings (T. A. Cleland et al., 2009), and environmental odour enrichment are known to reduce generalisation (N. Mandairon et al., 2006b), improving acuity and consequently the ability to discriminate between more similar odours. However, it has been shown more recently that rodents can be trained to generalise across odours too, and that such tasks reduce the ability to discriminate novel odours (J. Chapuis and D. A. Wilson, 2011; T. A. Cleland et al., 2012). A similar process has been observed in humans, where repeated presentation of two odours together increases the probability that one of the odours presented alone will be described as having some of the qualities of its former partner (R. J. Stevenson, 2001). Therefore, stored odour representations may be altered either to enhance the ability to generalise across odours, or to increase acuity, which improves the ability to discriminate odours (D. A. Wilson and R. M. Sullivan, 2011). The lesion data presented in chapter seven shows that this process can also occur in the context of alteration of bulbar odour representations (K. K. Yee

and R. M. Costanzo, 1998; B. Slotnick and N. Bodyak, 2002).

Plasticity in the piriform cortex has been suggested to mediate the ability to improve generalisation or increase acuity (D. A. Wilson, 2000; J. Chapuis and D. A. Wilson, 2011; D. A. Wilson and R. M. Sullivan, 2011). Training rats to discriminate similar odours sharpened single-unit odour receptive fields of anterior piriform cortical (aPCx) pyramidal neurons, while training them to generalise across odours broadened receptive fields (J. Chapuis and D. A. Wilson, 2011). Other studies suggest that aPCx and posterior piriform cortex (pPCx) may play opposing roles in increasing acuity and generalisation respectively (M. Kadohisa and D. A. Wilson, 2006). Odour representations in the aPCx have been reported to become less similar during odour discrimination training (D. A. Wilson, 2000), while neurons in the pPCx show a significant broadening of tuning and increase in correlated population responses (M. Kadohisa and D. A. Wilson, 2006). In agreement with this, studies in humans suggest that the aPCx may encode specific odour molecular structural features (e.g. aldehydes or ketone), while pPCx may encode broader associative features such as odour quality (e.g. cherry or pineapple) (J. A. Gottfried et al., 2006; C. Zelano et al., 2011).

The OB may also be a source of plasticity that alters acuity (W. Doucette and D. Restrepo, 2008). For example, odour exposure and discrimination training has been shown to cause a reduction in M/T cell activity (D. A. Wilson, 1998; M. L. Fletcher and D. A. Wilson, 2003; W. Doucette and D. Restrepo, 2008), which may last for months (H. K. Kato et al., 2012). A potential mechanism for

altering bulbar plasticity is altering the proportion of bulbar neurons that mediate inhibition. GCs and PG cells are known to be replenished throughout the lifetime of an animal (F. Lazarini and P. M. Lledo, 2011) and both odour enrichment and discrimination training coincide with increased survival of local inhibitory neurons when odours used evoke overlapping activity patterns (N. Mandairon et al., 2008; N. Mandairon and C. Linster, 2009). Increased GC numbers may promote M/T cell lateral inhibition, improving pattern decorrelation and thus discrimination acuity (Y. Gao and B. W. Strowbridge, 2009). Apart from neurogenesis, bulbar changes may also be due to changes in downstream centres altering activity of centrifugal inputs of the bulb (W. Doucette and D. Restrepo, 2008). For example, loss of cholinergic inputs to the OB increases generalisation between similar odours (C. Linster et al., 2001a; C. Linster and T. A. Cleland, 2002; D. A. Wilson et al., 2004; N. Mandairon et al., 2006c, 2006c), and olfactory cortex is thought to enhance M/T cell inhibition by enhancing GC activity (A. M. Boyd et al., 2012). This suggests that the perception of an odour is significantly subject to past olfactory experience and behavioural state (D. A. Wilson and R. M. Sullivan, 2011).

8.4. Future Directions

The variability of lesions caused by $ZnSO_{4\ LD}$, 3-MI, MeBr and direct surgical ablation (M. H. Sieck and H. D. Baumbach, 1974; D. H. Matulionis, 1975a, 1975b; B. M. Slotnick and L. A. Gutman, 1977) expose the need for a more precise method for investigating bulbar circuit function. Subsets of ORNs can be targeted by expression of diphtheria toxin under OR promoters (J. A. Gogos

et al., 2000) or by intranasal application of the herbicide dichlobenil, which targets a specific subpopulation of ORNs (V. Vedin et al., 2004). Furthermore, genetic alteration of ion channels in bulbar neurons can be used to investigate the behavioural impact of circuit alteration (N. M. Abraham et al., 2010). The expression of light-activated cation channel ChannelRhodopsin (ChR) in neurons allows transient manipulations of neural circuits (B. R. Arenkiel et al., 2007). The advantage of transient manipulations is that they can be repeated several times in the same animal. Mice can perform discrimination tasks based on activation of ChR expressing ORNs (R. Shusterman et al., 2011). Expression of ChR in ORNs or other bulbar neurons could be used to investigate their relative contributions to bulbar processes. Illumination from a digital mirror device could stimulate specific patterns of glomeruli (A. K. Dhawale et al., 2010) and combination with a head-fixed behavioural and imaging paradigm (D. A. Dombeck et al., 2007) would allow the effects of different manipulations of glomerular patterns on odour perception to be investigated. A *matching to sample* behavioural paradigm (X. C. Lu et al., 1993) would be ideal for such experiments; in this task, an animal receives a reward only if two stimuli presented to it in succession are identical, thus probing recognition of odour quality. Presenting two identical odours, but with the second in the presence of ChR activation could be used to determine the minimal alteration of spatiotemporal bulbar activity that causes a change in perception. The digital mirror device could be used to activate different glomeruli at different strengths, so importance of relative glomerular intensity to odour quality perception and for concentration invariance could be directly investigated. Sniff patterns could be monitored simultaneously to give a parallel

readout of change in odour quality perception. Halorhodopsin, a light-activated chloride channel, could ostensibly be used to reduce ORN activity and mimic lesions. However, ORNs are anomalous in that intracellular chloride levels are maintained at high levels with respect to the outside by a Na+-K+-2Cl− cotransporter, NKCC1 (G. Lowe and G. H. Gold, 1993; J. Reisert et al., 2005), so activation of halorhodopsin expressed in ORNs would be likely to cause depolarisation due to Cl- efflux.

Rodents in their natural habitats are subject to complex and varied odours, and the experiments proposed above could introduce increasingly difficult odours until even sham animals make mistakes (B. M. Slotnick and J. E. Ptak, 1977). Pushing the olfactory system to its limits in this way is likely to reveal much about the function of various circuit motifs and furthermore, determine which features of olfactory processing, if any, are redundant.

8.5. Conclusion

The findings presented here are at odds with the widely held view that the olfactory system makes little use of the detailed information in odour-evoked activity maps. Furthermore, they support work that shows that stored stimulus templates are labile and can be expanded to incorporate altered stimuli depending on experience (N. Mandairon et al., 2006b; N. Mandairon et al., 2006a; O. Escanilla et al., 2008; N. Mandairon and C. Linster, 2009; J. Chapuis and D. A. Wilson, 2011; T. A. Cleland and C. Linster, 2012; O. Escanilla et al., 2012). Acknowledgement that the olfactory system is a highly sensitive detection system that uses all available sensory inputs to form representations

should inform study of the detailed circuitry that underlies olfactory perception. From a clinical perspective, impairment of olfactory function is thought to precede the onset of neurodegenerative diseases such Parkinson's (R. L. Doty, 2012) or Alzheimer's (R. S. Wilson et al., 2009; W. Li et al., 2010). More sensitive behavioural methods for testing rodent models of disease may help advance understanding of these debilitating illnesses.

Appendix

A

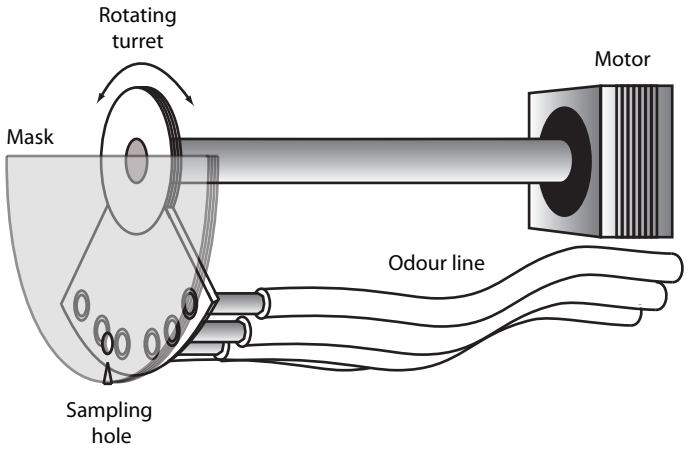

B

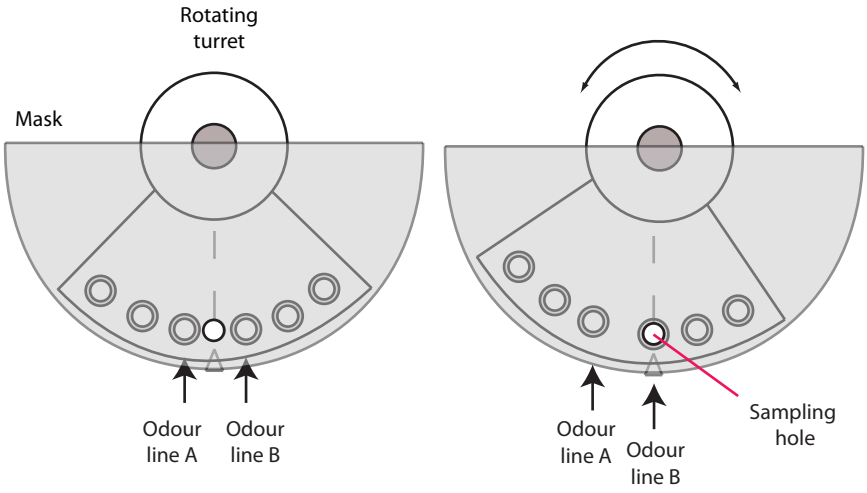

Rotating odour delivery system

A. Odours can anneal to the common joints in the tubing of olfactometers and need several minutes to be flushed effectively (B. M. Slotnick and B. J. Nigrosh, 1974). A mechanised delivery device was therefore designed to ensure all odours were kept in separate delivery channels until stimulus delivery at the odour sampling port.

B. The rotating turret aligned an odour line to the sampling hole, which opened onto the sampling port of the olfactometer Perspex chamber. A mask blocked the view of rotating parts to ensure movements did not provide visual cues. Delivery lines were alternated whenever odours were replaced, i.e. every 20 blocks.

References

Abraham NM, Spors H, Carleton A, Margrie TW, Kuner T, Schaefer AT (2004) Maintaining accuracy at the expense of speed: stimulus similarity defines odor discrimination time in mice. Neuron 44:865-876.

Abraham NM, Egger V, Shimshek DR, Renden R, Fukunaga I, Sprengel R, Seeburg PH, Klugmann M, Margrie TW, Schaefer AT, Kuner T (2010) Synaptic inhibition in the olfactory bulb accelerates odor discrimination in mice. Neuron 65:399-411.

Alberts JR, Galef BG, Jr. (1971) Acute anosmia in the rat: a behavioral test of a peripherally-induced olfactory deficit. Physiol Behav 6:619-621.

Andine P, Axelsson R, Jacobson I (1995) The effect of anosmia on MK-801-induced behaviour in mice. Neurosci Lett 190:113-116.

Antonini A, Fagiolini M, Stryker MP (1999) Anatomical correlates of functional plasticity in mouse visual cortex. J Neurosci 19:4388-4406.

Archunan G, Dominic CJ (1990) Stud male protection of implantation in food-deprived mice: evaluation of the involvement of olfactory-vomeronasal systems. Exp Clin Endocrinol 96:30-36.

Arenkiel BR, Peca J, Davison IG, Feliciano C, Deisseroth K, Augustine GJ, Ehlers MD, Feng G (2007) In vivo light-induced activation of neural circuitry in transgenic mice expressing channelrhodopsin-2. Neuron 54:205-218.

Arevian AC, Kapoor V, Urban NN (2008) Activity-dependent gating of lateral inhibition in the mouse olfactory bulb. Nat Neurosci 11:80-87.

Armstrong CM, DeVito LM, Cleland TA (2006) One-trial associative odor learning in neonatal mice. Chem Senses 31:343-349.

Aroniadou-Anderjaska V, Ennis M, Shipley MT (1997) Glomerular synaptic responses to olfactory nerve input in rat olfactory bulb slices. Neuroscience 79:425-434.

Aroniadou-Anderjaska V, Ennis M, Shipley MT (1999) Dendrodendritic recurrent excitation in mitral cells of the rat olfactory bulb. J Neurophysiol 82:489-494.

Aroniadou-Anderjaska V, Zhou FM, Priest CA, Ennis M, Shipley MT (2000) Tonic and synaptically evoked presynaptic inhibition of sensory input to the rat olfactory bulb via GABA(B) heteroreceptors. J Neurophysiol 84:1194-1203.

Aungst JL, Heyward PM, Puche AC, Karnup SV, Hayar A, Szabo G, Shipley MT (2003) Centre-surround inhibition among olfactory bulb glomeruli. Nature 426:623-629.

Bakalyar HA, Reed RR (1990) Identification of a specialized adenylyl cyclase that may mediate odorant detection. Science 250:1403-1406.

Barbour DL (2011) Intensity-invariant coding in the auditory system. Neurosci Biobehav Rev 35:2064-2072.

Barth TM, Jones TA, Schallert T (1990) Functional subdivisions of the rat somatic sensorimotor cortex. Behav Brain Res 39:73-95.

Bathellier B, Lagier S, Faure P, Lledo PM (2006) Circuit properties generating gamma oscillations in a network model of the olfactory bulb. J Neurophysiol 95:2678-2691.

Bathellier B, Buhl DL, Accolla R, Carleton A (2008) Dynamic ensemble odor coding in the mammalian olfactory bulb: sensory information at different timescales. Neuron 57:586-598.

Belluscio L, Katz LC (2001) Symmetry, stereotypy, and topography of odorant representations in mouse olfactory bulbs. J Neurosci 21:2113-2122.

Bevins RA, Besheer J (2006) Object recognition in rats and mice: a one-trial non-matching-to-sample learning task to study 'recognition memory'. Nat Protoc 1:1306-1311.

Bisulco S, Slotnick B (2003) Olfactory discrimination of short chain fatty acids in rats with large bilateral lesions of the olfactory bulbs. Chem Senses 28:361-370.

Bodyak N, Slotnick B (1999) Performance of mice in an automated olfactometer: odor detection, discrimination and odor memory. Chem Senses 24:637-645.

Bonino M, Cantino D, Sassoe-Pognetto M (1999) Cellular and subcellular localization of gamma-aminobutyric acidB receptors in the rat olfactory bulb. Neurosci Lett 274:195-198.

Boyd AM, Sturgill JF, Poo C, Isaacson JS (2012) Cortical feedback control of olfactory bulb circuits. Neuron 76:1161-1174.

Bozza T, McGann JP, Mombaerts P, Wachowiak M (2004) In vivo imaging of neuronal activity by targeted expression of a genetically encoded probe in the mouse. Neuron 42:9-21.

Briggman KL, Helmstaedter M, Denk W (2011) Wiring specificity in the direction-selectivity circuit of the retina. Nature 471:183-188.

Buck L, Axel R (1991) A novel multigene family may encode odorant receptors: a molecular basis for odor recognition. Cell 65:175-187.

Bunsey M, Eichenbaum H (1996) Conservation of hippocampal memory function in rats and humans. Nature 379:255-257.

Buonviso N, Chaput MA (1990) Response similarity to odors in olfactory bulb output cells presumed to be connected to the same glomerulus: electrophysiological study using simultaneous single-unit recordings. J Neurophysiol 63:447-454.

Buonviso N, Chaput MA, Scott JW (1991) Mitral cell-to-glomerulus connectivity: an HRP study of the orientation of mitral cell apical dendrites. J Comp Neurol 307:57-64.

Burd GD (1993) Morphological study of the effects of intranasal zinc sulfate irrigation on the mouse olfactory epithelium and olfactory bulb. Microsc Res Tech 24:195-213.

Can Guven S, Laska M (2012) Olfactory sensitivity and odor structure-activity relationships for aliphatic carboxylic acids in CD-1 mice. PLoS One 7:e34301.

Carey RM, Verhagen JV, Wesson DW, Pirez N, Wachowiak M (2009) Temporal structure of receptor neuron input to the olfactory bulb imaged in behaving rats. J Neurophysiol 101:1073-1088.

Carson KA (1984) Localization of acetylcholinesterase-positive neurons projecting to the mouse main olfactory bulb. Brain Res Bull 12:635-639.

Castillo PE, Carleton A, Vincent JD, Lledo PM (1999) Multiple and opposing roles of cholinergic transmission in the main olfactory bulb. J Neurosci 19:9180-9191.

Celerier A, Pierard C, Rachbauer D, Sarrieau A, Beracochea D (2004) Contextual and serial discriminations: a new learning paradigm to assess simultaneously the effects of acute stress on retrieval of flexible or stable information in mice. Learn Mem 11:196-204.

Chaigneau E, Tiret P, Lecoq J, Ducros M, Knopfel T, Charpak S (2007) The relationship between blood flow and neuronal activity in the rodent olfactory bulb. J Neurosci 27:6452-6460.

Chalansonnet M, Chaput MA (1998) Olfactory bulb output cell temporal response patterns to increasing odor concentrations in freely breathing rats. Chem Senses 23:1-9.

Chance B, Cohen P, Jobsis F, Schoener B (1962) Intracellular oxidation-reduction states in vivo. Science 137:499-508.

Chapuis J, Wilson DA (2011) Bidirectional plasticity of cortical pattern recognition and behavioral sensory acuity. Nat Neurosci 15:155-161.

Christie JM, Schoppa NE, Westbrook GL (2001) Tufted cell dendrodendritic inhibition in the olfactory bulb is dependent on NMDA receptor activity. J Neurophysiol 85:169-173.

Clarke S, Panksepp J, Trowill J, Pankseep J (1970) A method of recording sniffing in the free-moving rat. Physiol Behav 5:125-126.

Cleland TA (2009) Early transformations in odor representation. Trends Neurosci 33:130-139.

Cleland TA, Narla VA (2003) Intensity modulation of olfactory acuity. Behav Neurosci 117:1434-1440.

Cleland TA, Sethupathy P (2006) Non-topographical contrast enhancement in the olfactory bulb. BMC Neurosci 7:7.

Cleland TA, Linster C (2012) On-Center/Inhibitory-Surround Decorrelation via Intraglomerular Inhibition in the Olfactory Bulb Glomerular Layer. Front Integr Neurosci 6:5.

Cleland TA, Narla VA, Boudadi K (2009) Multiple learning parameters differentially regulate olfactory generalization. Behav Neurosci 123:26-35.

Cleland TA, Morse A, Yue EL, Linster C (2002) Behavioral models of odor similarity. Behav Neurosci 116:222-231.

Cleland TA, Johnson BA, Leon M, Linster C (2007) Relational representation in the olfactory system. Proc Natl Acad Sci U S A 104:1953-1958.

Cleland TA, Chen SY, Hozer KW, Ukatu HN, Wong KJ, Zheng F (2012) Sequential mechanisms underlying concentration invariance in biological olfaction. Front Neuroeng 4:21.

Cohen LB, Keynes RD, Landowne D (1972) Changes in axon light scattering that accompany the action potential: current-dependent components. J Physiol 224:727-752.

Compston A (2011) From the archives. Disturbances of vision from cerebral lesions, with special reference to the cortical representation of the macula. By Gordon Holmes and W. T. Lister (Consulting Ophthalmic Surgeon, BEF). Brain 1916: 39; 34-73; with A contribution to the cortical representation of vision. By Gordon Holmes. Brain 1931: 54; 470-479. Brain 134:634-637.

Costanzo RM (2000) Rewiring the olfactory bulb: changes in odor maps following recovery from nerve transection. Chem Senses 25:199-205.

Cury KM, Uchida N (2010) Robust odor coding via inhalation-coupled transient activity in the mammalian olfactory bulb. Neuron 68:570-585.

Davis BJ, Macrides F, Youngs WM, Schneider SP, Rosene DL (1978) Efferents and centrifugal afferents of the main and accessory olfactory bulbs in the hamster. Brain Res Bull 3:59-72.

Davison IG, Katz LC (2007) Sparse and selective odor coding by mitral/tufted neurons in the main olfactory bulb. J Neurosci 27:2091-2101.

De Saint Jan D, Hirnet D, Westbrook GL, Charpak S (2009) External tufted cells drive the output of olfactory bulb glomeruli. J Neurosci 29:2043-2052.

Devor A, Dunn AK, Andermann ML, Ulbert I, Boas DA, Dale AM (2003) Coupling of total hemoglobin concentration, oxygenation, and neural activity in rat somatosensory cortex. Neuron 39:353-359.

Devore S, Manella LC, Linster C (2012) Blocking muscarinic receptors in the olfactory bulb impairs performance on an olfactory short-term memory task. Front Behav Neurosci 6:59.

Dhawale AK, Hagiwara A, Bhalla US, Murthy VN, Albeanu DF (2010) Non-redundant odor coding by sister mitral cells revealed by light addressable glomeruli in the mouse. Nat Neurosci 13:1404-1412.

Djurisic M, Popovic M, Carnevale N, Zecevic D (2008) Functional structure of the mitral cell dendritic tuft in the rat olfactory bulb. J Neurosci 28:4057-4068.

Dombeck DA, Khabbaz AN, Collman F, Adelman TL, Tank DW (2007) Imaging large-scale neural activity with cellular resolution in awake, mobile mice. Neuron 56:43-57.

Doty RL (2012) Olfactory dysfunction in Parkinson disease. Nat Rev Neurol 8:329-339.

Doucette W, Restrepo D (2008) Profound context-dependent plasticity of mitral cell responses in olfactory bulb. PLoS Biol 6:e258.

Duchamp-Viret P, Chaput MA, Duchamp A (1999) Odor response properties of rat olfactory receptor neurons. Science 284:2171-2174.

Duchamp-Viret P, Duchamp A, Chaput MA (2000) Peripheral odor coding in the rat and frog: quality and intensity specification. J Neurosci 20:2383-2390.

Ducray A, Bondier JR, Michel G, Bon K, Millot JL, Propper A, Kastner A (2002) Recovery following peripheral destruction of olfactory neurons in young and adult mice. Eur J Neurosci 15:1907-1917.

Dugue GP, Mainen ZF (2009) How serotonin gates olfactory information flow. Nat Neurosci 12:673-675.

Duncan HJ, Beauchamp GK, Yamazaki K (1992) Assessing odor generalization in the rat: a sensitive technique. Physiol Behav 52:617-620.

Edwards DA, Burge KG (1973) Olfactory control of the sexual behavior of male and female mice. Physiol Behav 11:867-872.

Edwards DA, Thompson ML, Burge KG (1972) Olfactory bulb removal vs peripherally induced anosmia: differential effects on the aggressive behavior of male mice. Behav Biol 7:823-828.

Ehrenstein H, Ehrenstein A (1999) Psychophysical Methods. Modern Techniques in Neuroscience Research 1999 Chapter 43:1212-1241.

Escanilla O, Mandairon N, Linster C (2008) Odor-reward learning and enrichment have similar effects on odor perception. Physiol Behav 94:621-626.

Escanilla O, Arrellanos A, Karnow A, Ennis M, Linster C (2010) Noradrenergic modulation of behavioral odor detection and discrimination thresholds in the olfactory bulb. Eur J Neurosci 32:458-468.

Escanilla O, Alperin S, Youssef M, Ennis M, Linster C (2012) Noradrenergic but not cholinergic modulation of olfactory bulb during processing of near threshold concentration stimuli. Behav Neurosci 126:720-728.

Eyre MD, Antal M, Nusser Z (2008) Distinct deep short-axon cell subtypes of the main olfactory bulb provide novel intrabulbar and extrabulbar GABAergic connections. J Neurosci 28:8217-8229.

Fantana AL, Soucy ER, Meister M (2008) Rat olfactory bulb mitral cells receive sparse glomerular inputs. Neuron 59:802-814.

Fleischmann A, Shykind BM, Sosulski DL, Franks KM, Glinka ME, Mei DF, Sun Y, Kirkland J, Mendelsohn M, Albers MW, Axel R (2008) Mice with a "monoclonal nose": perturbations in an olfactory map impair odor discrimination. Neuron 60:1068-1081.

Fletcher ML, Wilson DA (2002) Experience modifies olfactory acuity: acetylcholine-dependent learning decreases behavioral generalization between similar odorants. J Neurosci 22:RC201.

Fletcher ML, Wilson DA (2003) Olfactory bulb mitral-tufted cell plasticity: odorant-specific tuning reflects previous odorant exposure. J Neurosci 23:6946-6955.

Fletcher ML, Masurkar AV, Xing J, Imamura F, Xiong W, Nagayama S, Mutoh H, Greer CA, Knopfel T, Chen WR (2009) Optical imaging of postsynaptic odor representation in the glomerular layer of the mouse olfactory bulb. J Neurophysiol 102:817-830.

Fried HU, Fuss SH, Korsching SI (2002) Selective imaging of presynaptic activity in the mouse olfactory bulb shows concentration and structure dependence of odor responses in identified glomeruli. Proc Natl Acad Sci U S A 99:3222-3227.

Friedrich RW, Korsching SI (1997) Combinatorial and chemotopic odorant coding in the zebrafish olfactory bulb visualized by optical imaging. Neuron 18:737-752.

Friedrich RW, Yaksi E, Judkewitz B, Wiechert MT (2009) Processing of odor representations by neuronal circuits in the olfactory bulb. Ann N Y Acad Sci 1170:293-297.

Frostig RD, Lieke EE, Ts'o DY, Grinvald A (1990) Cortical functional architecture and local coupling between neuronal activity and the microcirculation revealed by in vivo high-resolution optical imaging of intrinsic signals. Proc Natl Acad Sci U S A 87:6082-6086.

Gangrade BK, Dominic CJ (1983) Effect of zinc sulphate-induced anosmia on estrous cycle of the laboratory mice. Indian J Exp Biol 21:425-427.

Gao Y, Strowbridge BW (2009) Long-term plasticity of excitatory inputs to granule cells in the rat olfactory bulb. Nat Neurosci 12:731-733.

Gogos JA, Osborne J, Nemes A, Mendelsohn M, Axel R (2000) Genetic ablation and restoration of the olfactory topographic map. Cell 103:609-620.

Gomez C, Brinon JG, Barbado MV, Weruaga E, Valero J, Alonso JR (2005) Heterogeneous targeting of centrifugal inputs to the glomerular layer of the main olfactory bulb. J Chem Neuroanat 29:238-254.

Gottfried JA, Zelano C (2011) The value of identity: olfactory notes on orbitofrontal cortex function. Ann N Y Acad Sci 1239:138-148.

Gottfried JA, Winston JS, Dolan RJ (2006) Dissociable codes of odor quality and odorant structure in human piriform cortex. Neuron 49:467-479.

Grinvald A, Lieke E, Frostig RD, Gilbert CD, Wiesel TN (1986) Functional architecture of cortex revealed by optical imaging of intrinsic signals. Nature 324:361-364.

Gross-Isseroff R, Lancet D (1988) Concentration-dependent changes of perceived odor quality. Chem Senses 13:191-204.

Gurden H, Uchida N, Mainen ZF (2006) Sensory-evoked intrinsic optical signals in the olfactory bulb are coupled to glutamate release and uptake. Neuron 52:335-345.

Guthrie KM, Gall CM (1995a) Odors increase Fos in olfactory bulb neurons including dopaminergic cells. Neuroreport 6:2145-2149; discussion 2103.

Guthrie KM, Gall CM (1995b) Functional mapping of odor-activated neurons in the olfactory bulb. Chem Senses 20:271-282.

Guthrie KM, Anderson AJ, Leon M, Gall C (1993) Odor-induced increases in c-fos mRNA expression reveal an anatomical "unit" for odor processing in olfactory bulb. Proc Natl Acad Sci U S A 90:3329-3333.

Haberly LB, Price JL (1977) The axonal projection patterns of the mitral and tufted cells of the olfactory bulb in the rat. Brain Res 129:152-157.

Haddad R, Weiss T, Khan R, Nadler B, Mandairon N, Bensafi M, Schneidman E, Sobel N (2010) Global features of neural activity in the olfactory system form a parallel code that predicts olfactory behavior and perception. J Neurosci 30:9017-9026.

Harding JW, Getchell TV, Margolis FL (1978) Denervation of the primary olfactory pathway in mice. V. Long-term effect of intranasal ZnSO4 irrigation on behavior, biochemistry and morphology. Brain Res 140:271-285.

Hayar A, Shipley MT, Ennis M (2005) Olfactory bulb external tufted cells are synchronized by multiple intraglomerular mechanisms. J Neurosci 25:8197-8208.

Hayar A, Karnup S, Ennis M, Shipley MT (2004) External tufted cells: a major excitatory element that coordinates glomerular activity. J Neurosci 24:6676-6685.

Hendrickson A, Boles J, McLean EB (1977) Visual acuity and behavior of monocularly deprived monkeys after retinal lesions. Invest Ophthalmol Vis Sci 16:469-473.

Hill DK, Keynes RD (1949) Opacity changes in stimulated nerve. J Physiol 108:278-281.

Ho SL, Johnson BA, Leon M (2006a) Long hydrocarbon chains serve as unique molecular features recognized by ventral glomeruli of the rat olfactory bulb. J Comp Neurol 498:16-30.

Ho SL, Johnson BA, Chen AL, Leon M (2006b) Differential responses to branched and unsaturated aliphatic hydrocarbons in the rat olfactory system. J Comp Neurol 499:519-532.

Homma R, Cohen LB, Kosmidis EK, Youngentob SL (2009) Perceptual stability during dramatic changes in olfactory bulb activation maps and dramatic declines in activation amplitudes. Eur J Neurosci 29:1027-1034.

Imai T, Sakano H, Vosshall LB (2010) Topographic mapping--the olfactory system. Cold Spring Harb Perspect Biol 2:a001776.

Imamura K, Mataga N, Mori K (1992) Coding of odor molecules by mitral/tufted cells in rabbit olfactory bulb. I. Aliphatic compounds. J Neurophysiol 68:1986-2002.

Isaacson JS, Strowbridge BW (1998) Olfactory reciprocal synapses: dendritic signaling in the CNS. Neuron 20:749-761.

Jiang M, Griff ER, Ennis M, Zimmer LA, Shipley MT (1996) Activation of locus coeruleus enhances the responses of olfactory bulb mitral cells to weak olfactory nerve input. J Neurosci 16:6319-6329.

Jobsis FF (1977) Non-invasive, infra-red monitoring of cerebral O2 sufficiency, bloodvolume, HbO2-Hb shifts and bloodflow. Acta Neurol Scand Suppl 64:452-453.

Johnson BA, Leon M (2000) Modular representations of odorants in the glomerular layer of the rat olfactory bulb and the effects of stimulus concentration. J Comp Neurol 422:496-509.

Johnson BA, Leon M (2007) Chemotopic odorant coding in a mammalian olfactory system. J Comp Neurol 503:1-34.

Johnson BA, Woo CC, Leon M (1998) Spatial coding of odorant features in the glomerular layer of the rat olfactory bulb. J Comp Neurol 393:457-471.

Johnson BA, Farahbod H, Leon M (2005a) Interactions between odorant functional group and hydrocarbon structure influence activity in glomerular response modules in the rat olfactory bulb. J Comp Neurol 483:205-216.

Johnson BA, Farahbod H, Saber S, Leon M (2005b) Effects of functional group position on spatial representations of aliphatic odorants in the rat olfactory bulb. J Comp Neurol 483:192-204.

Johnson BA, Woo CC, Hingco EE, Pham KL, Leon M (1999) Multidimensional chemotopic responses to n-aliphatic acid odorants in the rat olfactory bulb. J Comp Neurol 409:529-548.

Johnson BA, Ong J, Lee K, Ho SL, Arguello S, Leon M (2007) Effects of double and triple bonds on the spatial representations of odorants in the rat olfactory bulb. J Comp Neurol 500:720-733.

Jones DT, Reed RR (1989) Golf: an olfactory neuron specific-G protein involved in odorant signal transduction. Science 244:790-795.

Junek S, Kludt E, Wolf F, Schild D (2010) Olfactory coding with patterns of response latencies. Neuron 67:872-884.

Kadohisa M, Wilson DA (2006) Separate encoding of identity and similarity of complex familiar odors in piriform cortex. Proc Natl Acad Sci U S A 103:15206-15211.

Kashiwadani H, Sasaki YF, Uchida N, Mori K (1999) Synchronized oscillatory discharges of mitral/tufted cells with different molecular receptive ranges in the rabbit olfactory bulb. J Neurophysiol 82:1786-1792.

Kato HK, Chu MW, Isaacson JS, Komiyama T (2012) Dynamic sensory representations in the olfactory bulb: modulation by wakefulness and experience. Neuron 76:962-975.

Katoh K, Koshimoto H, Tani A, Mori K (1993) Coding of odor molecules by mitral/tufted cells in rabbit olfactory bulb. II. Aromatic compounds. J Neurophysiol 70:2161-2175.

Kaupp UB (2010) Olfactory signalling in vertebrates and insects: differences and commonalities. Nat Rev Neurosci 11:188-200.

Kay LM, Krysiak M, Barlas L, Edgerton GB (2006) Grading odor similarities in a Go/No-Go task. Physiol Behav 88:339-346.

Kent PF, Youngentob SL, Sheehe PR (1995) Odorant-specific spatial patterns in mucosal activity predict perceptual differences among odorants. J Neurophysiol 74:1777-1781.

Kent PF, Mozell MM, Youngentob SL, Yurco P (2003) Mucosal activity patterns as a basis for olfactory discrimination: comparing behavior and optical recordings. Brain Res 981:1-11.

Kim DS, Bonhoeffer T (1994) Reverse occlusion leads to a precise restoration of orientation preference maps in visual cortex. Nature 370:370-372.

Kleene SJ (2008) The electrochemical basis of odor transduction in vertebrate olfactory cilia. Chem Senses 33:839-859.

Klenoff JR, Greer CA (1998) Postnatal development of olfactory receptor cell axonal arbors. J Comp Neurol 390:256-267.

Kosaka T, Kosaka K (2011) "Interneurons" in the olfactory bulb revisited. Neurosci Res 69:93-99.

Krone D, Mannel M, Pauli E, Hummel T (2001) Qualitative and quantitative olfactometric evaluation of different concentrations of ethanol peppermint oil solutions. Phytother Res 15:135-138.

Kuffler SW (1953) Discharge patterns and functional organization of mammalian retina. J Neurophysiol 16:37-68.

Kumar KR, Archunan G (1999) Influence of the stage of the cycle on olfactory sensitivity in laboratory mice. Indian J Exp Biol 37:317-318.

Lagier S, Carleton A, Lledo PM (2004) Interplay between local GABAergic interneurons and relay neurons generates gamma oscillations in the rat olfactory bulb. J Neurosci 24:4382-4392.

Larsson L, Laska M (2011) Ultra-high olfactory sensitivity for the human sperm-attractant aromatic aldehyde bourgeonal in CD-1 mice. Neurosci Res 71:355-360.

Laska M, Persson O, Hernandez Salazar LT (2009) Olfactory sensitivity for alkylpyrazines-a comparative study in CD-1 mice and spider monkeys. J Exp Zool A Ecol Genet Physiol 311:278-288.

Lazarini F, Lledo PM (2011) Is adult neurogenesis essential for olfaction? Trends Neurosci 34:20-30.

Lecoq J, Tiret P, Charpak S (2009) Peripheral adaptation codes for high odor concentration in glomeruli. J Neurosci 29:3067-3072.

Lehmkuhle MJ, Normann RA, Maynard EM (2003) High-resolution analysis of the spatio-temporal activity patterns in rat olfactory bulb evoked by enantiomer odors. Chem Senses 28:499-508.

Leon M, Johnson BA (2009) Is there a space-time continuum in olfaction? Cell Mol Life Sci 66:2135-2150.

Li J, Bravo DS, Upton AL, Gilmour G, Tricklebank MD, Fillenz M, Martin C, Lowry JP, Bannerman DM, McHugh SB (2011) Close temporal coupling of neuronal activity and tissue oxygen responses in rodent whisker barrel cortex. Eur J Neurosci 34:1983-1996.

Li W, Howard JD, Gottfried JA (2010) Disruption of odour quality coding in piriform cortex mediates olfactory deficits in Alzheimer's disease. Brain 133:2714-2726.

Linster C, Cleland TA (2002) Cholinergic modulation of sensory representations in the olfactory bulb. Neural Netw 15:709-717.

Linster C, Garcia PA, Hasselmo ME, Baxter MG (2001a) Selective loss of cholinergic neurons projecting to the olfactory system increases perceptual generalization between similar, but not dissimilar, odorants. Behav Neurosci 115:826-833.

Linster C, Johnson BA, Morse A, Yue E, Leon M (2002) Spontaneous versus reinforced olfactory discriminations. J Neurosci 22:6842-6845.

Linster C, Johnson BA, Yue E, Morse A, Xu Z, Hingco EE, Choi Y, Choi M, Messiha A, Leon M (2001b) Perceptual correlates of neural representations evoked by odorant enantiomers. J Neurosci 21:9837-9843.

Liu S, Aungst JL, Puche AC, Shipley MT (2012) Serotonin modulates the population activity profile of olfactory bulb external tufted cells. J Neurophysiol 107:473-483.

Lowe G, Gold GH (1993) Nonlinear amplification by calcium-dependent chloride channels in olfactory receptor cells. Nature 366:283-286.

Lu XC, Slotnick BM (1994) Recognition of propionic acid vapor after removal of the olfactory bulb area associated with high 2-DG uptake. Brain Res 639:26-32.

Lu XC, Slotnick BM (1998) Olfaction in rats with extensive lesions of the olfactory bulbs: implications for odor coding. Neuroscience 84:849-866.

Lu XC, Slotnick BM, Silberberg AM (1993) Odor matching and odor memory in the rat. Physiol Behav 53:795-804.

Luo M, Katz LC (2001) Response correlation maps of neurons in the mammalian olfactory bulb. Neuron 32:1165-1179.

Ma J, Lowe G (2007) Calcium permeable AMPA receptors and autoreceptors in external tufted cells of rat olfactory bulb. Neuroscience 144:1094-1108.

Ma L, Qiu Q, Gradwohl S, Scott A, Yu EQ, Alexander R, Wiegraebe W, Yu CR (2012) Distributed representation of chemical features and tunotopic organization of glomeruli in the mouse olfactory bulb. Proc Natl Acad Sci U S A 109:5481-5486.

MacVicar BA, Hochman D (1991) Imaging of synaptically evoked intrinsic optical signals in hippocampal slices. J Neurosci 11:1458-1469.

Malnic B (2007) Searching for the ligands of odorant receptors. Mol Neurobiol 35:175-181.

Mandairon N, Linster C (2009) Odor perception and olfactory bulb plasticity in adult mammals. J Neurophysiol 101:2204-2209.

Mandairon N, Stack C, Linster C (2006a) Olfactory enrichment improves the recognition of individual components in mixtures. Physiol Behav 89:379-384.

Mandairon N, Didier A, Linster C (2008) Odor enrichment increases interneurons responsiveness in spatially defined regions of the olfactory bulb correlated with perception. Neurobiol Learn Mem 90:178-184.

Mandairon N, Stack C, Kiselycznyk C, Linster C (2006b) Enrichment to odors improves olfactory discrimination in adult rats. Behav Neurosci 120:173-179.

Mandairon N, Ferretti CJ, Stack CM, Rubin DB, Cleland TA, Linster C (2006c) Cholinergic modulation in the olfactory bulb influences spontaneous olfactory discrimination in adult rats. Eur J Neurosci 24:3234-3244.

Mao T, O'Connor DH, Scheuss V, Nakai J, Svoboda K (2008) Characterization and subcellular targeting of GCaMP-type genetically-encoded calcium indicators. PLoS One 3:e1796.

Marella S, Ermentrout B (2010) Amplification of asynchronous inhibition-mediated synchronization by feedback in recurrent networks. PLoS Comput Biol 6:e1000679.

Margrie TW, Schaefer AT (2003) Theta oscillation coupled spike latencies yield computational vigour in a mammalian sensory system. J Physiol 546:363-374.

Markopoulos F, Rokni D, Gire DH, Murthy VN (2012) Functional properties of cortical feedback projections to the olfactory bulb. Neuron 76:1175-1188.

Martin C, Grenier D, Thevenet M, Vigouroux M, Bertrand B, Janier M, Ravel N, Litaudon P (2007) fMRI visualization of transient activations in the rat olfactory bulb using short odor stimulations. Neuroimage 36:1288-1293.

Matulionis DH (1975a) Ultrastructural study of mouse olfactory epithelium following destruction by ZnSO4 and its subsequent regeneration. Am J Anat 142:67-89.

Matulionis DH (1975b) Light and electron microscopic study of the effects of ZnSO4 on mouse nasal respiratory epithelium and subsequent responses. Anat Rec 183:63-82.

Mayer AD, Rosenblatt JS (1993) Peripheral olfactory deafferentation of the primary olfactory system in rats using ZnSO4 nasal spray with special reference to maternal behavior. Physiol Behav 53:587-592.

McBride K, Slotnick B (2006) Discrimination between the enantiomers of carvone and of terpinen-4-ol odorants in normal rats and those with lesions of the olfactory bulbs. J Neurosci 26:9892-9901.

McBride K, Slotnick B, Margolis FL (2003) Does intranasal application of zinc sulfate produce anosmia in the mouse? An olfactometric and anatomical study. Chem Senses 28:659-670.

McGann JP, Pirez N, Wachowiak M (2006) Imaging odor coding and synaptic plasticity in the mammalian brain with a genetically-encoded probe. Conf Proc IEEE Eng Med Biol Soc 1:664-667.

McGann JP, Pirez N, Gainey MA, Muratore C, Elias AS, Wachowiak M (2005) Odorant representations are modulated by intra- but not interglomerular presynaptic inhibition of olfactory sensory neurons. Neuron 48:1039-1053.

McLean JH, Shipley MT (1987a) Serotonergic afferents to the rat olfactory bulb: I. Origins and laminar specificity of serotonergic inputs in the adult rat. J Neurosci 7:3016-3028.

McLean JH, Shipley MT (1987b) Serotonergic afferents to the rat olfactory bulb: II. Changes in fiber distribution during development. J Neurosci 7:3029-3039.

Meister M, Bonhoeffer T (2001) Tuning and topography in an odor map on the rat olfactory bulb. J Neurosci 21:1351-1360.

Miesenbock G, De Angelis DA, Rothman JE (1998) Visualizing secretion and synaptic transmission with pH-sensitive green fluorescent proteins. Nature 394:192-195.

Mittmann W, Wallace DJ, Czubayko U, Herb JT, Schaefer AT, Looger LL, Denk W, Kerr JN (2011) Two-photon calcium imaging of evoked activity from L5 somatosensory neurons in vivo. Nat Neurosci 14:1089-1093.

Miyamichi K, Serizawa S, Kimura HM, Sakano H (2005) Continuous and overlapping expression domains of odorant receptor genes in the olfactory epithelium determine the dorsal/ventral positioning of glomeruli in the olfactory bulb. J Neurosci 25:3586-3592.

Mombaerts P, Wang F, Dulac C, Chao SK, Nemes A, Mendelsohn M, Edmondson J, Axel R (1996) Visualizing an olfactory sensory map. Cell 87:675-686.

Mori K, Yoshihara Y (1995) Molecular recognition and olfactory processing in the mammalian olfactory system. Prog Neurobiol 45:585-619.

Mori K, Mataga N, Imamura K (1992) Differential specificities of single mitral cells in rabbit olfactory bulb for a homologous series of fatty acid odor molecules. J Neurophysiol 67:786-789.

Mori K, Takahashi YK, Igarashi KM, Yamaguchi M (2006) Maps of odorant molecular features in the Mammalian olfactory bulb. Physiol Rev 86:409-433.

Mouly AM, Vigouroux M, Holley A (1985) On the ability of rats to discriminate between microstimulations of the olfactory bulb in different locations. Behav Brain Res 17:45-58.

Murthy VN (2011) Olfactory maps in the brain. Annu Rev Neurosci 34:233-258.

Nagayama S, Enerva A, Fletcher ML, Masurkar AV, Igarashi KM, Mori K, Chen WR (2010) Differential axonal projection of mitral and tufted cells in the mouse main olfactory system. Front Neural Circuits 4.

Nakamura T, Gold GH (1987) A cyclic nucleotide-gated conductance in olfactory receptor cilia. Nature 325:442-444.

Niessing J, Friedrich RW (2010) Olfactory pattern classification by discrete neuronal network states. Nature 465:47-52.

O'Connell RJ, Mozell MM (1969) Quantitative stimulation of frog olfactory receptors. J Neurophysiol 32:51-63.

O'Keefe J (1979) A review of the hippocampal place cells. Prog Neurobiol 13:419-439.

O'Keefe J, Dostrovsky J (1971) The hippocampus as a spatial map. Preliminary evidence from unit activity in the freely-moving rat. Brain Res 34:171-175.

Orona E, Rainer EC, Scott JW (1984) Dendritic and axonal organization of mitral and tufted cells in the rat olfactory bulb. J Comp Neurol 226:346-356.

Pain F, L'Heureux B, Gurden H (2011) Visualizing odor representation in the brain: a review of imaging techniques for the mapping of sensory activity in the olfactory glomeruli. Cell Mol Life Sci.

Petzold GC, Hagiwara A, Murthy VN (2009) Serotonergic modulation of odor input to the mammalian olfactory bulb. Nat Neurosci 12:784-791.

Pinching AJ, Powell TP (1971a) The neuropil of the glomeruli of the olfactory bulb. J Cell Sci 9:347-377.

Pinching AJ, Powell TP (1971b) The neuropil of the periglomerular region of the olfactory bulb. J Cell Sci 9:379-409.

Pressler RT, Strowbridge BW (2006) Blanes cells mediate persistent feedforward inhibition onto granule cells in the olfactory bulb. Neuron 49:889-904.

Price JL, Powell TP (1970) The synaptology of the granule cells of the olfactory bulb. J Cell Sci 7:125-155.

Rall W, Shepherd GM (1968) Theoretical reconstruction of field potentials and dendrodendritic synaptic interactions in olfactory bulb. J Neurophysiol 31:884-915.

Rall W, Shepherd GM, Reese TS, Brightman MW (1966) Dendrodendritic synaptic pathway for inhibition in the olfactory bulb. Exp Neurol 14:44-56.

Rancz EA, Franks KM, Schwarz MK, Pichler B, Schaefer AT, Margrie TW (2011) Transfection via whole-cell recording in vivo: bridging single-cell physiology, genetics and connectomics. Nat Neurosci 14:527-532.

Reisert J, Matthews HR (2001) Response properties of isolated mouse olfactory receptor cells. J Physiol 530:113-122.

Reisert J, Lai J, Yau KW, Bradley J (2005) Mechanism of the excitatory Cl- response in mouse olfactory receptor neurons. Neuron 45:553-561.

Ressler KJ, Sullivan SL, Buck LB (1994) Information coding in the olfactory system: evidence for a stereotyped and highly organized epitope map in the olfactory bulb. Cell 79:1245-1255.

Rubin BD, Katz LC (1999) Optical imaging of odorant representations in the mammalian olfactory bulb. Neuron 23:499-511.

Rubin BD, Katz LC (2001) Spatial coding of enantiomers in the rat olfactory bulb. Nat Neurosci 4:355-356.

Schaefer AT, Margrie TW (2007) Spatiotemporal representations in the olfactory system. Trends Neurosci 30:92-100.

Schaefer AT, Margrie TW (2012) Psychophysical properties of odor processing can be quantitatively described by relative action potential latency patterns in mitral and tufted cells. Front Syst Neurosci 6:30.

Schoppa NE (2006) Synchronization of olfactory bulb mitral cells by precisely timed inhibitory inputs. Neuron 49:271-283.

Schoppa NE, Urban NN (2003) Dendritic processing within olfactory bulb circuits. Trends Neurosci 26:501-506.

Schoppa NE, Kinzie JM, Sahara Y, Segerson TP, Westbrook GL (1998) Dendrodendritic inhibition in the olfactory bulb is driven by NMDA receptors. J Neurosci 18:6790-6802.

Schwob JE, Youngentob SL, Ring G, Iwema CL, Mezza RC (1999) Reinnervation of the rat olfactory bulb after methyl bromide-induced lesion: timing and extent of reinnervation. J Comp Neurol 412:439-457.

Shepard RN (1987) Toward a universal law of generalization for psychological science. Science 237:1317-1323.

Shepard RN, Chang JJ (1963) Stimulus generalization in the learning of classifications. J Exp Psychol 65:94-102.

Shepherd GM, Chen WR, Greer CA (2004) Olfactory Bulb. The Synaptic Organization fo the Brain Fifth Edition:165-216.

Shimshek DR, Bus T, Kim J, Mihaljevic A, Mack V, Seeburg PH, Sprengel R, Schaefer AT (2005) Enhanced odor discrimination and impaired olfactory memory by spatially controlled switch of AMPA receptors. PLoS Biol 3:e354.

Shipley MT, Adamek GD (1984) The connections of the mouse olfactory bulb: a study using orthograde and retrograde transport of wheat germ agglutinin conjugated to horseradish peroxidase. Brain Res Bull 12:669-688.

Shusterman R, Smear MC, Koulakov AA, Rinberg D (2011) Precise olfactory responses tile the sniff cycle. Nat Neurosci.

Sieck MH, Baumbach HD (1974) Differential effects of peripheral and central anosmia producing techniques on spontaneous behavior patterns. Physiol Behav 13:407-425.

Skinner BF (1948) Superstition in the pigeon. J Exp Psychol 38:168-172.

Slotnick B (2007a) Response accuracy and odor sampling time in mice trained to discriminate between enantiomers of carvone and those of terpinen-4-ol. Chem Senses 32:721-725.

Slotnick B (2007b) Olfactory performance of rats after selective deafferentation of the olfactory bulb by 3-methyl indole. Chem Senses 32:173-181.

Slotnick B, Bodyak N (2002) Odor discrimination and odor quality perception in rats with disruption of connections between the olfactory epithelium and olfactory bulbs. J Neurosci 22:4205-4216.

Slotnick B, Bisulco S (2003) Detection and discrimination of carvone enantiomers in rats with olfactory bulb lesions. Neuroscience 121:451-457.

Slotnick B, Glover P, Bodyak N (2000) Does intranasal application of zinc sulfate produce anosmia in the rat? Behav Neurosci 114:814-829.

Slotnick B, Cockerham R, Pickett E (2004) Olfaction in olfactory bulbectomized rats. J Neurosci 24:9195-9200.

Slotnick BM, Katz HM (1974) Olfactory learning-set formation in rats. Science 185:796-798.

Slotnick BM, Nigrosh BJ (1974) Olfactory stimulus control evaluated in a small animal olfactometer. Percept Mot Skills 39:583-597.

Slotnick BM, Gutman LA (1977) Evaluation of intranasal zinc sulfate treatment on olfactory discrimination in rats. J Comp Physiol Psychol 91:942-950.

Slotnick BM, Ptak JE (1977) Olfactory intensity-difference thresholds in rats and humans. Physiol Behav 19:795-802.

Slotnick BM, Kufera A, Silberberg AM (1991) Olfactory learning and odor memory in the rat. Physiol Behav 50:555-561.

Slotnick BM, Graham S, Laing DG, Bell GA (1987) Detection of propionic acid vapor by rats with lesions of olfactory bulb areas associated with high 2-DG uptake. Brain Res 417:343-346.

Slotnick BM, Panhuber H, Bell GA, Laing DG (1989) Odor-induced metabolic activity in the olfactory bulb of rats trained to detect propionic acid vapor. Brain Res 500:161-168.

Slotnick BM, Bell GA, Panhuber H, Laing DG (1997) Detection and discrimination of propionic acid after removal of its 2-DG identified major

focus in the olfactory bulb: a psychophysical analysis. Brain Res 762:89-96.

Smallwood PM, Olveczky BP, Williams GL, Jacobs GH, Reese BE, Meister M, Nathans J (2003) Genetically engineered mice with an additional class of cone photoreceptors: implications for the evolution of color vision. Proc Natl Acad Sci U S A 100:11706-11711.

Smith CG (1938) Changes in the Olfactory Mucosa and the Olfactory Nerves Following Intranasal Treatment with One Per Cent Zinc Sulphate. Can Med Assoc J 39:138-140.

Sokoloff L, Reivich M, Kennedy C, Des Rosiers MH, Patlak CS, Pettigrew KD, Sakurada O, Shinohara M (1977) The [14C]deoxyglucose method for the measurement of local cerebral glucose utilization: theory, procedure, and normal values in the conscious and anesthetized albino rat. J Neurochem 28:897-916.

Soucy ER, Albeanu DF, Fantana AL, Murthy VN, Meister M (2009) Precision and diversity in an odor map on the olfactory bulb. Nat Neurosci 12:210-220.

Spors H, Grinvald A (2002) Spatio-temporal dynamics of odor representations in the mammalian olfactory bulb. Neuron 34:301-315.

Spors H, Wachowiak M, Cohen LB, Friedrich RW (2006) Temporal dynamics and latency patterns of receptor neuron input to the olfactory bulb. J Neurosci 26:1247-1259.

Spors H, Albeanu DF, Murthy VN, Rinberg D, Uchida N, Wachowiak M, Friedrich RW (2012) Illuminating vertebrate olfactory processing. J Neurosci 32:14102-14108.

Stawski RS, Sliwinski MJ, Smyth JM (2009) The effects of an acute psychosocial stressor on episodic memory. Eur J Cogn Psychol 21:897-918.

Stevenson RJ (2001) Associative Learning and Odor Quality Perception: How

Sniffing an Odor Mixture Can Alter the Smell of Its Parts. Learning and Motivation 32:154-177.

Stewart WB, Kauer JS, Shepherd GM (1979) Functional organization of rat olfactory bulb analysed by the 2-deoxyglucose method. J Comp Neurol 185:715-734.

Stosiek C, Garaschuk O, Holthoff K, Konnerth A (2003) In vivo two-photon calcium imaging of neuronal networks. Proc Natl Acad Sci U S A 100:7319-7324.

Svoboda K, Denk W, Kleinfeld D, Tank DW (1997) In vivo dendritic calcium dynamics in neocortical pyramidal neurons. Nature 385:161-165.

Thor DH, Carty RW, Flannelly KJ (1976) Prolonged peripheral anosmia in the rat by multiple intranasal applications of zinc sulfate solution. Bull Psychon Soc 7:41-43.

Uchida N, Mainen ZF (2003) Speed and accuracy of olfactory discrimination in the rat. Nat Neurosci 6:1224-1229.

Uchida N, Mainen ZF (2008) Odor concentration invariance by chemical ratio coding. Front Syst Neurosci 1:3.

Uchida N, Takahashi YK, Tanifuji M, Mori K (2000) Odor maps in the mammalian olfactory bulb: domain organization and odorant structural features. Nat Neurosci 3:1035-1043.

Urban NN, Sakmann B (2002) Reciprocal intraglomerular excitation and intra- and interglomerular lateral inhibition between mouse olfactory bulb mitral cells. J Physiol 542:355-367.

Urban NN, Arevian AC (2009) Computing with dendrodendritic synapses in the olfactory bulb. Ann N Y Acad Sci 1170:264-269.

Vassar R, Chao SK, Sitcheran R, Nunez JM, Vosshall LB, Axel R (1994) Topographic organization of sensory projections to the olfactory bulb. Cell 79:981-991.

Vedin V, Slotnick B, Berghard A (2004) Zonal ablation of the olfactory sensory neuroepithelium of the mouse: effects on odorant detection. Eur J Neurosci 20:1858-1864.

Vincis R, Gschwend O, Bhaukaurally K, Beroud J, Carleton A (2012) Dense representation of natural odorants in the mouse olfactory bulb. Nat Neurosci 15:537-539.

Vucinic D, Cohen LB, Kosmidis EK (2006) Interglomerular center-surround inhibition shapes odorant-evoked input to the mouse olfactory bulb in vivo. J Neurophysiol 95:1881-1887.

Wachowiak M, Cohen LB (2001) Representation of odorants by receptor neuron input to the mouse olfactory bulb. Neuron 32:723-735.

Wachowiak M, Cohen LB (2003) Correspondence between odorant-evoked patterns of receptor neuron input and intrinsic optical signals in the mouse olfactory bulb. J Neurophysiol 89:1623-1639.

Wachowiak M, Shipley MT (2006) Coding and synaptic processing of sensory information in the glomerular layer of the olfactory bulb. Semin Cell Dev Biol 17:411-423.

Wachowiak M, Cohen LB, Zochowski MR (2002) Distributed and concentration-invariant spatial representations of odorants by receptor neuron input to the turtle olfactory bulb. J Neurophysiol 87:1035-1045.

Wachowiak M, Zochowski M, Cohen LB, Falk CX (2000) The spatial representation of odors by olfactory receptor neuron input to the olfactory bulb is concentration invariant. Biol Bull 199:162-163.

Wallis G, Backus BT, Langer M, Huebner G, Bulthoff H (2009) Learning illumination- and orientation-invariant representations of objects through temporal association. J Vis 9:6.

Wellis DP, Scott JW, Harrison TA (1989) Discrimination among odorants by single neurons of the rat olfactory bulb. J Neurophysiol 61:1161-1177.

Wesson DW, Verhagen JV, Wachowiak M (2009) Why sniff fast? The relationship between sniff frequency, odor discrimination, and receptor neuron activation in the rat. J Neurophysiol 101:1089-1102.

Wesson DW, Carey RM, Verhagen JV, Wachowiak M (2008a) Rapid encoding and perception of novel odors in the rat. PLoS Biol 6:e82.

Wesson DW, Donahou TN, Johnson MO, Wachowiak M (2008b) Sniffing behavior of mice during performance in odor-guided tasks. Chem Senses 33:581-596.

Whitesell JD, Sorensen KA, Jarvie BC, Hentges ST, Schoppa NE (2013) Interglomerular lateral inhibition targeted on external tufted cells in the olfactory bulb. J Neurosci 33:1552-1563.

Wiechert MT, Judkewitz B, Riecke H, Friedrich RW (2010) Mechanisms of pattern decorrelation by recurrent neuronal circuits. Nat Neurosci 13:1003-1010.

Willhite DC, Nguyen KT, Masurkar AV, Greer CA, Shepherd GM, Chen WR (2006) Viral tracing identifies distributed columnar organization in the olfactory bulb. Proc Natl Acad Sci U S A 103:12592-12597.

Wilson DA (1998) Habituation of odor responses in the rat anterior piriform cortex. J Neurophysiol 79:1425-1440.

Wilson DA (2000) Odor specificity of habituation in the rat anterior piriform cortex. J Neurophysiol 83:139-145.

Wilson DA, Sullivan RM (2011) Cortical processing of odor objects. Neuron 72:506-519.

Wilson DA, Fletcher ML, Sullivan RM (2004) Acetylcholine and olfactory perceptual learning. Learn Mem 11:28-34.

Wilson RI (2008) Neural and behavioral mechanisms of olfactory perception. Curr Opin Neurobiol 18:408-412.

Wilson RI, Mainen ZF (2006) Early events in olfactory processing. Annu Rev Neurosci 29:163-201.

Wilson RS, Arnold SE, Schneider JA, Boyle PA, Buchman AS, Bennett DA (2009) Olfactory impairment in presymptomatic Alzheimer's disease. Ann N Y Acad Sci 1170:730-735.

Winans SS, Powers JB (1977) Olfactory and vomeronasal deafferentation of male hamsters: histological and behavioral analyses. Brain Res 126:325-344.

Wright GA, Thomson MG, Smith BH (2005) Odour concentration affects odour identity in honeybees. Proc Biol Sci 272:2417-2422.

Wu KN, Tan BK, Howard JD, Conley DB, Gottfried JA (2012) Olfactory input is critical for sustaining odor quality codes in human orbitofrontal cortex. Nat Neurosci 15:1313-1319.

Xu F, Greer CA, Shepherd GM (2000) Odor maps in the olfactory bulb. J Comp Neurol 422:489-495.

Yaksi E, Friedrich RW (2006) Reconstruction of firing rate changes across neuronal populations by temporally deconvolved Ca2+ imaging. Nat Methods 3:377-383.

Yaksi E, Judkewitz B, Friedrich RW (2007) Topological reorganization of odor representations in the olfactory bulb. PLoS Biol 5:e178.

Yaksi E, von Saint Paul F, Niessing J, Bundschuh ST, Friedrich RW (2009) Transformation of odor representations in target areas of the olfactory bulb. Nat Neurosci 12:474-482.

Yee KK, Costanzo RM (1998) Changes in odor quality discrimination following recovery from olfactory nerve transection. Chem Senses 23:513-519.

Yokoi M, Mori K, Nakanishi S (1995) Refinement of odor molecule tuning by dendrodendritic synaptic inhibition in the olfactory bulb. Proc Natl Acad Sci U S A 92:3371-3375.

Youngentob SL, Schwob JE (2006) Odorant identification and quality perception following methyl bromide-induced lesions of the olfactory epithelium. Behav Neurosci 120:1346-1355.

Youngentob SL, Markert LM, Mozell MM, Hornung DE (1990) A method for establishing a five odorant identification confusion matrix task in rats. Physiol Behav 47:1053-1059.

Youngentob SL, Johnson BA, Leon M, Sheehe PR, Kent PF (2006) Predicting odorant quality perceptions from multidimensional scaling of olfactory bulb glomerular activity patterns. Behav Neurosci 120:1337-1345.

Zelano C, Mohanty A, Gottfried JA (2011) Olfactory predictive codes and stimulus templates in piriform cortex. Neuron 72:178-187.

Zhang X, Firestein S (2002) The olfactory receptor gene superfamily of the mouse. Nat Neurosci 5:124-133.

Zhou J, Dong Q, Zhuang LJ, Li R, Wang P (2012) Rapid odor perception in rat olfactory bulb by microelectrode array. J Zhejiang Univ Sci B 13:1015-1023.

Zhou Z, Belluscio L (2012) Coding odorant concentration through activation timing between the medial and lateral olfactory bulb. Cell Rep 2:1143-1150.